Danger from Above - The Economic Impacts of Floods

Dino Collalti

Inauguraldissertation zur Erlangung der Würde eines

DOCTOR RERUM OECONOMICARUM

der Wirtschafts- und Sozialwissenschaftlichen Fakultät

der Universität Bern

July 2023

The faculty accepted this thesis on the 24. August 2023 at the request of the reviewers Prof. Dr. Eric Strobl and Prof. Dr. Luisito Bertinelli as dissertation, without wishing to comment on the views expressed therein.

Die Fakultät hat diese Arbeit am 24. August 2023 auf Antrag der Gutachter Prof. Dr. Eric Strobl und Prof. Dr. Luisito Bertinelli als Dissertation angenommen, ohne damit zu den darin ausgesprochenen Auffassungen Stellung nehmen zu wollen.

"Don't aim at success. The more you aim at it and make it a target, the more you are going to miss it. For success, like happiness, cannot be pursued; it must ensue, and it only does so as the unintended side effect of one's personal dedication to a cause greater than oneself or as the by-product of one's surrender to a person other than oneself. Happiness must happen, and the same holds for success: you have to let it happen by not caring about it. I want you to listen to what your conscience commands you to do and go on to carry it out to the best of your knowledge. Then you will live to see that in the long-run—in the long-run, I say!—success will follow you precisely because you had forgotten to think about it."

Viktor E. Frankl, Man's Search for Meaning

Preface

First, I thank my supervisor Eric Strobl for his support and guidance in the past years. His advice not only contributed substantially to this dissertation but also to my personal academic development. He sparked my interest in interdisciplinary work and showed me what potential there is. I have been able to grow enormously, thanks to him.

I am also indebted to my co-author of the second chapter, Nekeisha Spencer. Without her help and support, I could not have written with conviction about the Caribbean Nation of Jamaica. I especially remember my visit to the University of the West Indies and the hearty laughter during our hunt for the ripest fruits all over Kingston.

I would also like to thank the faculty of the Department of Economics, particularly Jeanne Tschopp, Max von Ehrlich, and Mike Gerfin. In their way, they each helped me write this thesis and develop my critical academic thinking. Similarly, I want to thank the Oeschger Centre for Climate Change for introducing me to true interdisciplinary research. Academia can be pretty daunting for any Ph.D. student, and it was even more so when the first part of the journey was online only due to the Corona Pandemic. The additional and diverse guidance I received sheltered my spark for research, for which I am grateful.

Further thank goes to all my peers that helped me with their comments and suggestions. I am grateful to have spent my time at the university among many inspiring fellow Ph.D. students, where different generations came and went. Special thank goes to Tamara Bischof and Jonas Meier for sharing their experience and setting an example for a young economist, Martina Pons for her honest remarks, Frederic Kluser for his enthusiasm, and

Moritz Weik for keeping the mood light. I also want to express my gratitude to the Secretariat and the Dean's office. Not only did they support me in all organizational affairs and other circumstances. Fiona Scheidegger, Kathrin Balmer, Gabriella Winistörfer, and Patrizia Vernon helped me in all aspects in the beginning as the Student Advisor in Economics, for which my only qualification was to have spent a long time studying in Bern.

This thesis would not have been possible without my family and friends. My parents made it possible that I could always do what inspires me, and thanks to my older brother Fabio, I was always ahead on my way. Their love and support, together with my friends who have accompanied me all those years, made me who I am today.

My final and most profound thank goes to Selina. You have critically reflected on my work and arguments time and time again, have supported me when I needed it, and helped me to put everything into perspective. Thank you for all you have provided me with and for always being by my side.

Bern, July 2023 *Dino Collalti*

Contents

List of Figures

List of Tables

Introduction

The scientific evidence decisively attributes natural hazards' increasing intensity and frequency to global warming. The Synthesis Report of the 6^{th} IPCC Assessment Report, which has just been finalized in March 2023, states:

In the near term, every region in the world is projected to face further increases in climate hazards (medium to high confidence, depending on region and hazard), increasing multiple risks to ecosystems and humans (very high confidence).

These risks of climate hazards include heat-related human mortality, biodiversity loss, and the spread of diseases, to name a few. Concerning the hazards themselves, floods, landslides, and water availability have the potential to lead to severe consequences for people, infrastructure, and the economy. Their study is highly relevant because climate hazards constitute a causal channel through which anthropogenic climate change influences the economy. For instance, estimates of their social and economic costs provide evidence for setting the social cost of carbon emissions. Given the projections from the natural sciences, it is striking that the discipline of economics has made little effort to assess the economic impact of many hazards.

This thesis comprises four papers investigating the economic impacts of floods from extreme rainfall in Central America and the Caribbean. Chapter One provides empirical evidence that a non-negligible part of hurricanes' direct damages can be attributed to extreme rainfall. Chapter Two then shifts the focus from large-scale hurricanes to small-scale flash floods. It develops a statistical method to detect potential flash flood events from satellite rainfall data. In Chapters Three and Four, I then use this method

to study the economic impacts of flash floods consistently across Central America and the Caribbean. Specifically, Chapter Three looks at the dynamics in night light activity following a flood, whereas Chapter Four analyzes the flood's impact on establishments.

In the first chapter of my thesis, co-authored with Eric Strobl and published in *Natural Hazards*, we revisit the common notion of modeling the impacts of hurricanes solely via their local wind speed. In recent years, some of the most destructive hurricanes, such as Morakot in Taiwan 2009, Harvey in Texas 2017, and Idai in Mozambique 2019, are characterized not by particularly strong wind but by a tremendous amount of rainfall. Relying on a model and a damage function that ignores rainfall and subsequent flooding is thus bound to yield biased results. Furthermore, there is a consensus that rainfall-heavy hurricanes will likely become more common with global warming (Grossmann and Morgan, 2011; Walsh et al., 2016; Knutson et al., 2019). A priori, it is not clear how to best assess the rainfall flood risk and relate it to damages. For instance, adequate rainfall measurements at a high spatial resolution during a hurricane are generally unavailable.

To this end, we link remote sensing precipitation data to regional damage data for five hurricanes in Jamaica from 2001 to 2012. We find that the maximum rainfall intensity during a hurricane in a region is a significant determinant of economic damages, explaining much of the variation. Next, we use extreme value modeling of precipitation and combine the return periods with an estimated damage function and satellite-derived night light intensity to assess the local risk in monetary terms. This allows us to quantify the monetary risk for different horizons. For instance, the damage risk for a 20-year rainfall event in Jamaica is estimated to be at least 238 million USD, i.e., about 1.5% of Jamaica's yearly GDP.

In my second chapter, co-authored with Nekeisha Spencer and Eric Strobl, we set out to study the rainfall conditions that trigger floods, particularly flash floods. These are a type of highly localized flood that is directly caused by short but intense episodes of rainfall (Borga et al., 2007). Compared to river floods that require catchment-type hydrological modeling, they can occur almost anywhere given intense rainfall and are, as such, one of

the most common natural hazards.[1] The Caribbean is especially at risk from flash floods since urbanization is often unregulated and soil degradation common such that excess rainfall can not run off quickly (Gencer, 2013; Pinos and Quesada-Román, 2021).

We set out to assess rainfall characteristics of previous flash flood events to create a classification method above what threshold a rainfall event likely causes a flash flood. For this, we gather information on all 93 confirmed flash floods in Jamaica from 2001 to 2018. We link these to remote sensing precipitation data, with which we further construct the location-specific yearly maximum rainfall events. By employing the copula method to create intensity-duration-frequency (IDF) curves, we model the intensity and duration of the annual maximum events separately and flexibly from their respective marginal distribution. The estimated Normal copula has Weibull and generalized extreme value (GEV) marginals for duration and intensity, respectively. The parametric IDF curve with an associated return period of $2\frac{1}{6}$ years is then the optimal threshold for flash flood event classification. The simple nature of connecting the copula method for IDF curves with a classification for flash floods potentially opens up many applications in parametric insurance programs, regional risk mapping, and hazard warning systems.

I then investigate the local dynamic economic response after a flash flood in the third chapter. The idea that a natural disaster influences economic performance and organization not only on impact but over time has entertained several empirical studies that try to estimate these. These include the study of tropical storms (Nordhaus, 2010; Strobl, 2012; Hsiang and Jina, 2014), earthquakes (Barone and Mocetti, 2014; Fabian, Lessmann, and Sofke, 2019), droughts (Barrios, Bertinelli, and Strobl, 2010; Hornbeck, 2012) and floods (Loayza et al., 2012; Kocornik-Mina et al., 2020). The studies on floods focus on large-scale disasters and reports in global databases that neglect localized flash flood events. Conceptually, a natural hazard causes destruction upon impact that might depress local economic activity, cause its re-location or spur innovation and growth in the future. Given the high frequency of extreme rainfall events in many developing countries, they

[1] For instance, according to the Centre for Research on the Epidemiology of Disasters (CRED) Emergency Events Database (EM-DAT), the number of affected people in 2022 by flash floods (0.9 M) is significantly more than river floods (0.1 M) or forest fires (0.03 M).

could be a primary mechanism for how climate and environmental degradation impacts their economic development.

I employ the method from Chapter Two to construct a high-resolution physically based indicator of flash flood occurrence for Central America and the Caribbean. With that, I estimate the local economic response to an event via changes in local night light emissions from satellite data. After accounting for tropical cyclone activity, flash floods have a delayed, short-term negative effect on economic activity. In countries with a low to medium human development index (HDI), the average effect can be up to -5.7%. Back-of-the-envelope calculations suggest that, due to their high frequency, flash floods in these countries cause GDP growth to fall by -0.84 percentage points. Countries with higher development appear to be only marginally affected. I also find evidence for negative spatial spillovers from floods in neighboring locations.

In my fourth chapter, I shift my focus from the dynamic perspective to the economic agents. With a limited capacity to adapt to climate change, it is important to study the mechanisms through which climate change affects the economy to guide policymakers (Mendelsohn, 2012). In the case of flash floods, such mechanisms likely include local establishments as the main economic agents.

I again use the method from Chapter Two and link the indicator of flash flood occurrence to the Worldbank Enterprise Surveys for Central America and the Caribbean. They uniquely provide a large number of consistent, geo-located surveys across the study region. After controlling for the location-specific extreme rainfall history, I find that a flash flood significantly decreases sales and the number of employees but increases capital productivity. The negative effects are driven by establishments for which financial market access is an obstacle, whereas the increased capital productivity occurs in establishments with sufficient financial market access. Flash floods similarly affect different industries, with the notable exception of the construction sector. The construction sector is not negatively affected in terms of output and employment. My results suggest that flash floods

negatively impact firms and that their increase due to global warming will likely influence economic activity. Improving financial market access appears to be an effective adaptation strategy to increase establishments' resilience.

Chapter 1

Economic Damages due to Extreme Precipitation during Tropical Storms: Evidence from Jamaica

joint with Eric A. Strobl

"*We are not an endangered species ourselves yet, but this is not for lack of trying*."

Douglas Adams, Last Chance to See

Acknowledgments: This chapter has been published as Collalti and Strobl (2022). We would like to thank the editors, two anonymous reviewers, and attendees of the EAERE 2021 (Berlin, Online), as well as seminar participants at the University of Bern, for their valuable comments. Special thanks go to Jeanne Tschopp for her input at an early stage of the manuscript that helped mature the work. This research did not receive any specific grant from funding agencies in the public, commercial, or not-for-profit sectors.

1.1 Introduction

Tropical cyclones (TCs) are among the most destructive natural disasters, estimated to have caused over 800 USD billion in damages globally over the last 20 years.[1] Damages attributable to these storms are mainly due to three factors, namely extreme wind, storm surge, and torrential rainfall (Bakkensen, Park, and Sarkar, 2018; Park, van de Lindt, and Li, 2013; Lin et al., 2010). The literature modeling the economic impact has, however, mainly focused on damages as a result of wind and to a lesser extent storm surge (Emanuel, 2005; Nordhaus, 2006; Hu et al., 2016; Baradaranshoraka et al., 2017; Masoomi et al., 2019; Hatzikyriakou and Lin, 2018; Do, van de Lindt, and Cox, 2020), due to the difficulties associated with large scale flood modeling as a result of extreme precipitation (Murnane and Elsner, 2012; Zhai and Jiang, 2014). This is often justified on the grounds that wind is strongly correlated with rainfall during a TC and thus that wind exposure will capture damages due to rainfall as well. However, recent evidence suggests that rainfall is not absolutely dependent on TC intensity, *"...suggesting that stronger TCs do not have systematically higher maximum rain rates than weaker storms."* (Yu et al., 2017). It has also been shown that the positive correlation between wind speed and rainfall may only be true over the ocean and not on land (Jiang et al., 2008).

The failure to take account of extreme precipitation in damage estimation arguably neglects an important driver of the economic costs due to TCs (Czajkowski, Simmons, and Sutter, 2011; Rezapour and Baldock, 2014; Rappaport, 2014; Park et al., 2015; Bakkensen, Park, and Sarkar, 2018). For instance, available data for the Caribbean suggest that rainfall is either the primary or secondary cause of damages in 75% of TC events.[2] While the influence of anthropogenic climate change on TC frequency, general intensity, and affected areas is still a matter of debate, there is a general consensus that rainfall-heavy TCs will likely become more frequent in the future (Emanuel, 2013; Knutson et al., 2019; Van Oldenborgh et al., 2017; Villarini et al., 2014b; Grossmann and Morgan, 2011; Walsh et al., 2016). Nevertheless, the link between extreme rainfall and economic damages

[1] Authors' own calculation using EMDAT database.
[2] Authors' own calculations using the EMDAT database on damages due to natural disasters.

is not well understood yet (Villarini et al., 2014a; Rosenzweig et al., 2018; Rözer et al., 2019). While non-hazard measures such as risk awareness, building type, and topography are important aspects, the most influential determinants for whether a building is damaged by flooding are local water depth and accumulated rainfall (Spekkers et al., 2013; Van Ootegem et al., 2015, 2018; Rözer et al., 2019). At the same time, short-duration and high-intensity rainfall have been shown to be a major factor for the occurrence of landslides (Dou et al., 2019). Case studies have demonstrated that hazard scales that include rainfall in addition to wind speed are able to better predict the cost of TCs (Rezapour and Baldock, 2014) and that wind-only damage functions systematically underestimate damages by rainfall-heavy typhoons in the Philippines (Eberenz, Lüthi, and Bresch, 2021).

The current study explicitly focuses on estimating the damage and risk associated with extreme precipitation during TCs, using Jamaica as a case study. Jamaica is arguably a particularly interesting setting for this purpose since the island is frequently afflicted by TCs. Excess rainfall is a major cause of destruction by inducing flash floods and landslides (Laing, 2004). Moreover, due to the absence of large rivers and the volcanic origin of many hill-slopes, such floods and landslides are common throughout most of the island (Miller, Brewer, and Harris, 2009). This allows the exploitation of spatial variation in rainfall intensity during TCs for the estimation of a rainfall-based damage function.

Importantly, the Planning Institute of Jamaica (PIOJ) has compiled consistent and detailed damage reports for most storms since the turn of the century. The lack of consistently reported damages often introduces additional uncertainty (Bakkensen, Shi, and Zurita, 2018). Here, reports for five major TCs over the period of 2001-2012 are used to construct parish-level information on economic damages.[3] Given that excess rainfall damages during TCs are often due to short, high-intensity events (Larsen and Simon, 1993), These damage data are coupled with high resolution, high-frequency remote sensing precipitation data from the Global Precipitation Measurement Mission (Huffman et al., 2015a; Hou et al., 2014). Remote sensing information like the Tropical Rainfall

[3]Parish is the main administrative regional breakdown of Jamaica.

Measuring Mission (TRMM) has been used extensively for the monitoring of TCs (Lonfat, Marks Jr, and Chen, 2004; Chen, Knaff, and Marks Jr, 2006; Lau, Zhou, and Wu, 2008; Hendricks et al., 2010; Jiang, Liu, and Zipser, 2011; Villarini et al., 2011; Hence and Houze Jr, 2011; Matyas and Silva, 2013).

Using our data, we estimate a precipitation-dependent damage function via regression analysis while controlling for the maximum wind speed during the storm. We then employ the precipitation data to generate return level maps using an extreme value model in the spirit of Demirdjian, Zhou, and Huffman (2018). Such a statistical approach has been shown to model extreme rainfall risk well in several case studies (Sugahara, Da Rocha, and Silveira, 2009; Beguería et al., 2011; Tramblay et al., 2013). In conjunction with the estimated damage function and a proxy of the economic activity distribution derived from remote sensing night light intensity, information on the severity of a rainfall event occurring with a certain probability yields risk maps of economic damages due to extreme rainfall in Jamaica. The outlined method does not rely on large-scale hydrological models and should easily extend to other regions where gauge-based precipitation data is scarce.

The remainder of the paper is organized as follows: Section 1.2 presents the study region and describes the data. Section 1.3 details the methodology. Section 1.4 presents results, while section 1.5 discusses the findings. Finally, Section 1.6 concludes.

1.2 Study Region & Data

1.2.1 Study Region

Jamaica is an island country situated in the Caribbean and is the third-largest island of the Greater Antilles after Cuba and Hispaniola. With a population of 2.9 M (World Bank Group, 2020), Jamaica is one of the larger states in the region and is ranked as a high-development country by the UN human development index (Conceição, 2019). Jamaica consists of 14 parishes, which is the highest regional administrative unit for the island. The country's economy is mixed but increasingly based on tourism and finance while the export of agricultural commodities is declining (Johnston and Montecino, 2012). Jamaica

has two major cities, the capital Kingston in the southeast and Montego Bay in the northwest, known for its tourism. The islands' geography is dominated by its central high plains and mountains. The Blue Mountains in the east, famous for their coffee plantations, constitute Jamaica's highest point at 2.256 m. Jamaica is highly exposed to natural disasters such as TCs, earthquakes, and droughts (Carby, 2018). Between 1988 and 2012, 11 named storms made landfall in Jamaica and caused severe destruction (The World Bank Group, 2018). The climate in Jamaica is tropical with little seasonality in temperature. However, due to the northeast trade winds, the period from November to March is dry, and the rainy season lasts from April to October. The highest rainfall on the island occurs in the east, the northeastern coast averaging more than 400 mm a year. Near the peak of the Blue Mountains, the average is more than 625 mm a year (Nkemdirim, 1979). A summary of the data subsequently presented is given in Table 1.1.

TABLE 1.1: Data Summary

	Precipitation	Damages	Night Light	Wind
unit	mm/h	M USD	-	km/h
spatial	$0.1° \times 0.1°$	by parish	$30'' \times 30''$	$0.1° \times 0.1°$
temporal	1/2-hourly	by storm	monthly	hourly
source	GPM	PIOJ	DMSP/OLS	HURDAT
maximum	120	63.31	63	268.54
minimum	0	0.20	0	5.7
mean	0.04	15.84	9.87	59.3
st. dev.	0.72	13.65	10.69	51.24

Notes: Summary Statistics of data. The night light data does not have a specific measurement unit but is the average of the visible band digital values ranging from 0 to 63.

1.2.2 Damages

The Planning Institute of Jamaica (PIOJ) has produced consistent socio-economic damage reports after damaging tropical storms since Hurricane Michelle in October 2001. In this regard, the PIOJ follows the United Nations Economic Commission for Latin America and the Caribbean (UNECLAC) Damage and Loss Assessment (DaLA) methodology

(Bradshaw, 2003). Each report contains a precise description of the event, preliminary rainfall reports, a description of social trauma, emergency actions, and an assessment of economic damages. The assessment of economic damages considers damages in terms of three 'sectors', namely, agriculture (crop and livestock), public infrastructure (roads, schools, and others), and housing. Since not all reports provide this information at the parish level, the analysis in this study is restricted to events for which there is such a regional breakdown, i.e., five storms: Hurricane Michelle 2001, Hurricane Dean 2007, Hurricane Gustav 2008, Tropical Storm Nicole 2010 and Hurricane Sandy 2012. Additionally, even when there is regional information, in some reports not all three of the main sectors are necessarily covered sub-nationally. Table 1.2 shows which sectoral damages have been reported by the parish. When not all three sectors are covered sub-nationally, the damage measure was calculated as the proportion of damages with data at the parish level and scaled to total reported damages (including countrywide aggregates). For instance, during Hurricane Sandy in 2012, 25% ($3.7 M) of the damage to agriculture occurred in the parish of Portland, and 30% (5,190) of all damaged houses were located there. Thus, it was assumed that Portland accounted for 27.5% or 29.4 M USD of the estimated total damage of 106.6 M USD across all three sectors. One should note that in most reports the parish of Kingston is counted together with the parish of St. Andrew due to its small size and their proximity, leaving 13 distinct regions for the analysis. The per parish damages originally reported in USD are inflation-adjusted with the Federal Reserve Economic Data (FRED) consumer price index (U.S. Bureau of Labor Statistics, 2019, CPI), normalized to February 1st 2020 values. The data from the PIOJ reports for 13 Jamaican parishes and 5 TCs provide a total of 65 regional-level damage observations.

1.2.3 Precipitation

The source for precipitation data is version 06B of the Global Precipitation Measurement (GPM) Integrated Multi-satellitE Retrievals (IMERG), a satellite-based estimate (Huffman et al., 2015b). The satellite precipitation algorithm combines various microwave and infrared precipitation measurements to produce precipitation estimates, adjusted with

TABLE 1.2: Damage Data Availability

	Agricultural	Road Network	Housing	Schools
Hurricane Michelle 2001	✓	✓		
Hurricane Dean 2007	✓	✓	✓	✓
Storm Gustav 2008	✓	✓	✓	
Storm Nicole 2010	✓	✓	✓	
Hurricane Sandy 2012	✓		✓	

Notes: Overview of parish damage data availability for different tropical storms.

surface gauge data. The resulting product is a half-hourly data set with near-global coverage at a $0.1^\circ \times 0.1^\circ$ resolution for the sample period 01. June 2000 - 31. May 2019. The data has been pre-processed according to the accompanying tech report (Huffman et al., 2020). One should note that the GPM's predecessor, the Tropical Rainfall Measuring Mission (Huffman et al., 2007, TRMM), has been regularly used in the context of extreme value modeling in meteorology (Furrer and Katz, 2008; Demirdjian, Zhou, and Huffman, 2018) and hydrology (Collischonn, Collischonn, and Tucci, 2008; Li, Zhang, and Xu, 2012).

1.2.4 Storm Tracks

Information on the TCs in our analysis comes from the HURDAT Best Track Data (Landsea and Franklin, 2013). The data provides six hourly observations on all tropical cyclones in the North Atlantic Basin, including the position of the eye and the maximum wind speed of the storm. Additional information on the spatial extent of the TCs is taken from the Extended Best Track Dataset (Demuth, DeMaria, and Knaff, 2006).

1.2.5 Night Lights

The economic exposure to extreme precipitation during a TC is unlikely to be evenly distributed even within a parish. Ideally, this should be taken into account when estimating a damage function using parish-level damages. Given the lack of localized economic data from official statistical sources, night light intensity is often instead used as an alternative proxy (Chen and Nordhaus, 2011; Elliott, Strobl, and Sun, 2015). To this end, gridded

night light activity data from the Defense Meteorological Satellite Program (DMSP) Operational Linescan System (OLS) is used. The DMSP-OLS is available monthly at a high resolution of $30'' \times 30''$ (approx. 1 km $\times$ 1 km). Since the night light data is at a higher resolution than the GPM and damage data, the former is employed to aggregate the latter.[4]

1.3 Methodology

1.3.1 Framework

The risk of natural disasters consists of a combination of multiple factors (Peduzzi et al., 2012): the hazard itself (frequency and intensity), exposure (economic value, number of people), and vulnerability (the degree of loss given a hazard). Few attempts have been made to incorporate extreme rainfall into the TC damage function. Li, Fang, and Duan (2019) define a precipitation intensity index analog to the commonly used wind speed based power dissipation index. However, they do not derive or validate this functional form. Bakkensen, Park, and Sarkar (2018) utilizes the natural logarithm of maximum TC lifetime-rainfall of any weather station in a province, analog to their use of the natural logarithm of maximum wind speed anywhere in the province. While both approaches highlight the importance of rainfall as a potential source of TC damages, they mimic their functional form of max. wind speed. Our approach is to first construct parish-level wind and rainfall measures by TC, taking local exposure into account via the use of night light intensity measures. These measures are then combined with the parish-level damage reports to estimate a precipitation-specific damage function. The coefficient estimates, and an extreme value analysis of precipitation are then combined to create spatial risk maps for Jamaica.

[4]For instance, the parish-level damage data requires parish-level rainfall data. The GPM precipitation measurements do not naturally match the parish borders. Thus, the DMSP-OLS night light acts as an intermediary in aggregating the GPM to the parish data.

1.3.2 Rainfall Damage Function

Windfield Model

Following Strobl (2011) in calculating the local wind exposure during a storm, the Boose, Serrano, and Foster (2004) version of the well-known Holland (1980) wind field model is utilized. The model estimates the location-specific wind speed by taking into account the maximum sustained wind velocity anywhere in the storm, the forward path of the storm, the transition speed of the storm, the radius of maximum winds, and the radial distance to the storm's eye. The model further adjusts for gust factor, surface friction, asymmetry due to the forward motion of the storm, and the shape of the wind profile curve. The source of storm data used is the HURDAT Best Track Data (Landsea and Franklin, 2013). These 6-hourly track data are linearly interpolated to hourly observations. $WIND_{cst}$, the wind experienced at any point c, during storm s at time t is given by:

$$WIND_{cst} = GD\left[V_{mst} - S\left(1 - \sin(T_{cst})\right)\frac{V_{hst}}{2}\right] \times \left[\left(\frac{R_{mst}}{R_{cst}}\right)^{B_{st}} \exp\left\{1 - \left[\frac{R_{mst}}{R_{cst}}\right]^{B_{st}}\right\}\right]^{1/2} \tag{1.1}$$

where V_{mst} is the maximum sustained wind velocity anywhere in the storm, T_{cst} is the clockwise angle between the forward path of the storm and a radial line from the storm center to the c-th pixel of interest, V_{hst} is the forward velocity of the TC, R_{mst} is the radius of maximum winds, and R_{cst} is the radial distance from the center of the storm to point c. The remaining ingredients in Equation (1.1) consist of the gust factor G and the scaling parameters D for surface friction, S for the asymmetry due to the forward motion of the storm, and B, for the shape of the wind profile curve. Points c are set equal to the centroid coordinates of the GPM rainfall data and the storm-wise maximum wind speed for point c is given by $MWIND_{cs}$. Appendix A.2 provides additional information on the model parameters.

Rainfall

Rainfall measures for the five storms are obtained for every GPM cell whose centroid is within the storm's reach at a certain observational time.[5] This is judged by comparing the radius of the outermost closed isobar provided by the Extended Best Track Dataset (Demuth, DeMaria, and Knaff, 2006) with the distance to the storm's eye. If the distance of a GPM cell's centroid to the storm's eye is smaller than the radius of the outermost closed isobar, that cell is currently affected by the storm. The Extended Best Track Dataset provides 6-hourly observations which we linearly interpolate to match the half-hourly GPM precipitation measurements. Then, all rainfall observations $RAIN_{cst}$ can be summarized as the total rainfall $SRAIN_{cs}$ or maximum rainfall during that storm, $MRAIN_{cs}$. These two statistics are the extremes for describing the full distribution of $RAIN_{cst}$.

Parish Aggregation

The remote sensing information of rainfall and thus the calculated wind speed does not match the parish borders.[6] The monetary damages are, however, reported on the parish level. An intuitive way to aggregate rain and wind is to weigh the cells by the share of night light activity in that cell relative to total parish night lights. The grid of the night light activity is approx. $100\times$ finer compared to the rainfall and wind speed grid. This allows one to down-weight cells that lie not entirely within a parish if weighted only by the within parish night light activity. It further controls for the value at risk of areas with more night light activity compared to areas that are unlit at night, e.g., large population centers. Cells are only added to the sum when their centroid lies within the parish. Specifically, j denotes a $30'' \times 30''$ night light activity cell and w_{js} the associated 3-month mean night light intensity prior to storm s and c is a $0.1^\circ \times 0.1^\circ$ rainfall or wind speed cell.[7] The night light weight is the fraction of the sum of night light activity in cell c that lies in parish i, divided by the total night light activity in parish i,

[5] Even though many studies focus on landfalling TCs only, it has been shown that non-landfalling TCs can be equally destructive (López-Marrero and Castro-Rivera, 2019).

[6] The data of rainfall and wind speed is on a $0.1^\circ \times 0.1^\circ$ grid.

[7] Note that many night light cells j are in one rainfall (wind) cell c and many such cells c are in one parish i.

$$W_{csi} = \frac{\sum_{j \in c | j \in i} w_{js}}{\sum_{j \in i} w_{js}}, \quad W_{csi} \in (0,1). \tag{1.2}$$

With these weights, the gridded data can be aggregated to the parish level:

$$SRAIN_{is} = \sum_{c \in i} \Big(SRAIN_{cs} \times W_{csi} \Big), \tag{1.3}$$

$$MRAIN_{is} = \sum_{c \in i} \Big(MRAIN_{cs} \times W_{csi} \Big), \tag{1.4}$$

$$MWIND_{is} = \sum_{c \in i} \Big(MWIND_{cs} \times W_{csi} \Big), \tag{1.5}$$

where $SRAIN_{is}$ and $MRAIN_{is}$ are the parish i, storm s total and maximum rainfall and $MWIND_{is}$ the respective maximum wind measure.

Damage Function Regression

The functional form which is assumed for the damage function has to be imposed in the regression. In this regard, it is well established that the destruction of TCs relates roughly to the cube of the maximum wind speed (Emanuel, 2005). It is used as a control for tropical storms' power dissipation (Bertinelli and Strobl, 2013). A priori, it's unclear whether the maximum rainfall during a TC or the total rainfall adequately represents the effect of heavy rainfall during a TC. It follows that both measures should be included. Additionally, differences in parish economic endowment and thus potential damage is accounted for by parish indicators. The linear regression is then given by

$$\begin{aligned} DAMAGES_{is} = \alpha + \beta_1 MRAIN_{is} + \beta_2 SRAIN_{is} \\ + \beta_3 MWIND^3{}_{is} + \gamma PARISH_i + \varepsilon_{is}. \end{aligned} \tag{1.6}$$

where $DAMAGES_{is}$ are the reported monetary damages, $MRAIN_{is}$ the maximum

hourly rainfall in a parish, $SRAIN_{is}$ the sum of total rainfall, ${MWIND^3}_{is}$ is the cube of the maximum wind speed and $PARISH_i$ are indicator variables for parish i.[8] Potentially, other functional forms like polynomials or non-linear models might provide a better fit to the data. Given the small sample size (n=65), more evolved models could overfit.[9] Estimates obtained with an ordinary least squares regression of Equation 1.6 are likely to generalize well and are interpretable.

We run several alternative specifications of Equation 1.6. In Equation 1.7 we use parish population POP_i measured by Jamaica's 2011 census to control for local economic endowment (Statistical Institute of Jamaica, 2011) instead of parish indicators. This has the advantage of leaving more degrees of freedom for the model estimation. Robustness to outliers drives our results by omitting extreme observations as determined by Cook's distance (Cook, 1977).[10] The data without outliers are then used to estimate Equation 1.7.

$$DAMAGES_{is} = \alpha + \beta_1 MRAIN_{is} + \beta_3 {MWIND^3}_{is} + \delta POP_i + \varepsilon_{is}. \tag{1.7}$$

1.3.3 Extreme Value Modelling

The objective of statistical extreme value analysis (EVA) is to quantify the tail behavior of a process, for instance, extreme rainfall occurring at a certain location. Such an EVA can be categorized into either a block maxima or a peaks-over-threshold approach. Both allow us to fit a distribution to the extreme values of any sequence of i.i.d. random variables but differ in how they make use of the available information. The half-hourly

[8] This corresponds to a parish fixed effects model. The inclusion of binary indicator variables results in group (parish) fixed means. This allows for heterogeneity in the mean damage of a parish for different storms.

[9] A model overfits if it captures residual variation (noise) that is not part of the data-generating process. Such a model would not predict future observations reliably.

[10] We define observation as an outlier if it is $6\times$ more influential than the average observation.

time series X_i of rainfall in mm/h of GPM cell i with 333'072 observations from June 2000 to May 2019 are the subject of this EVA. Extreme rainfall in Jamaica often happens during TCs which occur 10-17 times in the Atlantic basin (NOAA, 2019), not all affecting Jamaica. Due to this irregular pattern, a peak-over-threshold approach appropriately represents the physical phenomenon while making better use of the available information. The peaks-over-threshold approach is based on the Pickands–Balkema–de Haan theorem stating that threshold excesses $y = (X - u|X > u)$ have a corresponding generalized Pareto distribution (GPD) if the threshold u is sufficiently high (Coles et al., 2001, p. 75):

$$GPD(y) = \begin{cases} 1 - \left[1 + \xi \left(\frac{y}{\tilde{\sigma}}\right)\right]^{-\frac{1}{\xi}} & \text{for } \xi \neq 0, \\ 1 - \exp\left(-\frac{y}{\tilde{\sigma}}\right) & \text{for } \xi = 0, \end{cases} \tag{1.8}$$

$$\text{where} \quad \tilde{\sigma} = \sigma + \xi(u - \mu). \tag{1.9}$$

The parameters of the GPD distribution are location μ, scale σ and shape ξ. Here, a Poisson point-process (PPP) representation of threshold excesses is used, which allows one to a) directly estimate the likelihood function in terms of location μ, scale σ and shape ξ parameter, b) model non-stationarity in these parameters, and c) include the Poisson distributed threshold exceedance rate together with the threshold excesses in the inference. The EVA is carried out on the cell level by separately estimating $GPD(y_i)$ as in Equation 1.8 where $y_i = (X_i - u_i|X_i > u_i)$ are the threshold excess of GPM cell i. The vector X_i contains the GPM rainfall measurements of cell i and u_i is the cell-specific threshold derived in subsection 1.3.3. Estimation is carried out via the *extRemes* library in *R* (Gilleland and Katz, 2016).

Threshold Selection

The selection of an appropriate threshold above which an observation is considered extreme is a classical case of the bias-variance trade-off. Too low a threshold violates the

underlying asymptotic basis and leads to bias, while too high a threshold discharges valid observations resulting in an unnecessarily high variance. A plethora of competing threshold selection techniques exist (Scarrott and MacDonald, 2012). The traditional procedure is graphical via mean residual life plot (Davison and Smith, 1990, MRL) which is subjective and becomes quickly infeasible for a large number of time series. An alternative by Northrop, Attalides, and Jonathan (2017) proposes the use of Bayesian cross-validation, comparing thresholds based on their predictive ability at extreme levels. This method scales well while directly addressing the desired property for a threshold - if the threshold is too low, threshold excesses will not follow a GPD and predictions will be off. For this study the size of the posterior sample simulated at each threshold is set to be 50'000 and 100 different thresholds are considered for the estimation of the quality of predictive inference. The training thresholds correspond to the 0.95 - 0.9995 quantiles at each GPM cell in increments of 0.0005.

Dependence

Rainfall tends to occur in temporal clusters, violating the independence assumption necessary for extreme value modeling. To overcome the issue of temporal dependence, the common method of declustering is implemented (Demirdjian, Zhou, and Huffman, 2018; Gilleland and Katz, 2006). The time series are declustered cell-wise such that the resulting series are near-independent if the observations are sufficiently distant in time. Such a series will have a dependence structure with no effect on the limit laws for extremes. This "runs" declustering algorithm requires first some threshold u where the values below are not considered extreme (Coles et al., 2001). Second, it starts a cluster at every first entry v with $v > u$ which runs until r consecutive observations are below u. Third, only the cluster maxima are retained, and all other observations are rendered to zero. The same declustering scheme as in Demirdjian, Zhou, and Huffman (2018) is adopted, with a threshold equal to the 99-th percentile and $r = 5$.

Non-Stationarity

The Pickands-Balkema-de Haan theorem requires the extreme values to be i.i.d. random variables which implies stationarity. Rainfall observations constitute by their very nature a non-stationary process. The PPP representation enables one to incorporate non-stationarity in the GPD parameters. In this regard, a first-order sinusoidal function of the day of the year in the location μ and scale parameters σ is allowed, analogous to Demirdjian, Zhou, and Huffman (2018).[11] Additionally, a binary variable $STORM_{ct}$ for cell c at time t is included to allow for a different distribution of rainfall observations that are within the spatial extent of a TC:

$$\mu_c(t) = \mu_{0c} + \mu_{1c} STORM_{ct} + \mu_{2c}\left[\sin\left(\frac{2\pi t}{365.25}\right)\right] + \mu_{3c}\left[\cos\left(\frac{2\pi t}{365.25}\right)\right] \tag{1.10}$$

$$\log\left[\sigma_c(t)\right] = \sigma_{0c} + \sigma_{1c} STORM_{ct} + \sigma_{2c}\left[\sin\left(\frac{2\pi t}{365.25}\right)\right] + \sigma_{3c}\left[\cos\left(\frac{2\pi t}{365.25}\right)\right]. \tag{1.11}$$

Note that for calculating return levels of a non-stationary EV model, one has to assume values for the non-stationary parameters. Here, this is done by fixing the day of the year t and storm dummy $STORM_{ct}$. The day of the year t is assumed to be $t = 0$ and not to influence multi-year return levels. Jamaica is on average for around 3% of the year within the outermost closed isobar of a TC. Thus we assume that the frequency of TCs stays the same and set the storm dummy $STORM_{ct}$ parameter equal to the sample probability $\Pr[STORM_c = 1] \approx 0.03$ for the calculation of the return levels.

1.3.4 Monetary Return Levels

The estimated return levels can be used in the damage function to obtain the n year extreme rainfall return level in monetary terms. The location of economic endowment also plays a role in the monetary risk. Average night light activity W_{ci} serves as the weight for economic endowment, analogously to Equation 1.3, where it was employed

[11] We refrain from modeling non-stationarity in the shape parameter, as it is customary in the literature.

to obtain rainfall by parish per storm.[12] Projected parish i damage for a return period of r is then given by

$$PDAMAGES_{ir} = \beta \times \sum_{c \in i} (RAIN_{cr} \times W_{ci}), \tag{1.12}$$

where $RAIN_{cr}$ is the estimated rainfall return level in cell c and β the coefficient of rainfall from the damage function estimation. $PDAMAGES_{ir}$ is the projected extreme rainfall damage during TCs in parish i that is expected to occur every r years. These parish-level estimates can then be aggregated to the country level and compared to Jamaica's GDP.

1.4 Results

1.4.1 Damage Function

Table 1.3 shows the mean damages, rainfall, and wind speed per storm across parishes, whereas appendix A.1 shows the damages by storm and parish. Hurricane Dean 2007 is associated with the strongest winds, while Storm Nicole 2010 brought the heaviest rainfall to Jamaica. These two storms were also the most damaging of the five storms. Figure 1.1 displays the co-occurrence of rainfall, wind speed, night light activity and damages of Hurricane Sandy. Both rainfall and wind are strongest in the northeast. The heaviest rainfall has been observed slightly more inland compared to wind speed, which peaked at the coast. While there is a strong relationship between the two, it is evident that these are two distinct physical phenomena with distinct spatial distributions. The map depicting night lights clearly outlines the capital city of Kingston as the largest convolution of night lights. A comparison with the map of damages suggests that parishes that undergo severe economic damages are also those with more night light activity, high winds, and much rainfall.

[12] W_{ci} here is the average night light activity for the period 2001 - 2013 as opposed to the storm-specific night light activity W_{csi} in Equation 1.2. Specifically, W_{ci} is calculated as $W_{ci} = \frac{\sum_{j \in c | j \in i} w_j}{\sum_{j \in i} w_j}$, $W_{ci} \in (0,1)$ with $w_j = \frac{1}{|T|} \sum_{t \in T} w_{j,t}$ being the average night light activity in night light cell j.

TABLE 1.3: Statistics per Storm

	Damage	Max. Rain	Total Rain	Max. Wind
Michelle 2001	5.17	7.75	23.32	61.96
Dean 2007	31.99	18.33	48.45	195.19
Gustav 2008	19.50	13.99	62.26	72.14
Nicole 2010	21.87	40.49	112.91	18.25
Sandy 2012	10.83	22.96	85.82	83.33

Notes: Per storm mean parish value for variables of interest.

Regression Results

Estimates of the regression specified in section 1.3.2 are displayed in Table 1.4. Baseline regression (1) (given by Equation 1.6) shows max. wind speed to be a significant predictor of parish-level damages while both maximum and total rainfall are insignificant. Since the latter two are highly collinear[13] we consider them separately by estimating Equation 1.6 without either $MRAIN_{is}$ or $SRAIN_{is}$ in columns (2) and (3), respectively. Accordingly, total rainfall during a storm is an imprecise predictor of damages. Maximum rainfall in regression (3), in contrast, is a statistically significant (10%-level) determinant of damages. Switching from parish fixed effects, which reduce the degrees of freedom considerably, to alternatively including parish population as in Equation 1.7 for regression (4) yields virtually the same result. Furthermore, results do not change significantly in regression (5), based on the same Equation 1.7 but without outliers as defined by Cook's Distance. The R^2 and adjusted R^2 is higher in models (1)-(3) compared to (4) and (5).[14] Since there are twelve parish indicators compared to one variable for population, the R^2 is expected to fall. The adjusted R^2 takes this change in degrees of freedom into account - one would thus expect that the adjusted R^2 in (4) and (5) should not be lower than in (1)-(3). This is not the case. Likely, the parish indicators contain more information than just the population number, and thus a model that contains these indicators

[13]The linear correlation coefficient is 0.9, and Spearman's rank correlation is 0.89. Note that the other variables are nearly independent. Pearson's correlation coefficient is -0.07 between max. wind speed and max. rainfall, 0.05 between max. wind speed and population and 0.11 between max. rainfall and population. Thus, we do not expect to have issues with collinearity besides the one already mentioned.

[14]The R^2 is the proportion of variation in the dependent variable that is explained by the independent variables. The adjusted R^2 further takes into account the reduction in degrees of freedom.

FIGURE 1.1: Hurricane Sandy

(A) Max. Rainfall

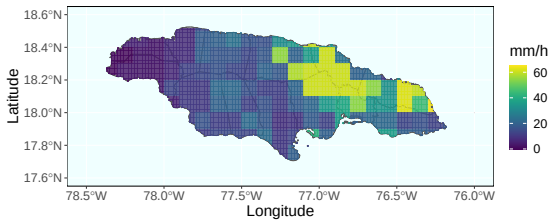

(B) Max. Windspeed

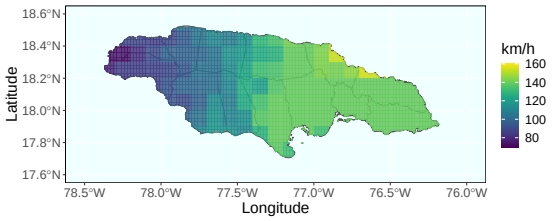

(C) Night Light

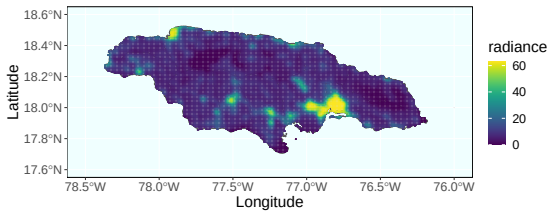

(D) Damages

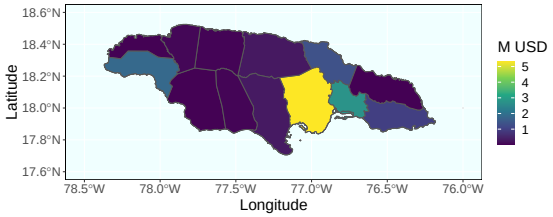

Notes: Cell-wise maximum hourly rainfall and maximum wind speed during Hurricane Sandy 2012, average monthly night light intensity 2000-2013 normalized to 0-63, and parish level damages of Hurricane Sandy 2012.

will have a higher R^2. From a model selection perspective, the Bayesian Information Criterion (BIC) favors models (4) and (5).[15]

1.4.2 Extreme Value Modelling

Threshold & Parameter Estimates

The average threshold chosen by the Bayesian cross-validation is 3.24 mm/h. However, the selected thresholds are spatially heterogeneous as depicted in Figure 1.2. This highlights the extent to which meteorological conditions vary across the island. Two examples of the model fitting are given in Figure 1.3. Panel a) shows the diagnostic plot for the cell that covers the capital city of Kingston close to the Blue Mountains while panel b) shows the diagnostic plot for the cell with the lowest 40-year return level (which is a candidate

[15]Note that a smaller BIC means a smaller information loss relative to the true (data generating) model. Thus, one typically selects the model with the smallest BIC.

TABLE 1.4: Regression Results

	Dependent Variable: Damages in M USD				
	(1)	(2)	(3)	(4)	(5)
$MRAIN_{is}$	0.13 (0.48)		0.24* (0.15)	0.22* (0.12)	0.23** (0.12)
$SRAIN_{is}$	0.05 (0.20)	0.09 (0.07)			
$MWIND_{is}^3/10^3$	0.01*** (0.00)	0.01*** (0.00)	0.01*** (0.00)	0.01*** (0.00)	0.01*** (0.00)
POP_i				0.03*** (0.01)	0.03*** (0.01)
Constant	9.15 (6.87)	8.54 (5.90)	10.03 (6.82)	1.32 (3.95)	1.45 (3.97)
Observations	65	65	65	65	63
R^2	0.57	0.57	0.57	0.39	0.41
$PARISH_i$	✓	✓	✓		
Outlier					✓

Notes: Standard errors in parentheses clustered by storm. *p<0.1; **p<0.05; ***p<0.01

for potential threshold-misspecification). The plots show estimated measures of predictive performance, normalized to sum to 1, against the training threshold. In panel a), the highest threshold weight and thus the selected threshold is at 0.56 mm/h while panel b) peaks at 0.49 mm/h.[16] We see that both plots give the most mass of threshold weight to values in the range of $0.5 - 3$ mm/h. As such, the specific choice of threshold appears not to have a large impact on the results as long as the threshold is within a certain range.

FIGURE 1.2: Threshold Map

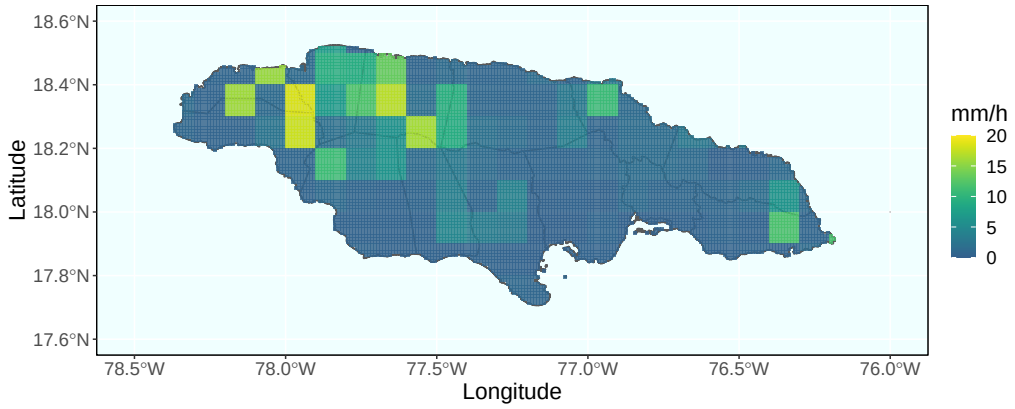

Notes: Map of the selected thresholds by Bayesian cross-validation detailed in section 1.3.3 by rainfall cell.

[16]The x-axis is scaled on the quantiles, thus the relative distance between the two plots is hard to compare.

FIGURE 1.3: Threshold Selection Diagnostic

(A) Kingston/Blue Mountains

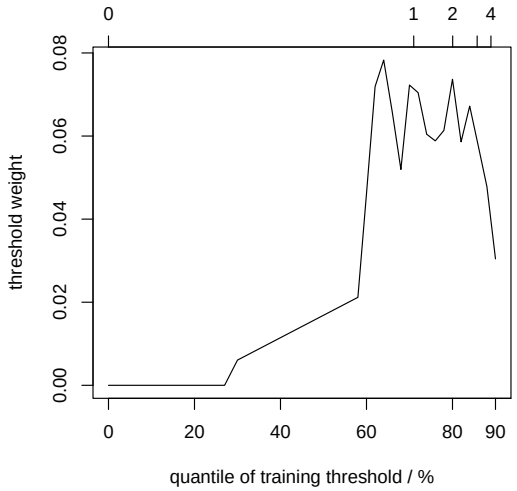

(B) Low Threshold

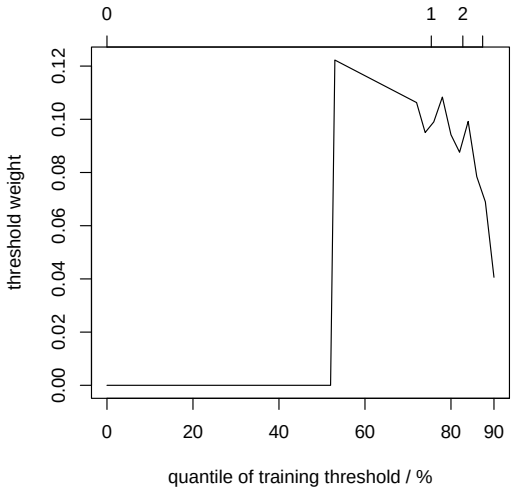

Notes: Example diagnostic plots of estimated measures of predictive performance. (a) shows the threshold selection for the cell-centered at (18.05,-76.75) which is a cell that covers the capital of Kingston close to the Blue Mountains. (b) shows the threshold selection for the cell-centered at (17.95,-77.25) which exhibits the lowest 40-year return level. For details about the procedure to produce the plots, see Equations (7) and (14) in Northrop, Attalides, and Jonathan (2017).

Parameter estimates from the extreme value GPD models are shown as boxplots in Figure 1.4. The estimated GPDs are shifted to the right (large μ), smoothly decreasing ($\sigma \gg 0$), are not degenerate[17] and have a mean ($\xi \leq 1$). Estimates of the non-stationary parameters can be found in Appendix A.3.

Return Levels

Return levels are summarized in the maps in Figure 1.5. The spatial pattern over different return periods stays the same with an increase in the average level as we extrapolate to less frequent events. The highest return levels can be found in the northeastern parish of Portland, around the city of Port Antonio.

[17] If $\xi \ll 0$ then the GPDs support is $0 \leq x \leq -1/\xi$ and is, in the case of extreme rainfall, degenerate.

FIGURE 1.4: GPD Parameter Boxplot

(A) Location μ (B) Scale σ (C) Shape ξ

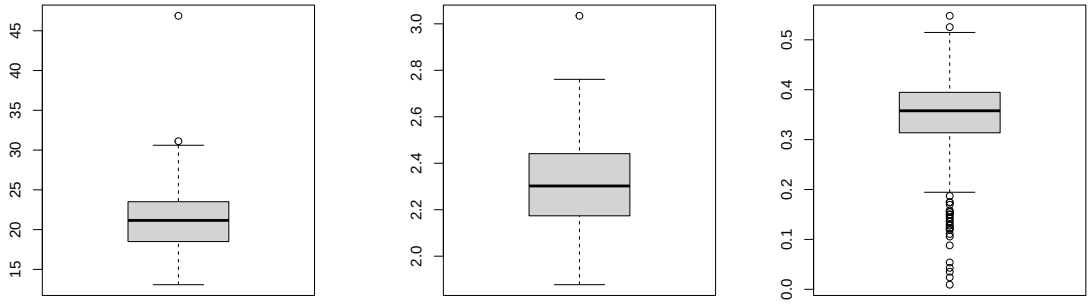

Notes: Boxplot of the location μ, scale σ and ξ parameter under the non-stationarity assumption as discussed in section 1.3.3.

We use the coefficient of 0.22 from the fourth column damage function regression in Table 1.4 as the damage function parameter to calculate predicted monetary damages in Figure 1.6. These can be summed up to the country level: projected damages are for 5, 10, 20, and 40-year return periods 138.3 M USD (0.9% of Jamaica's 2019 GDP), 183.1 M USD (1.1%), 238.0 M USD (1.5%) and 306.5 M USD (1.9%), respectively.

FIGURE 1.5: Return Level Map

(A) 5 Year

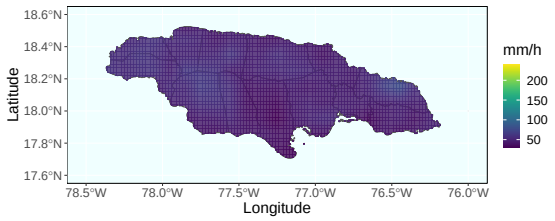

(B) 10 Year

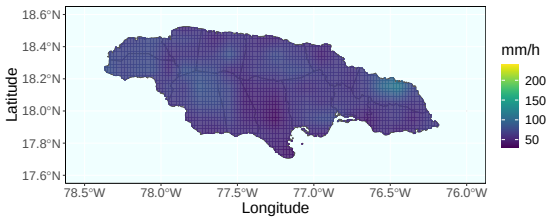

(C) 20 Year

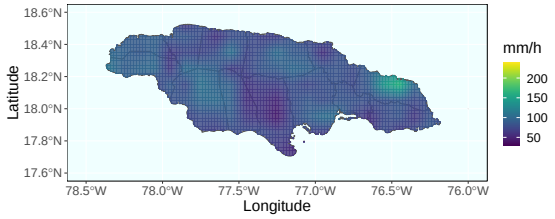

(D) 40 Year

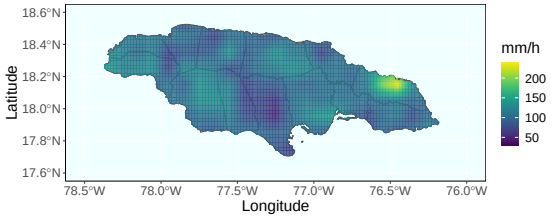

Notes: Maps of return levels drawn by disaggregating every cell into 64 sub-cells which are then bilinearly interpolated.

FIGURE 1.6: Projected Damages Map

(A) 5 Year

(B) 10 Year

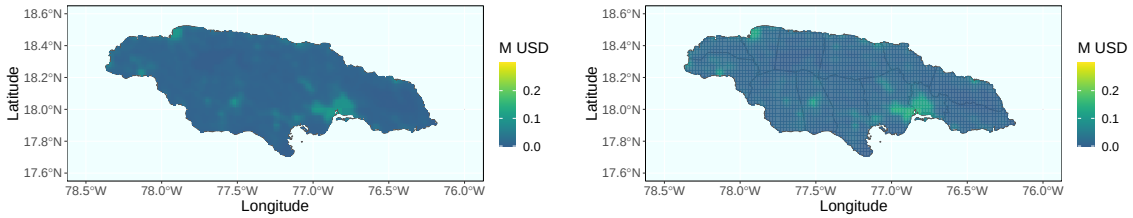

(C) 20 Year

(D) 40 Year

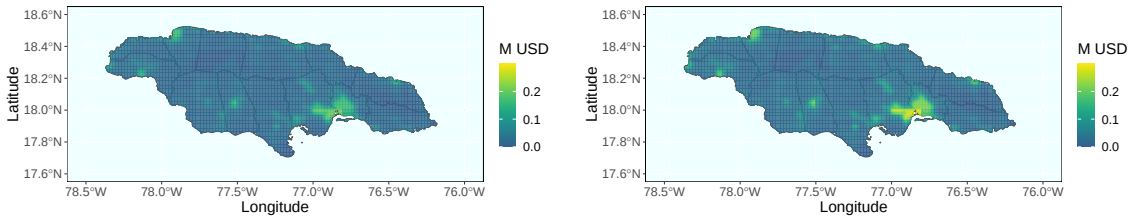

Notes: Maps of projected damages for different return periods calculated as in Equation 1.12.

1.5 Discussion

This paper makes three contributions. It adds to the recent literature that acknowledges the importance of rainfall in a TC damage function, especially with regard to climate change interactions. Employing the recent, high-resolution GPM rainfall data for an extreme value analysis in Jamaica identifies the spatial distribution of extreme rainfall. Lastly, we propose a simple approach to combine the damage function with return levels and transform them into monetary risk.

The estimated linear coefficient suggests that if maximum rainfall during a TC increases by 1 mm/h in a parish, the inflicted damage increases by 0.22 M USD. Depending on the TC, this can constitute a sizeable part of the damages. On average for these five storms, ex-post projected max. rainfall damages are 25.5% of total damages.[18] However, there can be considerable differences, also depending on the wind exposure during the storm: the average contribution of max. wind speed is 34% while residual damages are 40.5%.[19] For example, during tropical storm Nicole in 2010, the average parish max. rainfall was 40.5 mm/h, which translates into 8.9 M USD, while average parish damages were 21.9 M USD. In contrast, when Hurricane Dean brought strong winds over the island of Jamaica in 2007, the average parish max. rainfall was only 18.3 mm/h resulting 4 M USD damages (compared to the average 32 M USD per parish) while 67% (21.4 M USD) can be attributed to max. wind speed. This supports the view expressed in Eberenz, Lüthi, and Bresch (2021) that wind-only damage functions fail to predict the destruction of rainfall-heavy TCs. When comparing the observed events to the risk estimates, the extreme value analysis suggests that a rainfall-heavy event like Nicole in 2010 has a lower return period than 10 years. If extrapolated to less frequent events with a 20 or 40-year return period, the potential damages due to rainfall quickly dwarf those observed in any of the storms examined.

It is insightful to compare the return level estimates to those found in the literature.

[18] That is calculated as the fraction of projected damages against total reported damages.

[19] Damages not explained in the model come from factors such as storm surge and residual variation in the data.

Demirdjian, Zhou, and Huffman (2018), who employ a PPP approach on a global scale with the TRMM data, estimate 25-year return levels in the range of 150 - 180 mm/h for southern Florida.[20] Burgess et al. (2015) use long rainfall time series of two airports in Jamaica and estimate the 30 min. 25-year return level to be 110 and 128 mm/h, respectively. In comparison, if we consider the location of these two airports (Montego Bay and Kingston) the 20-year return level estimated in this analysis is around 80 to 90 mm/h for both.[21] Unsurprisingly we find that the area north of the Blue Mountains is most susceptible to extreme rainfall during a TC. This is likely because TCs often first make landfall in the northeast of Jamaica. The orographic lift of the Blue Mountains in the northeastern parishes increases the prevalence of heavy rainfall in that area further (Laing, 2004).

Our risk estimates could arguably be useful for policy. More precisely, from a damage mitigation perspective, modeling the spatial distribution of risk is necessary for the planning and execution of ex-ante mitigation interventions (Holcombe and Anderson, 2010; Anderson et al., 2011). For example, we find that the north-eastern parish of Portland is most susceptible to extreme rainfall and should therefore be a priority area for preventive measures such as proper surface water management to decrease landslide risk. Nevertheless, while our damage estimates serve to give an indication of the loss of assets from extreme precipitation during a TC, one should note that they only constitute part of the economic impact. More specifically, the direct damages are likely to result also in indirect damages through disruption of economic activity (Hallegatte and Przyluski, 2010). Strobl (2012) for example estimates the macroeconomic reduction in output for the average hurricane strike in the Central American and Caribbean region to be at least 0.83 percentage points, although this estimate was solely based on damages due to wind exposure. The estimates here suggest that projected direct damages for a 5 and 40-year return period event are in value 0.9% and 1.9% of Jamaica's GDP. However, these figures cannot a priori tell us how the damages will translate into changes in aggregate output as this will depend on the indirect consequences, disaster relief, and whether the damaged

[20] Note that the TRMM data is 3-hourly compared to the half-hourly GPM.
[21] The cities are in more than one grid cell.

assets are replaced, among others. For instance, Lenzen et al. (2019) show that TC Debby 2017 caused significant disruption through the supply chain to regions and industries in Australia that were not themselves hit by the storm. These spillover effects could be an avenue for future research.

There are a number of weaknesses inherent in our methodological approach that future research could address. Firstly, the magnitude of the projected damages crucially depends on the damage function estimate for extreme rainfall. While the coefficient of interest in Table 1.4 does not change statistically significant across specifications (3) - (5),[22] there are still a number of caveats to be made in this approach. First, both the dependent variable (reported damages) and the independent variables are subject to measurement error.[23] Measurement error in the dependent variable is less problematic (if it is not systematic) since it "only" increases the unexplainable part of the regression and will simply result in less precise estimates. Measurement error in the extreme rainfall, our independent variable of interest, is more of a concern since a sufficient amount of such will induce attenuation bias of the estimates towards zero (Frost and Thompson, 2000). A second caveat is the focus on statistical modeling and the omission of a hydrological perspective. Extreme rainfall during TCs is itself not a hazard but the cause for hazards such as floods and landslides (Yumul et al., 2012; Nolasco-Javier, Kumar, and Tengonciang, 2015; Nolasco-Javier and Kumar, 2018). Hydrological models would be able to decipher this relationship more precisely. The challenge of employing a hydrological model instead of a statistical approach is, however, in terms of feasibility and generalizability. Complete multi-hazard large-scale hydrological models are still an active research area (Lung et al., 2013; Koks et al., 2019). With the additional complexity of a model that makes use of the extent of river catchments, local soil type, and hill slopes, any result from the analysis could only be in terms of these specific conditions. The precision gained by a realistic

[22] A Wald-test of the preferred model (4)'s coefficient (0.22) against the coefficient from model (3) cannot reject their equality at any conventional level (p-value = 0.82).

[23] Damages are constructed and interpolated from incomplete reports, as discussed in section 1.2.2. Wind and rainfall observations are constructed from a parametric model or remote sensing information, and both are aggregated to a larger spatial scale. All these steps in the data construction are sources of measurement error.

model is thus paid with a narrower transferability of the results. The last restriction concerns the valuation of non-monetary damages. More specifically, the monetary damages figures used here do not account for other non-monetized impacts like the erosion and deterioration of soil, which can be linked to extreme rainfall events (Rawlins et al., 1998) as well as psychological and mental health impacts to the exposed population (Lindell and Prater, 2003; Bourque et al., 2006).

1.6 Conclusion

While the overall effect of climate change on the frequency and severity of TCs is a matter of debate and may be ocean basin specific, there is a general consensus that rainfall-heavy TCs will likely become more common with global warming (Grossmann and Morgan, 2011; Walsh et al., 2016; Knutson et al., 2019). In considering what greater precipitation in future TCs will mean in terms of economic impact, much of the current literature has focused on estimating the impact in terms of wind-induced damages. Even if one assumes that wind is a sufficient proxy for TC damages, a wind-only damage function likely underestimates future damage in climate change scenarios. The analysis presented in this case study of Jamaica shows that extreme rainfall during TCs is also potentially an important driver. Depending on the specification, a conservative estimate suggests that rainfall during a TC causes direct damage of 1.5% of GDP for a 20-year event. Thus failing to take into account extreme precipitation in risk assessments may not only underestimate future damage but substantially bias current risk assessments.

Chapter 2

Flash Flood Detection via Copula-based IDF Curves: Evidence from Jamaica

joint with Nekeisha Spencer and Eric A. Strobl

"The trouble with having an open mind, of course, is that people will insist on coming along and trying to put things in it."

Terry Pratchett, Diggers

Acknowledgments: We would like to thank the participants of the EAERE-ETH Winter School 2020 (Ascona), the Workshop on Compound Weather and Climate Events 2021 (Bern, Online), and the IPWSD 2021 (Columbia University, Online) for their valuable comments. This research did not receive any specific grant from funding agencies in the public, commercial, or not-for-profit sectors.

2.1 Introduction

Over the last twenty years, more people have been affected by floods than by any other natural disaster.[1] Among pluvial floods, flash floods have the highest average mortality (Jonkman, 2005). The Caribbean is especially at risk from flash floods. The region, in particular, is prone to hydro-meteorological hazards, urbanization is often unregulated, and soil degradation is common such that floods are frequently triggered (Gencer, 2013; Pinos and Quesada-Román, 2021). For instance, heavy rain on March 5^{th} 2022 in Northern Hispaniola caused severe flash floods, leading to 2 deaths and hundreds being displaced.[2] Flash floods follow shortly after heavy rainfall and are highly localized phenomena that occur in basins of no more than a few hundred square kilometers and have a response time of a few hours (Borga et al., 2007). Steep slopes, impermeable surfaces, and saturated soils are factors that can transform a heavy rainfall event into a flash flood hazard (Norbiato et al., 2008). The high localization and multidimensionality involved in flash floods make their study particularly involved.

It has long been a primary objective of weather service providers to create a warning system that connects rainfall to floods and landslides (Keefer et al., 1987). Warning system typically uses some lower bound or threshold above which a warning would be issued (Caine, 1980). Empirical thresholds for when rainfall events become hazardous connect the intensity (I) to the duration (D) and are used for the construction of so-called intensity-duration-frequency (IDF) curves (Koutsoyiannis, Kozonis, and Manetas, 1998). Commonly, estimation of IDF curves requires assumptions on the marginal distribution of I and D or the two marginals were assumed to be independent.[3] Using copula functions for conditional sampling allows the flexible and separate definition of marginals and dependence. Multiple studies employ the said method to estimate rainfall IDF curves for landslides and heavy rainfall events (Singh and Zhang, 2007; Ariff et al.,

[1] Authors' calculation using EMDAT database. Since 2000, 1.7 Billion people have been affected by floods, followed by droughts (1.4 Billion), storms (0.8 Billion), and earthquakes (0.12 Billion).

[2] `https://floodlist.com/` Accessed last on January 11^{th} 2023.

[3] There are also some instances where a specific dependence has been assumed from theoretical considerations, see Koutsoyiannis, Kozonis, and Manetas (1998)

2012; Bezak, Šraj, and Mikoš, 2016; Li et al., 2019). These studies often define the yearly maximum event of measurement stations by some decision rule and model the resulting time series. This allows for a good statistical fit and a well-described dependence between I and D. However, since the data does not necessarily contain hazardous events, little inference can be made about these.

This study aims to construct IDF curves with information from confirmed flash flood events in Jamaica. This allows for inference with regard to the hazard by comparing the odds ratio of flood occurrence given a frequency, where less frequent events are more severe and vice versa. The calculation of the odds ratio requires a set of extreme but non-hazardous events as well as a set of hazardous rainfall events. Following the literature, the local yearly maximum rainfall events are defined. Additionally, a complete and confirmed list of Jamaican flash floods by the Office of Disaster and Preparedness Management (ODPEM) is utilized to define hazardous events. These observed flash flood events are linked with 11 km $\times$ 11 km cells of remote sensing rainfall information. These remotely sensed data have several advantages compared to station data, such as consistency in sensors and resolution. While direct in-situ measurements are factual, they depend on the location and continuous operation of stations. Currently, the number of modern automatic weather stations in Jamaica is well below the remote sensing resolution, with the exception of the area around the capital Kingston.[4] Subsequently, the IDF curve threshold, which separates the confirmed hazard events from the rest via odds ratio, is determined. This threshold can serve as a simple decision rule for the identification of flash flood triggering rainfall events.

There are a number of reasons why the Caribbean and Jamaica in particular is an interesting case study. Small island states in the Caribbean, such as Jamaica, have long been identified as especially vulnerable to extreme meteorological events and associated flooding (IPCC, 2012; Wilson et al., 2014). Moreover, extreme precipitation events show an increased frequency since 1950 in the Caribbean region (Peterson et al., 2002). At the same time, there is little information on the local rainfall risk. In this regard, it is common

[4] `http://metservice.gov.jm/aws/` Accessed last on January 3rd 2023.

practice to transfer IDF curves for some Caribbean island nations to others, despite their different rainfall characteristics (Lumbroso et al., 2011). Burgess et al. (2015) therefore developed IDF curves for Jamaica with long historical data. Linearly projecting the historical parameter estimates to 2100, they find that the intensity of a 100-year return event increases by 27% to 59% as a result of increasing variability due to climate change.

Quantifying extreme rainfall-induced hazards has important applications, such as for risk maps, warning systems, or re-insurance schemes, particularly for the Caribbean. For example, the Climate Risk Early Warning Systems (CREWS) aims to strengthen hydro-meteorological and early warning services in the Caribbean, focusing on hurricanes and other hydro-meteorological hazards. Its first assessment in 2015 identified the need for increased forecasting of secondary hazards such as coastal flooding and flash floods. Currently, pilot projects to strengthen national multi-hazard early warning systems in the Caribbean community countries are devised through CREWS. The Caribbean Risk Information System (CRIS) platform, created by the Caribbean Disaster Emergency Management Agency (CDEMA), aims to support informed decision-making by providing access to information on hazards and does so via geospatial data for risk and hazard mapping, disaster preparedness, and response operations. This input data relies on research in the hazard, exposure, and vulnerability domain.[5] Another example is the Caribbean Catastrophe Risk Insurance Facility (CCRIF), which since 2013 has provided insurance against excess rainfall to member countries (Linkin, 2014). More specifically, its CCRIF Excess Rainfall (XSR) product is a parametric insurance based on specific rainfall thresholds that determine payouts.

The remainder of the paper is organized as follows: Section 2.2 presents the study region and describes the data. Section 2.3 details the methodology of conditional copula modeling and how the two samples are used to determine an IDF curve based flash flood

[5]Most commonly, risk is defined as the combination of the three components hazard, exposure, and vulnerability. Hazard relates to the physical phenomenon, in this case, flash floods. Exposure could be in terms of people, buildings, or economic assets at risk of the hazard. Vulnerability then links the hazard to the exposure and translates it to risk. For instance, given a flash flood hazard, the vulnerability of urban or agricultural settlements (exposure) is different, and as such, the risk is different as well.

threshold. Section 2.4 then presents the results. Section 2.5 discusses the findings and section 2.6 concludes.

2.2 Study Region & Data

2.2.1 Study Region

Jamaica is the third-largest Caribbean island by land area after Cuba and Hispaniola. The island's topography is characterized by interior mountain ranges descending to coastal plains where the eastern Blue Mountains historically experience the most rainfall (Nkemdirim, 1979). Jamaica lies in the Atlantic Hurricane Belt and is especially at risk of climate change (Monioudi et al., 2018). Tropical cyclones and the accompanying heavy rainfall are frequent and cause severe destruction (Spencer and Polachek, 2015; Collalti and Strobl, 2022). For instance, between June 2007 and August 2021, the CCRIF made 54 payouts for a total of USD 245 million, of which USD 135 million are for tropical cyclones, USD 60 million for excess rainfall and USD 49 million for earthquakes (mainly the devastating 2021 Haiti earthquake). Thus, local susceptibility to floods has become vital to planning and development in Jamaica (Nandi et al., 2016).

2.2.2 Flash Floods

The source of flash flood information is the Office of Disaster and Preparedness Management (ODPEM), whose responsibility includes monitoring extreme weather events in Jamaica and implementing measures to mitigate their impact. From the ODPEM, shapefiles of all 48 known flood events are obtained from 2001 to 2018. Many of these events correspond to a specific meteorological event, like a tropical storm that caused flooding in more than one location in Jamaica. We treat each event location separately if it falls uniquely in a remote-sensing rainfall cell. For example, during heavy rain on May $14th - 15th$ in 2017, several places around Cave Valley (parish of St. Ann) in central Jamaica, as well as, to the south, around Morgan's Pass in the parish of Clarendon, experienced severe flooding. These locations are approximately 20 km apart, lie on two sides

of the north/south watershed, and are thus treated as two incidents in their respective rainfall cell. Some flood events in the OPDEM shapefiles could not be verified by any report and were therefore dropped, as were a few riverine floods that would require explicit hydrological modeling, which is beyond the scope of this study. Some events where the exact day(s) are not included in the data are identified using local newspaper reports. A total of 93 flash flood events were localized for Jamaica with approximate timing.

2.2.3 Precipitation

The source for precipitation data is Version 06B of the Global Precipitation Measurement (GPM) Integrated Multi-satellitE Retrievals (IMERG, Huffman et al. (2015b)). The satellite precipitation algorithm combines microwave and infrared precipitation measurements to produce precipitation estimates, adjusted with surface gauge data. The resulting product is a half-hourly data set with near-global coverage at a $0.1^\circ \times 0.1^\circ$ resolution since June 2000. Compared to other remote sensing or reanalysis products, the GPM-IMERG has a considerably higher spatial and temporal resolution than its competitors. Also, the number of distinct cells and, thus, spatial resolution is considerably higher than the number of measurement stations in Jamaica. One major drawback of the GPM-IMERG, its short timeframe, does not apply to this study because all the OPDEM events are fully captured in the observational period since June 2000. Note that the quality of satellite rainfall data has leapfrogged in the last decade: An inter-comparison of rain-gauge, radar, and GPM-IMERG for rainfall-runoff modeling by Gilewski and Nawalany (2018) in a mountainous catchment in Poland identified that radar and GPM-IMERG outperform rain-gauge data. Tang et al. (2020) provides a comprehensive overview of different satellite precipitation and reanalysis products, reporting good performance for GPM-IMERG and it is continuously improving in more recent versions.

2.3 Methodology

2.3.1 Event Definition

The data on confirmed flash flood events provides location and start date information, but no sub-daily timing of rainfall onset and its ending. We thus need to find and define rainfall events that start before the flood (potentially lasting longer than the reported date). We resort to the common inter-event time definition (IETD) method to delimit the events (Ariff et al., 2012; Bezak, Šraj, and Mikoš, 2016). The IETD refers to the minimum duration without rain between consecutive rainfall events. An IETD of a few hours is typically selected for floods, while for landslides the IETD is longer, i.e., up to several days (Huff, 1967). For confirmed events, the event definition starts with a window of +/- 7 days around the date given by the OPDEM or newspapers. Within that window, the event with the maximum cumulative rainfall is regarded as the flood-inducing rainfall event. Figure 2.1 illustrates the procedure. The yearly maximum events are constructed the same way, though for each cell each year is considered separately. Note that a minimum threshold of 0.1 mm/h for a given observation to start an event is imposed to reduce the number of events.

2.3.2 Conditional Copula Modelling

Informally, copulas can be described as "functions that join or couple multivariate distribution functions to their one-dimensional marginal distribution functions" (Nelsen, 2007). More formally, given a 2-dimensional (joint) distribution function H with univariate margins $F_1 and F_2$, there exists, by the first part of Sklar's Theorem, a 2-dimensional copula C such that

$$H(\boldsymbol{x}) = C\big(F_1(x_1), F_2(x_2)\big), \quad \boldsymbol{x} \in \mathbb{R}^2. \tag{2.1}$$

The copula C is uniquely defined on $\prod_{j=j}^{2} \mathrm{ran} F_j$ and there given by

$$C(\boldsymbol{u}) = H\big(F_1^{\leftarrow}(u_1), F_2^{\leftarrow}(u_2)\big), \quad \boldsymbol{u} \in \prod_{j=1}^{d} \mathrm{ran}\ F_j, \tag{2.2}$$

FIGURE 2.1: Event Definition

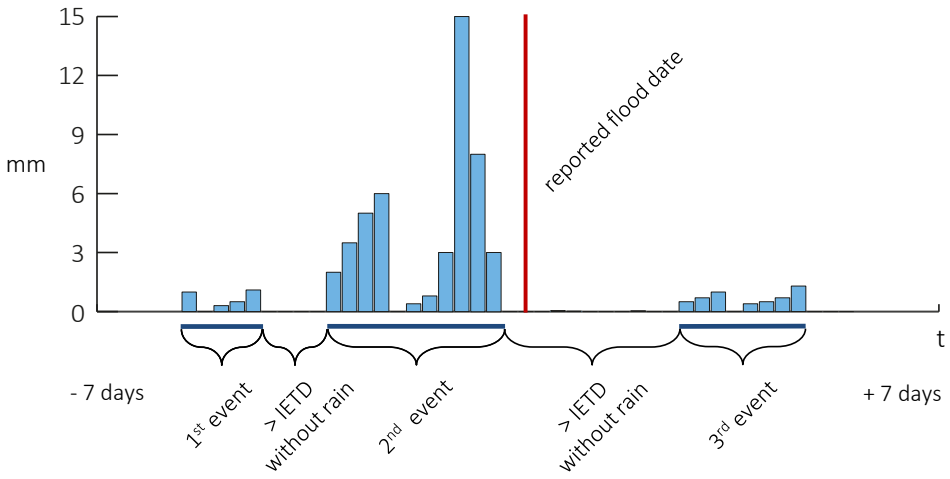

Notes: Illustration of the event definition in the case of a confirmed event with the reported date from OPDEM or newspapers in red. In the time frame +/- 7 days around this date, three separate events are defined given an IETD and a minimum threshold of 0.1 mm/h. Three events result, where the second event is the maximum event measured by cumulative rainfall and is considered the flood-inducing rainfall event.

where $F^{\leftarrow}$ denotes the generalized inverse, which equals the regular inverse F^{-1} for continuous and strictly increasing distribution functions (dfs). By the definition of a cumulative distribution function, ran $F_j \in (0,1)$ such that the copulas univariate margins are standard uniform $U(0,1)$ (Hofert et al., 2018). Three attributes follow: the copula function (1) uniquely specifies the dependence for the whole distribution, (2) can be recovered from data on joint and marginal distribution, and (3) imposes no constraint on the shape of the dependence.

The conditional copula method has previously been used to estimate IDF curves (Singh and Zhang, 2007; Ariff et al., 2012; Bezak, Šraj, and Mikoš, 2016). Let C be the 2-dimensional copula and let $\boldsymbol{U} \sim C$, $u_1 \in (0,1)$ and $u_2 \in [0,1]$, then

$$C_{2|1}(u_2|u_1) = \mathbb{P}(U_j \leq u_j | U_1 = u_1). \tag{2.3}$$

If one fixes for some value of $u_1 \in (0,1)$, the conditional copula function $C_{2|1}(u_2|u_1)$ is a

distribution function on $[0, 1]$ and can be used for conditional sampling. The evaluation of $C_{2|1}(u_2|u_1)$ however involves the evaluation of partial derivatives instead of densities (Hofert, Mächler, and McNeil, 2012; Hofert et al., 2018).

Consider that $C_{U,V}(u, v)$ is the copula function of interest and let intensity $I = i$ and duration $D = d$ have marginal distribution functions $V = F_I(i)$ and $U = F_D(d)$. For a known value of $U = u$, $C_{V|U=u}$ gives realizations of marginal V. The corresponding value of u can be obtained by the marginal distribution function. From u and v, the respective i and d can be recovered easily since $d = F_D^{-1}(u)$ and $i = F_I^{-1}(v)$. The conditional copula function can be written as

$$C_{V|U=v}(v|U = u) = \frac{\partial}{\partial u} C_{U,V}(u, v)\Big|_{U=u.} \tag{2.4}$$

The conditional copula, which is a conditional bivariate distribution, relates to the return period T as follows

$$C_{V|U=v}(v|U = u) = 1 - \frac{1}{T}. \tag{2.5}$$

For a given value of u and a return period T, solving Equation 2.4 and 2.5 simultaneously yields the corresponding v. Via the marginal distribution function, the respective values of i and d are recovered and represent a point on the IDF curve for a return period T. For every return period T, many values of u are chosen to get an approximately smooth IDF curve. That process is repeated for other T to construct IDF curves which are increasing in severity with T.

2.3.3 Two Sample Approach

Rainfall events of interest are those that lead to flash floods. However, a block maxima approach, partitioning the data into yearly blocks, allows a direct relation with return periods and is thus often chosen (Ariff et al., 2012). The proposed methodology uses information from block maxima as well as confirmed flood events. There are $m = 93$ confirmed flood events and, at these locations, $n = 1120$ yearly cell-wise maxima. The

yearly maximum events serve to estimate the copula function and the marginal distributions of intensity and duration for these extreme rainfall events. Conditional sampling from the copula enables the construction of IDF curves with T year return periods. One can then derive the IDF curve associated with a certain return period above which the likelihood of flash flood occurrence is maximized. For every return period the IDF curve is recovered and the ratio R of confirmed flash flood events m against the number of yearly maximum rainfall events n that lies above that curve is calculated,

$$R = \frac{\sum_{i=1}^{m} I\big(d_i \geq (\tilde{d}|U = u_i)\big)}{\sum_{j=1}^{n} I\big(d_j \geq (\tilde{d}|U = u_j)\big)}, \tag{2.6}$$

where $(\tilde{d}|U = u_i)$ is the estimated duration via conditional copula sampling and marginal transformation $\tilde{d} = F_D^{-1}(\tilde{u})$. The IDF curve with a return period associated with the highest ratio $R_{r:max}$ is the one that separates the events from non-events best. This constitutes a so-called critical layer $(d, i) \in L^2 : 1 - H((d, i) = P(D > d, I > i) = t$ where all combinations of i and $d \in L^2$ have the same probability $1 - H((d, i) = t$ (Salvadori et al., 2016). The critical region, which corresponds to a flash flood classification, is defined as $L_t^{>} = \{(i, d) \in L^2 : 1 - H(i, d) < t\}$ (De Michele et al., 2013). Subsequently, the return period $T^{>}$ of an event in the critical region is defined by the inverse probability of falling into the critical region (Zscheischler, Orth, and Seneviratne, 2017):

$$T^{>} = \frac{\mu}{P((D, I) \in L_t^{>})}, \tag{2.7}$$

where μ denotes the average time unit, which is 1 year in the case of yearly maxima.

2.3.4 Candidate Copulas

The selection of appropriate copula is carried out in two steps. First, a set of candidate copulas is defined. Second, the candidate copula is compared on the basis of fit, for both the event and the yearly maxima data. The first restriction on candidate copulas is that a conditional sampling algorithm exists. This is the case for the families of Archimedean and elliptical copulas (Hofert et al., 2018). The literature on landslides and flash flood

IDF curves has further established the negative relation between an event's duration and its intensity, which is the second restriction on candidates (Aleotti, 2004; Salvadori and De Michele, 2004). Table 2.1 shows the copulas for which conditional sampling algorithms exist and some of their properties. The two restrictions leave one with three potential copula classes, Normal, Frank, and t copula. Note that these copulas are all radially symmetric and exchangeable. Geometrically, radial symmetry is the symmetry of the density with respect to the point $\mathbf{1/2} = (1/2, ..., 1/2)$. Exchangeability is the symmetry of the density with respect to the main diagonal. Given a negative dependence, a copula that is not radial symmetric is one whose lower tail dependence is different from its upper tail dependence, whereas a copula that is not exchangeable is one whose dependence changes with the order of the marginals. The best candidate copula is selected on the basis of the Cross-Validation Copula Criterion (CIC) by Grønneberg and Hjort (2014), which is an Akaike Information Criterion (AIC)-like criterion on a Maximum-Pseudo-Likelihood Estimate (MPLE) of semi-parametrically (i.e., with non-parametric estimated margins) estimated copula. The methodology is implemented in the R package "Copula", with which all the subsequent copula modeling is carried out (Kojadinovic and Yan, 2010).

TABLE 2.1: Candidate Copula Families

Name	Attainable Dependence	Radial-Symmetry	Exchange-ability	Negative Dependence
Gaussian	(-1,1)	✓	✓	✓
t_v	(-1,1)	✓	✓	✓
AMH	[0, 1/3)		✓	
C	[0, 1)		✓	
F	(-1, 1)	✓	✓	✓
GH	[0, 1)	✓	✓	
J	[0, 1)	✓	✓	

Notes: Overview of candidate copula families with respect to their attributes.

2.3.5 Selection of Marginals

The IDF curve construction via conditional copula in section 2.3.2 requires the estimation of marginals for duration D and intensity I. Candidate marginal distributions are the Weibull, Gamma, Log-normal, and Generalized-Extreme-Value (GEV) distributions, and are all estimated via maximum-likelihood and assessed by AIC. The empirical probability density function is also inspected graphically against the marginal distributions' estimated probability density to assert its fit.

2.4 Results

2.4.1 Event Definition

The event definition in time requires an appropriate IETD. Values of IETD between 4 h and 24 h are considered. Graphical assessment of mean event intensity and duration revealed that an IETD of 12 hours best delimits the rainfall events. See Appendix section B.1 for a discussion and graphical examples for various IETD. Figure 2.2 shows the locations of confirmed flash flood events in Jamaica and the average intensity, duration, and total rainfall of the yearly maximum events. Average intensity is highest inland and to the West, but fairly evenly distributed. Average total rainfall is highest at the eastern shore north of the Blue Mountains, with a second agglomeration of high total rainfall cells in the West. Duration exhibits a similar pattern to total rainfall, with the longest events in the West. Since the confirmed flash flood events are evenly distributed across the island, variation in local conditions is expected to be captured well. Section B.2 in the Appendix further provides summary statistics for both yearly maximum and confirmed flash flood events.

2.4.2 Copula Selection

The shape of dependence can be assessed via pseudo-observations. Pseudo-observations are obtained by first estimating the empirical distribution functions $F_n(n, j)$ for $j \in (I, D)$,

FIGURE 2.2: Maps of Events and Rainfall Characteristics

(A) Confirmed Events

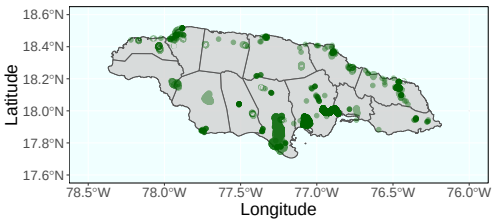

(B) Mean Intensity

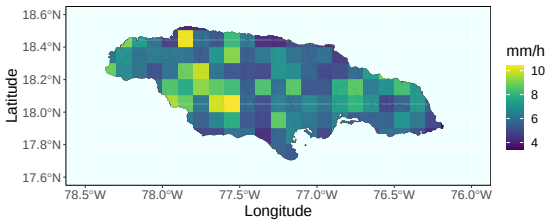

(C) Total Rainfall

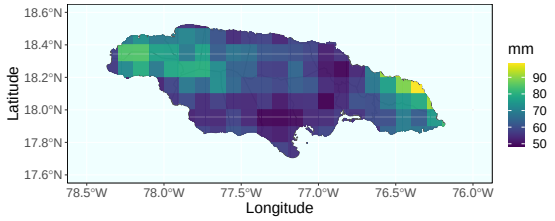

(D) Mean Duration

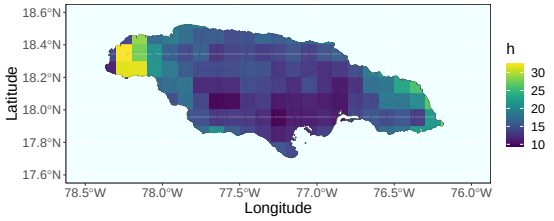

Notes: (a) Location of the confirmed flash flood events, (b) cell-wise mean intensity of locations maximum events, (c) cell-wise mean total rainfall of locations maximum events, and (d) cell-wise mean duration of locations maximum events.

$$F_{n,j} = \frac{1}{n+1} \sum_{i=1}^{n} 1(X_{i,j} < x), \quad x \in \mathbb{R}, \tag{2.8}$$

where $1(\cdot)$ is the indicator function. These estimated margins can then be used to form the sample:

$$U_{i,n} = \big(F_{n,D}(X_{i,D}), F_{n,I}(X_{i,I})\big), \quad i \in \{1, ..., n\}. \tag{2.9}$$

Figure 2.3 displays the pseudo-observations and demonstrates a strong negative dependence in both samples. This limits the set of potential copulas to the Normal, Frank, and t copula. Note that these copulas are all radially symmetric and exchangeable.

Estimates of the copula information criterion (CIC) are shown in Table 2.2. Selecting the Frank copula for the yearly maximum events leads to a higher CIC than the Normal or t copula. For the confirmed events, selecting the Frank copula leads to a lower CIC than

FIGURE 2.3: Pseudo-Observations

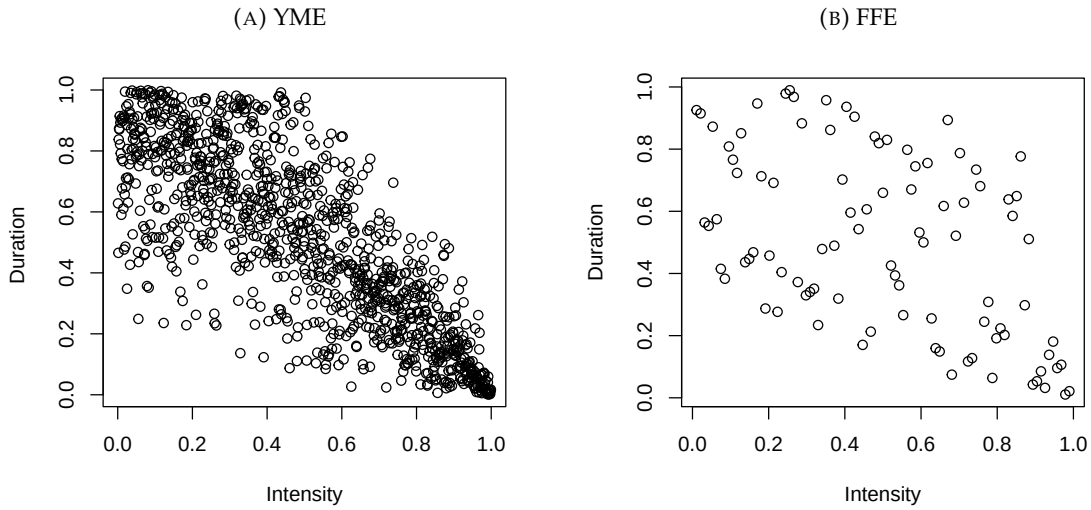

Notes: (a) Pseudo-observation of the yearly maximum rainfall events (YME) and (b) of the confirmed flash flood events (FFE). Ties in the duration variable due to the measurement scale are randomly split.

the Normal or t copula.

TABLE 2.2: Copula Cross-Validation Criterion

	Normal Copula	Frank Copula	t Copula
Maximum Events	513.3	551.4	521.3
Confirmed Events	15.92	12.02	15.93

Notes: Cross-Validation Copula Criterion (CIC) by Grønneberg and Hjort (2014) for both data samples. The t copula assumes $10 = v$ degrees of freedom.

Figure 2.4 displays pseudo-observations for both samples as well as a random sample of pseudo-observation under Frank and Normal copula. The sample of confirmed flash floods is too small to draw conclusive evidence regarding the optimal copula. There is also no clear visual indication around the locus of points for the Frank copula over the Normal copula or vice versa. However, the Normal copula exhibits tail dependence similar to the data, while the Frank copula is tail quadrant independent (Joe, 2014).

In summary, the Normal copula is better suited for the data and thus chosen for the analysis. It is more appropriate for yearly maximum events, which are the data on which the IDF curves are generated, as outlined in section 2.3.3 concerning the two sample approach. Additionally, the Normal copula is suitable for the confirmed events, as the CIC and graphical evidence shows.

FIGURE 2.4: Random Sample of Pseudo-Observations

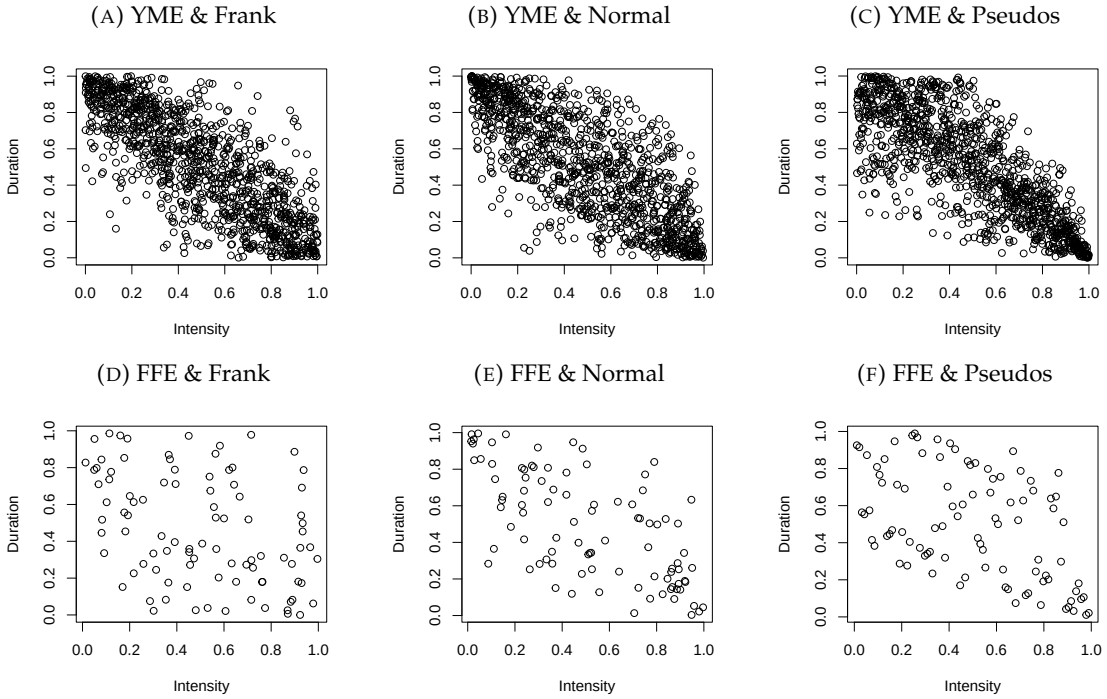

Notes: (a) random sample ($n = 1120$) of pseudo-observation of the yearly maximum rainfall events (YME) under the assumption of Frank copula, (b) under the assumption of Normal copula, and (c) the true pseudo-observation. (d) Random sample ($n = 93$) of pseudo-observation of the confirmed flash flood events (FFE) under the assumption of Frank copula, (e) under the assumption of Normal copula, and (f) the true pseudo-observation.

2.4.3 Estimation of Marginals

Table 2.3 reports the Akaike Information Criterion for both samples, where the parametric distributions are fitted via MLE to the marginals. For both samples' intensity, the generalized extreme-value (GEV) distribution results in the lowest information loss.

Similarly, for the duration, the Weibull distribution yields in both instances the lowest AIC.

TABLE 2.3: Akaike Information Criterion

	Yearly Maximum Events			
	Weibull	Gamma	Log-Normal	GEV
Intensity	7374.2	7327.5	7059.3	7029.1
Duration	7053.8	7061.3	7181.4	7196.5
	Flash Flood Events			
	Weibull	Gamma	Log-Normal	GEV
Intensity	493.7	487.8	447.5	428.8
Duration	632.7	634.6	650.2	648.3

Notes: Akaike Information Criterion (AIC) for both samples. A parametric distribution was fitted via MLE to the marginals, intensity and duration.

Figure 2.5 compares the estimated distributions and the empirical probability density. In all cases the two match well. The confirmed flood events are on average slightly longer (11.4 hours versus 9 hours) and less intense (5.2 mm/h versus 9.9 mm/h) compared to the yearly maximum events. It is notable that the flood events are, due to the smaller sample size, not as smoothly distributed. Both samples yield similar distributions and agree on the shape. Subsequent conditional copula modeling focuses on the more precisely estimated distributions from the large sample of yearly maximum events.

2.4.4 Conditional Copula IDF Curves

IDF curves corresponding to return periods between 2 and 40 years are shown in Figure 2.6. The curves are all convex, such that shorter events have a disproportionately higher intensity. Visually, the choice of marginals has little impact on the IDF curves. Higher return periods shift the IDF curve outwards to higher intensities for all durations. Interestingly, convexity decreases with higher return periods.

FIGURE 2.5: Marginal Probability Estimates

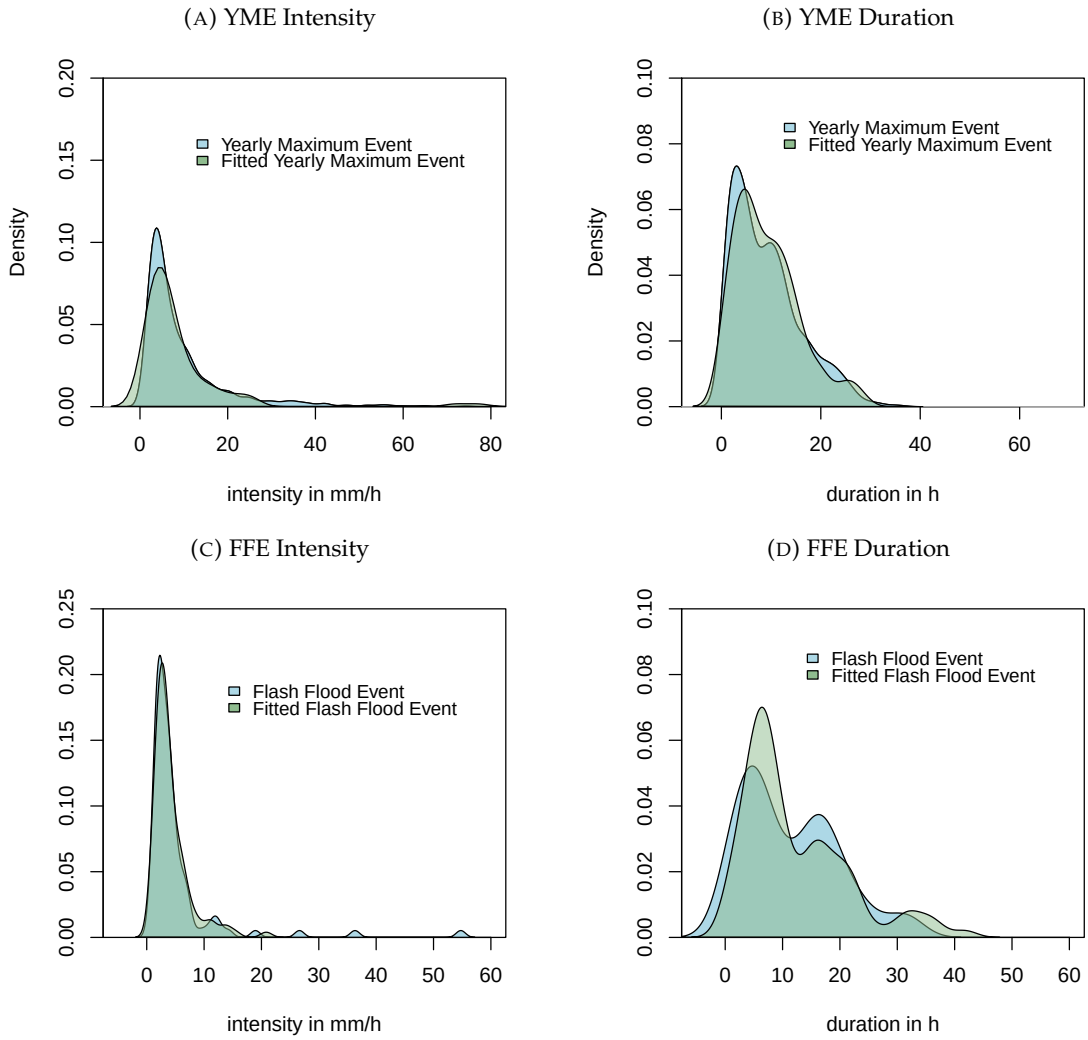

Notes: Comparison of estimated probability density function for (a) intensity of yearly maximum events (YME), (b) duration of yearly maximum events, (c) intensity of flash flood events and d) duration of flash flood events (FFE).

2.4.5 Best IDF Curve

IDF curves generated with the Normal copula, a generalized extreme-value distribution for intensity and a Weibull distribution for duration reliably quantify the joint severity of an event by linking a return period to it. The next step is to find the IDF curve above which the probability of a flood event is maximized. The highest odds ratio (0.66) is

FIGURE 2.6: IDF Curves

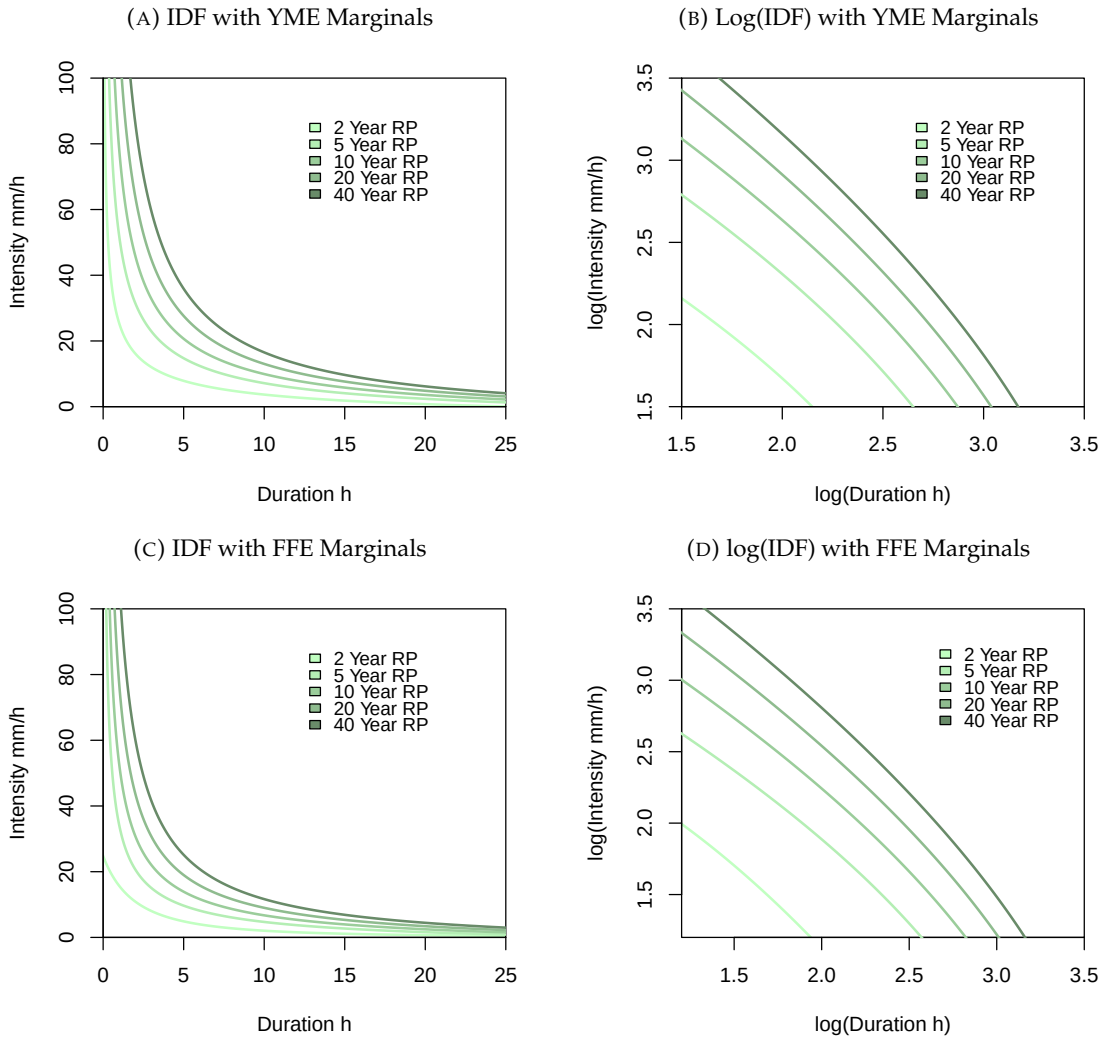

Notes: Intensity-Duration curves for frequencies corresponding to a return period of 2, 5, 10, 20 and 40 years. (a) shows these IDF curves for the Normal copula and marginals estimated from the yearly maximum events (YME), in logs in (b), and (c) shows the Normal copula from YME and marginals from flash flood events (FFE), in logs in (d).

reached with a return period of 2 years and 2 months. Rainfall events that potentially trigger flash floods are thus expected to be at least as severe as a 2.17-year return period event.[6]

[6]This threshold is naturally higher than the simple empirical analog of the 93 confirmed events in Jamaica during the 18-year period because the geographical resolution is higher: looking at smaller scale areas, each of these areas' flood probability has to be lower than that of the whole island.

2.5 Discussion

It is insightful to compare the IDF curves from this study with those that have been otherwise obtained for Jamaica. Burgess et al. (2015) provides the most recent IDF curves for Jamaica, using long-time series data from two stations in Jamaica, extending existing annual maximum records back to 1895. With a return period of 5 years and a duration of 12 h, they estimate intensities of around 7.2 - 11.4 mm/h, depending on the configuration. For a duration of 2 h and again a return period of 5 years, intensities are between 32 - 33 mm/h. For a return period of 5 years, the results from the current study suggest an intensity of 7.14 mm/h for 10 h and 22.8 mm/h for 3 h. The corresponding IDF curves are thus in a similar range but are more strongly convex than those in Burgess et al. (2015). This might be caused by the choice of the Normal copula, which is well suited to depict convex dependence. It might also be caused by the type of data input in that Burgess et al. (2015) uses data from stations in the two largest cities in Jamaica, namely Kingston and Montego Bay, while the remote sensing data employed in the current study covers the whole island. Arguably doing so can be advantageous for an average representation of the island.

The quantification of extreme rainfall hazards through the IDF curve classification has direct applications for policymakers. One may first consider the case of the CCRIF XSR parametric insurance against excess rainfall that is based on specific rainfall thresholds for payouts. The most recent version, XSR 2.5, utilizes separate exposure, vulnerability, and hazard modules for each member. For the Caribbean the module is triggered by rainfall events that exceed some country-specific average intensity threshold for a period of 12 h (short events) or 48 h (long events). These country-specific thresholds are optimized to increase the likelihood of detecting severe events while not capturing false positives. The results from the current study aims at a similar threshold identification as the XSR but differs in the methodology. However, feasibly the flash flood identification from conditional copula modeling could be coupled with a module of exposure and a specific vulnerability functional. The IDF curve can also provide thresholds for shorter than 12 h

events. For instance, a 6 h long rainfall event with an average intensity above 8.4 mm/h is potentially flash flood inducing. Such an integrated model based on the IDF curves would be an alternative verification to the CCRIF XSR and reduce model uncertainty.

The methodology proposed here could also be employed for hazard warning services. The Climate Risk Early Warning Systems (CREWS) Caribbean project aims at strengthening such services. One of the three project components is the institutional strengthening and capacity building of hydro-meteorological services and early warning systems. The simple decision rule within the intensity duration space derived in the current study could be adapted for such purposes. More precisely, given a local weather forecast for the next day and corresponding uncertainty, the risk of a potential flash flood event can be deduced. After the initial parameterization, a direct implementation into the forecasting routine comes at virtually no cost. Again, even if there exist other systems, introducing another model based on a different methodology can greatly reduce model uncertainty.

It must be pointed out that the proposed methodology suffers from two main shortcomings. The focus on rainfall events as measured at a certain location ignores general meteorological conditions as well as conditions on the ground. Additional information such as antecedent rainfall and soil moisture, soil type, or slope gradients can be employed to get a more precise decision rule. Likely, these factors play a crucial role in the actual development of a hazard given a specific rainfall event. The current methodology with a bivariate copula at its core is not directly suited for additional variables. While trivariate and higher dimensional copulas do exist, they are much less understood. Trivariate copulas also impose some limits on the attainable negative dependence. Furthermore, adding another variable to the copula requires a disproportionately larger sample, where the sample density decreases exponentially with the number of dimensions. One should note that several of these shortcomings such as the sample density apply to other methodologies as well. Another potentially more fruitful route might be to consider separate copula functions for different classes of topography or meteorological conditions instead of a unified model that explicitly accounts for these interdependencies.

The procedure also omits the role of tropical cyclones (TCs). It has long been recognized that in the Caribbean many instances of extreme rainfall and consequential flooding are due to TCs (Arenas, 1983; Laing, 2004). Ideally, a classification scheme would take into account synoptic scale weather events. If the proposed classification scheme for flash flood incidents will be used to estimate the effect of extreme rainfall on the economy or for insurance schemes, evidence is necessary to distinguish it from TCs. While the current study did verify via newspaper articles that the flash flood incidents are largely non-TC events, additional care is necessary for applications. For instance, Collalti and Strobl (2022) studies the economic impacts of flooding during tropical storms in Jamaica and finds that only a minor number of heavy rainfall events occur during tropical storms of hurricane strength compared to the number of flash flood incidents discussed in this study.

2.6 Conclusion

This study uses 93 confirmed flash flood events in Jamaica over the period 2001 to 2018 to estimate intensity-duration-frequency (IDF) curves via conditional copula sampling. Rainfall information of flash flood events is taken from remote sensing and additional data on location-specific yearly maximum rainfall events was constructed. This considerably larger sample of statistically similar events allows for higher robustness in the estimation. It further enables one to find an IDF curve threshold above which flash flood events become likely. This threshold corresponds to a return period of $2\frac{1}{6}$ years. A comparison with IDF curves for Jamaica in Burgess et al. (2015) yields similar results in terms of absolute level, but these are less convex with regard to extremely intense or long events. The simple nature of connecting the copula method for IDF curves with a classification for flash floods potentially opens up many applications in parametric insurance programs and regional risk mapping, as well as hazard warning systems. The current study abstracts from event-determining conditions other than local rainfall intensity and duration. Future research should therefore aim at including other factors,

such as soil type and terrain ruggedness in the conditional copula modeling, as well as incorporate synoptic scale meteorological conditions.

Chapter 3

The Economic Dynamics after a Flood: Evidence from Satellite Data

---

"*And, when you want something, all the universe conspires in helping you to achieve it.*"

Paulo Coelho, The Alchemist

Acknowledgments: I would like to thank Martina Pons, Eric Strobl, Jeanne Tschopp, and the participants of the EAERE 2022 (Rimini), the VI Econometric Models of Climate Change Conference 2022 (Toulouse), the Swiss Climate Summer School 2022 (Grindelwald), WECON 2023 (Kingston), as well as seminar participants at the University of Bern, for their valuable comments. This research did not receive any specific grant from funding agencies in the public, commercial, or not-for-profit sectors.

3.1 Introduction

Natural disasters can have a profound negative impact on economic assets. The idea that they also influence economic performance and organization has entertained a number of empirical studies to estimate these second-order impacts.[1] For instance, Deryugina (2017) finds that US hurricanes lead to a substantial increase in transfers to affected counties, significantly exceeding direct disaster transfers. Another example is Hornbeck and Naidu (2014) who document black out-migration and subsequent development of agricultural technology in the aftermath of the Great Mississippi Flood of 1927. The common denominator of the literature is the focus on large-scale, rare events. It is unclear whether the results with regard to transfers, migration or economic output translate to natural hazards that are characterized by a high frequency and local impacts. In particular, common hazards that are associated with extreme weather might be absorbed by spatial equilibrium effects or temporal smoothing of investment choices. I examine the effect of such a common hazard on economic activity using a novel, physically based indicator of flash flood incidence.

According to the Emergency Events Database (EM-DAT),[2] 0.9 Million people were affected by flash floods in 2022. This is the 5^{th} most among all natural hazard subtypes after droughts (107 Million), tropical cyclones (15 Million), earthquakes (3.6 Million), and convective storms (1.6 Million) but before river floods (0.1 Million) and forest fires (0.03 Million). It has also been the 6^{th} costliest natural hazard in total damage with 273 Million USD. These costs are a lower bound since many small-scale events are not included in the database, and even if they are, much of the damage is uninsured and not recorded (Panwar and Sen, 2020). Further, total damages in EM-DAT are an accounting figure of the direct destruction, not taking into account the indirect effects on livelihoods and impediments to economic organization. With respect to climate change, it is important to

[1] The direct impact can be viewed as the direct destruction or the cost to rebuild. The indirect impact is characterized by second-order effects, the re-organization of the economy. For instance, when an establishment of a firm is destroyed due to a natural hazard, this causes disruption along the value chain. Similarly, if the infrastructure is damaged, said infrastructure does not supply its public good until it is reconstructed.

[2] Centre for Research on the Epidemiology of Disasters (CRED), UCLouvain, Brussels, Belgium – www.emdat.be

understand how indirect effects work to prepare for an increase in natural hazards. The Caribbean and Central America are especially at risk from flash floods by being one of the world's most rainfall- and thunderstorm-heavy regions. Further aggravating the risk, urbanization is often unregulated, and soil degradation is common in many parts of the region (Pinos and Quesada-Román, 2021).

While the direct physical damage from natural hazards is self-evident, the economic consequences are not. For many countries, natural disasters are a primary reason for their lower economic development and a major channel through which climate and environmental degradation impact the economy (Felbermayr and Gröschl, 2014). A growing literature has thus started to study the economic impacts of various kinds of natural disasters: tropical storms (Nordhaus, 2010; Strobl, 2012; Hsiang and Jina, 2014; Deryugina, 2017), earthquakes (Barone and Mocetti, 2014; Fabian, Lessmann, and Sofke, 2019), droughts (Barrios, Bertinelli, and Strobl, 2010; Hornbeck, 2012) and urban floods (Kocornik-Mina et al., 2020). The literature that aims at estimating the effect of extreme rainfall and those estimating effects of flood events constitute two groups. Those concerned with extreme rainfall use aggregated weather data, for instance, the region-specific deviation in monthly rainfall, to estimate economic impacts of weather anomalies (Dell, Jones, and Olken, 2012; Felbermayr et al., 2022; Kotz, Levermann, and Wenz, 2022). These studies suffer from the fact that a monthly measure cannot directly identify short, extreme rainfall events that would cause flooding. The other group that is focused on floods uses flood report data to overcome this issue (Loayza et al., 2012; Fomby, Ikeda, and Loayza, 2013; Kocornik-Mina et al., 2020). The advantage of flood report data like EM-DAT or the Dartmouth Flood Observatory (DFO) is that it identifies the natural hazard impact. But it also comes at a cost: relying for instance on media reports to identify and locate flood events introduces reporting, selection, and endogeneity biases. To give an example, both insurance penetration and damages are highly correlated with a country's development (Felbermayr et al., 2022). The EM-DAT is known to have increased in coverage quality in recent years, which can be problematic given the potential for a

spurious correlation.[3] The DFO relies on satellite imagery on cloud-free days to quantify the flooded area. Since floods often occur in combination with heavy rainfalls and thus cloud coverage, some floods go by without being noticed, while large flood events are covered. To study the economic impacts of flash floods, it is thus necessary to develop a physically consistent index of occurrence that reliably identifies extreme events.

Despite the growing interest in the economics of natural disasters, the theoretical considerations have focused on classical growth models with the event as a one-time shock to the capital stock. However, it has been shown that these standard models cannot capture the effects of short-term shocks from natural hazards adequately to derive long-term impacts (Cavallo et al., 2013). In that sense, the question at hand has to be answered empirically for the various natural hazards. Each hazard is unique in the sense that some destroy a larger share of capital, some damage a larger share of public infrastructure, and others displace more people. It has also been recognized that with climate change making natural hazards more common in many parts of the world, jointly considering events based on their frequency and intensity is crucial when estimating the effects on growth. For instance, in a Solow-like model that allows for non-equilibrium dynamics, Hallegatte, Hourcade, and Dumas (2007) show that there is a sharp increase in GDP loss if natural hazards intensity or frequency increase above a certain threshold. The capacity of an economy to cope with a natural hazard, determining the threshold, is linked to its development (Hallegatte and Dumas, 2009). For instance, the more developed economy can cope better with severe shocks such as hurricanes as it has the necessary means for quick reconstruction. A similar argument will be made regarding shocks that are defined by their high frequency, such as flash floods.

To frame the analysis, there are four hypotheses regarding the total effects a natural disaster might have on the economy: a return to the same output level after a decline, a decline in output level without recovery, or an increase in the level of output either immediately or after some time of initial decline. This is closely linked to the question of

[3] For instance, there is a positive relation between global warming and the number of reported EM-DAT hazards that is in part due to the increased coverage quality.

whether there is an impact on the level or the growth rate of output. The same question has already been drawn without a conclusion focusing on high-impact natural disasters (Skidmore and Toya, 2002; Crespo Cuaresma, Hlouskova, and Obersteiner, 2008; Klomp, 2016). A critical part of this exercise is considering localized impacts on a high temporal resolution to adequately depict the reaction to the shock. Small-scale, high-frequency natural disasters are likely averaged out when considering country-by-year panel data. Further, temporal as well as spatial spillovers become more informative with regard to the mechanism through which the natural hazard has an indirect impact on the economy. My results thus draw from the dynamic effects estimated with high-resolution satellite data.

A critical part of the methodology is to detect extreme rainfall events that likely trigger flash floods. I use the flash flood intensity-duration classification from Collalti, Spencer, and Strobl (2023) as a physical measure for flood incidence. This classification is based on intensity-duration-frequency (IDF) curves from conditional copula sampling and information on 93 confirmed flash flood events in Jamaica from 2001 to 2018. Jamaica shares a similar topography, soil composition, and climate with the whole region of Central America and the Caribbean such that the classification is well-calibrated. I use rainfall information from the Integrated Multi-satellitE Retrievals for GPM (IMERG), which employs the Global Precipitation Measurement (GPM) constellation satellite data. In the period 2000 - 2021, I find that out of the 64 M cell-wise rainfall events in Central America and the Caribbean, 2.3 M or approximately 1.7% can be classified as a flash flood.

In the empirical exercise, I estimate a flash flood's effect on aggregate economic activity by using satellite images of night lights at a monthly frequency from the VIIRS Day/Night Band (DNB). Controlling for tropical storms and various types of fixed effects, I find that night lights decrease significantly by up to 5.7% in the following months for low and medium-development countries. Afterward, there is a quick recovery within the first year. A back-of-the-envelope calculation implies that there is a decrease in the

GDP growth rate by -0.84 percentage points for low- and medium-development countries in the region attributable to flash floods. For high and very high-development countries, I do not find a pronounced reaction in night lights after a flood.

These results are important for a number of reasons. First, the findings contribute to the literature on physically modeled natural disasters in economics (Nordhaus, 2010; Hsiang and Jina, 2014; Eichenauer et al., 2020). Second, extreme rainfall events and the associated pluvial floods are, after droughts, the extreme event most likely to increase in probability and intensity due to climate change. For instance, the 6^{th} IPCC Report states that *"Projected increases in direct flood damages are higher by 1.4 to 2 times at 2°C and 2.5 to 3.9 times at 3°C compared to 1.5°C global warming without adaptation."*.[4] It is important for economists to quantify how direct flood damages affect the economy indirectly. Knowledge regarding the propagation of such a natural hazard shock through the economy is necessary to adequately inform policymakers about climate change risks.

The remainder of the paper is organized as follows: Section 3.2 gives a background of flood types and presents the conceptual framework. Section 3.3 describes the data and provides summary statistics. In Section 3.4, the identification strategy is detailed, whereas Section 3.5 provides results which are discussed in Section 3.6. Finally, Section 3.7 concludes.

3.2 Background

The study region of Central America and the Caribbean is characterized by its proximity to the sea: no location is further away than 200 km from it (Encyclopedia Britannica, 2022). The climate is generally tropical, though tempered by elevation, latitude, and local topography. Rainfall occurs in a dry and wet season pattern and is heaviest between May and November. Topography is diverse: most countries have humid lowlands along the coast, while there are pronounced hills and mountain ranges. Natural vegetation is equally varied. Tropical forests occupy lowlands, while evergreen forests clothe hills and

[4] IPCC 6^{th} Report, Summary for Policymakers.

mountains. However, much of Central America and the Caribbean's timberland has been cleared for crop cultivation.

3.2.1 Typology of Floods

Let us consider the phenomenon of floods in detail and how the flood hazard depends on several factors. Floods come in various forms. Fluvial floods occur when the water level in a river or lake rises so much that it overflows and floods its surrounding area. Because river systems are connected to each other and overflow upstream cause overflows further downstream, these types of floods are analyzed on the catchment level. The severity of a fluvial flood is determined by the duration and intensity of rainfall in the catchment area and modulated water run-off. Coastal floods are due to the inland flow of seawater. Commonly, they are caused by storm surge and high tide. Inundation is particularly severe if these two factors coincide. The storm surge is created when a storm's wind builds up water on the windward side and pushes it in front of itself. The severity of a coastal flood is determined by the storm's wind speed and pressure as well as coastal topography. Lastly, there are pluvial floods, the subject of this study. A pluvial flood is caused by an extreme rainfall event, which can be further characterized into two types. Surface water floods are caused when rain falls over a prolonged period of time such that the drainage systems and general runoff are not able to deal with the amount of water, resulting in a shallow, standing flood. flash floods on the other side are characterized by shorter, more intense extreme rainfall events. Torrential rainfalls trigger these especially dangerous floods due to their quick onset and ravageous, debris-sweeping flow. They are an especially localized phenomenon that can occur almost everywhere and is hard to forecast.

3.2.2 Conceptual Framework

It is of particular interest to measure the effect of a natural hazard over time. That is, taking into account indirect losses - sometimes called higher-order effects - following causative after the hazard's destruction. Closely related to this is the question of

whether a hazard affects the output level or the growth rate in a neoclassical growth model (Klomp and Valckx, 2014). In the empirical literature studying the impacts of natural hazards, there are four hypotheses that describe the long-term evolution of output following the hazard (see e.g., Hsiang and Jina (2014)). The *creative destruction* hypothesis states that a disaster may temporarily stimulate economic growth since it acts as a demand shock due to aid flows and that it stimulates innovation (Skidmore and Toya, 2002). The *build-back-better* hypothesis suggests that a disaster may, after an initial decline in output, temporarily stimulate the economy to grow at a faster rate because lost capital gets replaced by better vintage (Crespo Cuaresma, Hlouskova, and Obersteiner, 2008). The *recovery to trend* hypothesis argues that growth declines in the beginning due to lost capital but then rebounds when, due to the higher marginal product of capital, the capital stock accrues until the same trajectory is reached again. Finally, the *no recovery* hypothesis states that the destruction of productive capital and durable goods reduces output. There is no rebound here because the positive effects that can occur in the other hypothesis are dominated by the direct loss of capital. For instance, destroyed capital to be replaced is then missing for investments elsewhere such that the economy will always lag behind.

3.2.3 Growth Theory

It is peculiar that neoclassical growth theory can be consistent with each of these four scenarios (Botzen, Deschenes, and Sanders, 2019). In its simplest form, a natural hazard is a shock to the capital stock. A standard model with a Cobb-Douglas production function with fixed savings and depreciation rate supports the *recovery to trend* hypothesis since exogenous technology determines the production frontier. If one endogenizes technical change by introducing vintage capital into the model, then one is in the *build-back-better* case: vintage capital represents the best technology at the time and, with technology becoming better with time, a large update of capital due to a natural disaster will increase productivity.[5] However, if one uses an AK representation instead of vintage capital to

[5]See the discussion in Botzen, Deschenes, and Sanders (2019) for a thorough treatment and a list of references.

make technology endogenous, then the *no recovery* hypothesis is supported. In *AK* models, the production function is supplemented with a productivity parameter A, which is linked to the level of accumulated capital K. When a natural disaster lowers the level of capital, productivity and, thus, output decreases permanently. In essence, growth theory cannot a priori say which model is appropriate for a specific natural hazard. Therefore, we should focus our aim on empirical evidence.

3.2.4 Weather vs. Hazard

Flash flood events are a different kind of hazard from those commonly studied in economics: they are frequent and highly localized phenomena instead of rare, disastrous events on, at least, the regional level. There is a duality between extreme rainfall, the weather event, and the flash flood, the hazard event. The difference in location-specific climate as a part of characteristics captured by local geography can explain large differences in economic outcomes (Dell, Jones, and Olken, 2014). An extreme rainfall event, like all weather events, is drawn from the climate distribution, albeit from its upper tail. Arguably, flash floods sit right in the middle between weather variation and large-scale natural hazards. One might therefore question whether the empirical evidence from the literature focused on weather anomalies or the literature on hurricanes and earthquakes can be translated to flash floods. I argue that the uniqueness of flash floods in terms of their high frequency as well as their small spatial scale justifies an analysis of its own. I find that of the 63 M rainfall events in the data, 98.3% are not hazardous, but there is often at least one potential flood event per year per location. Even if the effect of a flood is transitory and disappears after some time, the effect of flash floods as a phenomenon is akin to permanent. With this, I suggest that economic impact should not be thought only in terms of a single event but rather in terms of the phenomenon.

3.2.5 Spatial Scale

Flash floods are also defined by their localized impact. On one side, this directly requires a higher spatial resolution in the analysis. Sub-national level 1 and even level 2

government bodies (such as states and counties in the US) can be inadequate when considering flash floods. On the other side, there are implications of the localized direct impact of flash floods for spatial spillovers. If certain mechanisms through which natural hazards indirectly affect the economy work on a larger scale than the hazard itself, spatial spillovers allow us to touch on these. For instance, if a relatively small area is affected by a flash flood and a part of the road network cannot be used such that firms and households outside the hit area are indirectly affected, there will be a spillover effect attributable to changes in transportation cost. As shown subsequently, both spatial and temporal resolution is key in this exercise to adequately focus on the temporal dynamics as well as spatial spillovers.

3.3 Data

Three categories of variables are employed for this study. The first is concerned with hazards. This includes a satellite-derived rainfall measure and the subsequent creation of a flash flood indicator as the variable of interest. Also, I create an index of hurricane destructiveness. The second category is the economic variable, where I use night light data to infer changes in economic activity. Third, auxiliary data on topography and land use serve as sources for potential heterogeneity that I will explore.

3.3.1 Flash Floods

Flash floods are measured via a binary classification that indicates whether, in the course of a month, an episode of heavy rainfall likely triggered some flash flood at a location. The classification is from Collalti, Spencer, and Strobl (2023) who employ a hydrostatistical methodology and exhaustive data on confirmed flash flood events in Jamaica to estimate a decision rule for the optimal classification of flood incidence. Specifically, the procedure starts by first defining appropriate rainfall events that relate to weather conditions via an inter-event time definition, where 12 h without rainfall delimits a rainfall

FIGURE 3.1: Map of Flash Flood Distribution

(A) Average Number of Floods (B) Floods June 2015

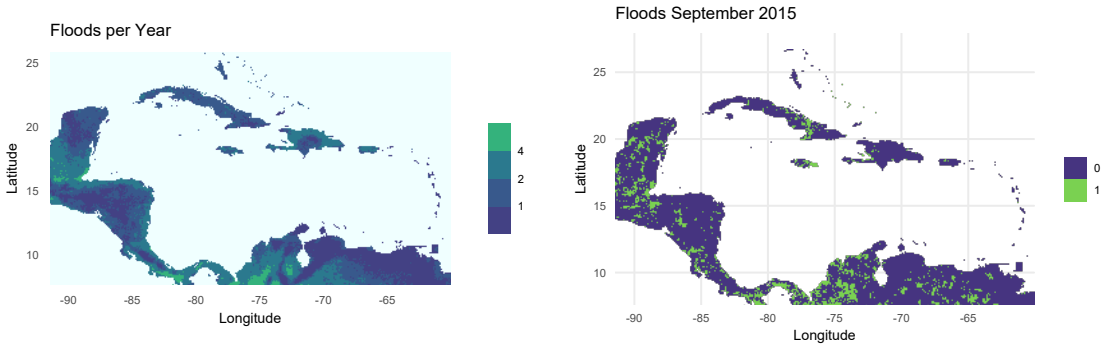

Notes: Map of the average number of flash floods per year from June 2000 to October 2021 and map of the flash flood incidents in June 2015.

event from another. By using remote sensing data from the Global Precipitation Measurement (GPM) Integrated Multi-satellitE Retrievals (IMERG) on a $0.1° \times 0.1°$ (approx. 11 km $\times$11 km at the equator) grid with half-hourly data, coverage is consistent for the whole study region (Huffman et al., 2015b). Local extreme events are then used to estimate the dependence between the intensity (mm/h) of such an event and its duration (h) via copula functions. The common method of generating intensity-duration-frequency (IDF) curves for some frequency corresponding to a return period is used to flexibly characterize the dependence structure. One IDF curve assigns for every duration of an event an intensity given a certain return period. This relationship is negative and concave. Finally, the IDF curve which best predicts the data on confirmed flash floods in Jamaica serves to classify rainfall into potential flood events. As a decision rule, I require that a rainfall event must have an intensity of at least 2 mm/h above the IDF curve to be classified as a flash flood in order to reduce the number of false positives. If an event is above this threshold, then I treat it as a flood-inducing rainfall event.[6]

I employ this decision rule on the same satellite-based rainfall estimate to recover flood events. The satellite precipitation algorithm combines various microwave and infrared

[6]Results do not change qualitatively for a threshold of 5 mm/h and can be found in section 3.5.3 of the results.

precipitation measurements to produce precipitation estimates, adjusted with surface gauge data. The sample period is June 1^{st} 2000 to June 30^{th} 2021. For every month with one rainfall event above the threshold, the corresponding GPM/IMERG grid cell area is considered treated by a flash flood.[7] In the study region, which is one of the most rainfall-intense regions in the world, locations experience a flash flood 1.7 times each year on average, according to the index. There is considerable spatial variation for the average occurrence probability but also spatial clustering for a given month, as Figure 3.1 shows. Table 3.1 provides summary statistics of all rainfall events.

TABLE 3.1: Flash Flood Summary Statistics

Statistic	Mean	St. Dev.	Min	Median	Max
Flash Flood Rainfall Events (N = 1'056'508)					
Intensity mm/h	6.61	3.31	3.93	5.50	113.18
Duration h	16.60	11.14	1.00	13.50	214.50
Year	2009.44	5.79	2000	2009	2021
Month	7.02	2.99	1	7	12
Longitude	−80.15	8.28	−91.95	−81.55	−58.05
Latitude	16.07	8.07	7.05	14.25	31.95
Non Flash Flood Rainfall Events (N = 63'049'303)					
Intensity mm/h	1.21	1.36	0.10	0.77	190.22
Duration h	6.65	10.84	0.50	3.50	3'875.00
Year	2010.49	6.12	2000	2011	2021
Month	6.83	3.05	1	7	12
Longitude	−78.00	9.22	−91.95	−79.65	−58.05
Latitude	15.73	7.54	7.05	13.95	31.95

Notes: Characteristics of flash flood and non-flash flood rainfall events.

3.3.2 Night Lights

The source of night light data is NASA's Black Marble product. Black Marble processing of the Visible Infrared Imaging Radiometer Suite (VIIRS) Day-Night Band (DNB) removes cloud-contaminated pixels and corrects for atmospheric and other light effects

[7] Flash floods that start in one month and end in the next are only assigned to the month when the rainfall event started.

such as gas flares, is calibrated across time, and validated against ground measurements (Román et al., 2018). The VIIRS DNB provides global daily measurements of nocturnal visible and near-infrared light. The VIIRS DNB is said to be ultra-sensitive in low light conditions making it suitable for monitoring remote areas as well as highly urbanized locations.

I use version VNP46A3, which provides monthly composites generated from daily observations. Monthly composites remove much of the noise in daily observations and also ensure continuous measurements even when there is cloud coverage for several days in a row, which is not uncommon in the tropics. Black Marble has been available globally since January 2012 on a 15 arc-second (approx. 500 m) linear latitude-by-longitude grid. Figure 3.2 shows lights at night in January 2012, where radiance was top-coded at 800 $W/(cm^2 - sr)$ to shrink the color scale and make differences at lowly lit places visible as well. For the analysis, all cells that are not on land are removed - both ocean and lakes.[8]

3.3.3 Tropical Storms

In analyzing the effect of floods which are due to extreme rainfall in the Caribbean and Central America, it is necessary to separate the flood effect from the effect of tropical storms' wind destruction. I follow Strobl (2011) in calculating the local wind exposure during a storm with the Boose, Serrano, and Foster (2004) version of the Holland (1980) wind field model. The model estimates the location-specific wind speed by taking into account the maximum sustained wind velocity anywhere in the storm, the forward path of the storm, the transition speed of the storm, the radius of maximum winds, and the radial distance to the storm's eye. The model further adjusts for gust factor, surface friction, asymmetry due to the storm's forward motion, and the shape of the wind profile curve. The source of storm data used is the HURDAT Best Track Data (Landsea and Franklin, 2013). These 6-hourly track data are linearly interpolated to hourly observations. $WIND_{cst}$, the wind experienced at any point i, during storm j at time t is given by:

[8] Due to ships, some cells do have night light activity even if not on land.

FIGURE 3.2: Map of Night Lights

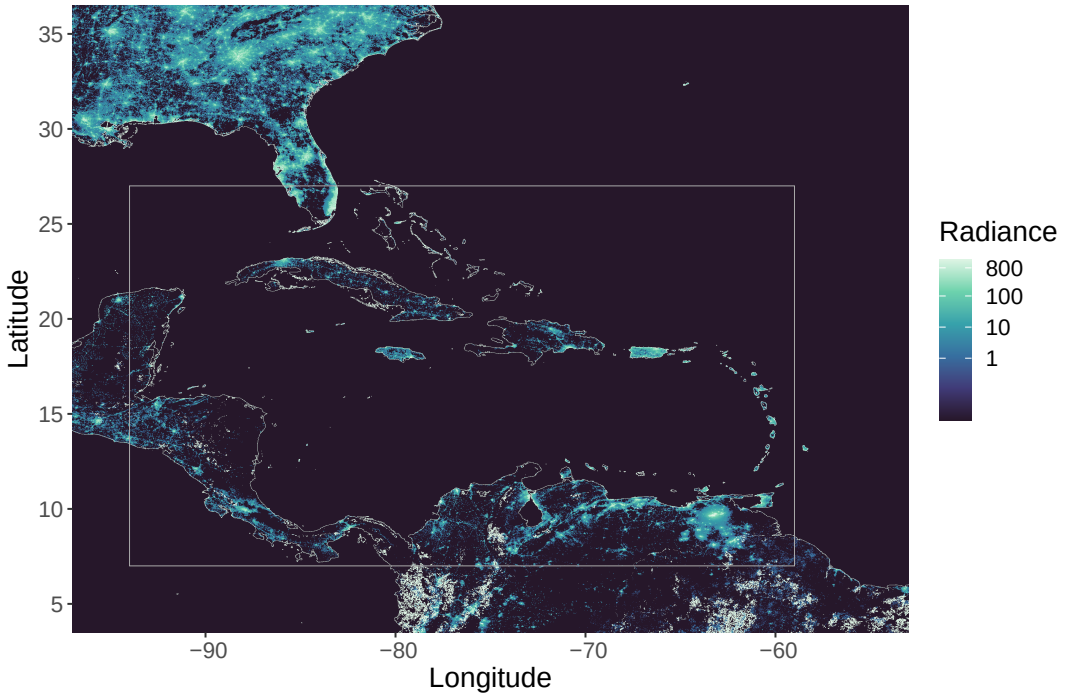

Notes: Night light map in January 2012 where the grey polygon indicates the study region.

$$V_{ijt} = GD\left[V_{mjt} - S\left(1 - \sin(T_{ijt})\right)\frac{V_{hjt}}{2}\right] \times \left[\left(\frac{R_{mjt}}{R_{ijt}}\right)^{B_{jt}} \exp\left\{1 - \left[\frac{R_{mjt}}{R_{ijt}}\right]^{B_{jt}}\right\}\right]^{1/2} \tag{3.1}$$

where V_{mst} is the maximum sustained wind velocity anywhere in the storm, T_{ijt} is the clockwise angle between the forward path of the storm and a radial line from the storm center to the i-th cell of interest, V_{hjt} is the forward velocity of the TC, R_{mjt} is the radius of maximum winds, and R_{ijt} is the radial distance from the center of the storm to point i. The remaining ingredients in Equation (3.1) consist of the gust factor G and the scaling parameters D for surface friction, S for the asymmetry due to the forward motion of the storm, and B, for the shape of the wind profile curve. Appendix C.1 provides additional

information on the model parameters.

The wind speed is then translated to an index of economic impact via the non-linear damage function by Emanuel (2011):

$$wn_{it} = \frac{v_{ijt}^3}{1 + v_{ijt}^3} \times 100 \tag{3.2}$$

with

$$v_{ijt} = \frac{\max(V_{ijt} - V_{thresh}, 0)}{V_{half} - V_{thresh}} \tag{3.3}$$

where V_{ijt} corresponds to the maximum wind speed of hurricane j in location i at time t. Then, $V_{thresh} = 92$ km/h is the lower threshold below which no damages are occurring, whereas $V_{half} = 203$ km/h is where 50% destruction is expected. Conveniently, a one-unit increase can be interpreted as a 1% increase in damages. The maximum v_{ijt} in a given month represents the tropical cyclone impact in subsequent analysis.

3.3.4 Topography

Data on topography are from Amatulli et al. (2018). They provide a suite of global topographic variables at a resolution of 1 km to 100 km, namely elevation and terrain ruggedness. The terrain ruggedness index (TRI) is defined as the mean of the absolute differences in elevation between a focal cell and its 8 surrounding cells. Elevation and TRI were gathered on the highest resolution of 1 km $\times$ 1 km, and then the average for each GPM/IMERG rainfall cell was calculated.

3.3.5 Land Cover

Data on the land cover are from the Copernicus Global Land Cover Layers - Collection 2 (Buchhorn et al., 2020). They provide global maps at a resolution of 100 m $\times$ 100 m for 23 land cover classes (discrete classification) or alternative 10 base classes for fractional classification. Classification accuracy is 80% for the discrete case. The base classes include built-up, permanent water, tree and cropland cover, which is sufficiently detailed for this

TABLE 3.2: Summary Statistics

Flash Flood Cell × Month Observations (N = 205′784)					
Statistic	Mean	St. Dev.	Min	Median	Max
Night Light	4.15	32.72	0.001	0.69	5′355.50
Wind Index	0.02	1.20	0.00	0.00	319.76
# Historical Floods	30.47	14.41	0	29	79
Longitude	−78.89	8.41	−91.95	−77.65	−60.05
Latitude	12.77	4.90	7.05	10.75	26.75
Year	2015.82	2.80	2012	2016	2021
Month	7.29	2.82	1	7	12
Elevation m	247.52	350.47	−0.52	113.54	4′145.80
Terrain Ruggedness	14.28	16.28	0.00	6.37	98.53
Non Flash Flood Cell × Month Observations (N = 1′356′244)					
Statistic	Mean	St. Dev.	Min	Median	Max
Night Light	7.08	65.92	0.001	0.66	7′010.11
Wind Index	0.01	0.78	0.00	0.00	327.47
# Historical Floods	21.54	13.18	0	20	79
Longitude	−77.08	9.42	−91.95	−76.05	−60.05
Latitude	12.98	4.78	7.05	11.15	26.75
Year	2016.33	2.74	2012	2′016	2′021
Month	6.20	3.51	1	6	12
Elevation m	344.08	510.79	−0.52	132.98	4′196.78
Terrain Ruggedness	16.44	18.97	0.00	6.93	110.82

Notes: Summary statistics grouped by treatment status.

analysis. Consolidated maps are available for the years 2015 - 2018. The map from 2018 is used for all the analysis as the most recent consolidate.[9] I use the fractional classification on the highest resolution before aggregating the fractions to the panel data cell level. That way, the fractional interpretation conserves its meaning.

[9] Arguably, land cover and flash flood severity are simultaneously and dynamically influencing each other, to some degree. Since there is no data available for the whole study period and definitely not on a monthly scale, the land cover data is static compared to the rainfall or the night light data. Note that the land cover data is only used for an exercise concerning heterogeneous effects for which the static picture of 2018 is likely a close enough approximation.

3.3.6 Summary Statistics

Table 3.2 displays summary statistics. There are 13'702 cells with 114 monthly observations starting in January 2012 and ending in June 2021 for a panel of 1.56 Million observations.[10] Out of these 1.56 Million observations, 205'784 or 15% are hit by a flash flood. Observations that are hit emit less light at night on average (4.15 vs. 7.08 $W/(cm^2 - sr)$), have, on average, been hit more frequently in the period 2000 - 2010 (30.5 vs. 21.5 times), have a lower average elevation (247.5 m vs. 344.08 m) and have a slightly less rugged terrain (14.28 vs. 16.44 TRI). In summary, the two groups of observation are not equal; local characteristics and seasonality likely affect whether a flash flood occurs. The subsequent empirical analysis has to consider these differences.

3.4 Empirical Strategy

An estimation strategy for the effect of a flash flood on subsequent months' light emissions is developed. First, we need to consider the nature of the phenomenon studied, our variable of interest, and its relation with the outcome. The variable of interest is a binary indicator of whether, within a given month and a certain location, a rainfall episode was so extreme that a flash flood had to be expected within the area. For identification, a Difference-in-Difference (DiD) setup with a two-way fixed effects model (TWFE) is suggested. The panel structure of the data readily allows for the estimation of such a model with ordinary least squares (OLS). There are three assumptions that have to be fulfilled for a causal interpretation of the effects: no anticipation effect, parallel trends, and linear additive effects. In the case of an extreme weather event, this is feasible. Weather, especially extreme rainfall, is nigh impossible to forecast for horizons longer than two weeks. There is seasonality in the likelihood of an extreme event, with seasons that are heavy in rain and seasons that are dry. Further, not all places bear the same risk: some areas that are close to mountains or in the path of persistent, high-moisture wind systems

[10] The rainfall data has been available since 2000. Thus, lags of flood events prior to 2012 have been supplemented to the panel.

are more likely than others to experience extreme rainfall. Even then, knowing the underlying probability of extreme events in a location or during a specific time of the year does not allow us to predict the occurrence of a single event with sufficient confidence in weather forecasts. Reversing that argument means that, given location and season, there are no further observable characteristics that would lead to selection bias. Thus, there is a quasi-randomness in the occurrence of a flood that can be exploited to estimate a causal effect when controlling for observed differences in flash flood risk. This can be done in a fixed effects regression with both individual and time fixed effects:

$$log(ntl_{it}) = \sum_{j=0}^{m} \beta_j f_{itj} + \gamma_i + \delta_t + \varepsilon_{it}. \tag{3.4}$$

where $log(ntl_{it})$ is the natural logarithm of night light at cell i at time t, f_{itj} are lagged flash flood indicators up to a length of m months afterwards and $\sum_{j=0}^{m} \beta_j$ are the corresponding constant coefficients. The γ_i are unobserved cell fixed effects, δ_t are the unobserved time fixed effects, and ε_{it} is the error term. Note that this and all subsequent regressions are estimated with ordinary least squares (OLS). This specification removes location and time-specific averages, reducing the remaining variation to estimate the coefficients of interest and potentially allowing for a causal interpretation. Cell-specific γ_i control for time-invariant effects that might be correlated with flood impact and economic activity. These fixed effects remove variation in night light emission that is correlated with the likelihood of a flash flood occurrence but is not causally linked to it. For instance, if a region experiences frequent flood events but enjoys prosperous economic development due to natural resources, then one should control for such region-specific effects. Similarly, δ_t controls for time fixed effects that are location invariant and might be correlated with flood destruction and economic activity. For instance, floods are more common during the rainy season when fewer tourists arrive.

Likely, several episodes of extreme rainfall are attributable to tropical cyclones (TCs). In order to separate the effect of TC wind damage from extreme rainfall, I include lags of

the wind index derived in Section 3.3.3. Also, there might be a spatial spillover of flood events across cells, for which I also include lags:

$$log(ntl_{it}) = \sum_{j=0}^{m} \beta_j f_{itj} + \sum_{j=0}^{m} \alpha_j wn_{itj} + \sum_{j=0}^{m} \nu_j nfl_{itj} + \gamma_i + \delta_t + \varepsilon_{it}. \tag{3.5}$$

where α_j gives us the effect of a 1% increase in economic damages due to TC winds j periods ago and ν_j the local effect for a flood event in a neighboring cell.[11]

Let us turn our attention to the dependent variable. Monthly emissions at night are the average of all daily measurements without cloud coverage. For approximately 6.3% of observations, there is not a single cloud-free night. Therefore, I fill in missing night light values as the average between the preceding and succeeding non-missing observations. This might be problematic because cloudy periods are correlated with high rainfall episodes. In the data, the linear correlation between a flood occurrence and no night light measurement for that cell is with 0.056 relatively modest but statistically significant due to the large sample size. Even after this processing, the underlying night light data remains noisy, especially for lower-level night light cells. I account for this in several specifications by first calculating a three-monthly moving average of night light.[12] Both the filling of missing observations and the moving average likely induces some bias toward zero for coefficient estimates of the flood impact on night lights. This is due to the combination of a positive correlation between the occurrence of a flood and missing observations in night lights and the smoothing from filling missing values and the moving average. Since the positive correlation is relatively modest, this bias should not be problematic and behave similarly to some attenuation bias in that the estimated coefficients are shrunk toward zero.

[11] Neighbors are defined by queen-type, one field away. Each cell, therefore, has 8 neighboring cells that are directly adjacent by moving one cell in either direction. Taking into account elevation by only considering higher elevation neighbors has no impact on results (not reported).

[12] A similar strategy has been employed by Naguib et al. (2022) to estimate the dynamic impacts after a Hurricane in India via night lights.

In addition, there are two other issues. For one, it might be that some countries have higher growth rates and structural changes in the likelihood of flood events during the study period, for instance, caused by climatic variation. These potential common country-specific trends in flash flood exposure and economic activity could bias the results in both directions. I thus include country-specific linear time trends. Second, it might be that the rainy season and yearly cycles of economic activity (e.g., due to tourism) are not aligned the same across all countries. Then, the time-fixed effect does not remove all confounding variation. I thus include month of the year by province fixed effects. The province is the level one administrative sub-unit for all countries but small island states, where the province is taken to be equal to the country.[13] This gives the following model specification:

$$log(MA_3(ntl_{it})) = \sum_{j=0}^{m} \beta_j f_{itj} + \sum_{j=0}^{m} \alpha_j wn_{itj} + \sum_{j=0}^{m} \nu_j nfl_{itj} + \gamma_i + \delta_t + \pi_c time_t + \omega_{pt}(month_t \times province_i) + \varepsilon_{it}. \tag{3.6}$$

with π_c being the country c specific linear time trend and ω_{pt} the month of the year by province p fixed effect. The dependent variable $log(MA_3(ntl_{it}))$ is the natural logarithm of the three-monthly moving average transformed night light.

So far, little attention has been given to the error term. Neighboring cells likely affect the error term of the focal cell. With the current assumptions, such dependence is ruled out and potentially biases the estimation. Also, given the panel structure of the data, there is likely autocorrelation in the error term. To account for both, I use Driscoll and Kraay (1998) standard errors. The treatment of missing values in night light and the moving average specification suggest an autocorrelation length of three months.

[13] This yields a total of 282 provinces. Examples where the country equals the province include Saint Lucia and Martinique.

3.5 Results

Regression results estimated with ordinary least squares (OLS), restricted to a maximum lag length $m = 3$ for conciseness, are displayed in Table 3.3. Results in column (1) are from the simplest model in Equation 3.4. It suggests that there is a positive contemporaneous effect of 4% in the month of the flash flood that then reverses to -3% three months after. The same can be found in column (2) with the model from Equation 3.5, which adds controls for tropical storm wind speed and neighboring cells' flood incidents. An increase of the tropical storm wind destruction index by one percentage point decreases light emissions by 0.8% contemporaneously, an effect that weakens but persists over the course of the following months. Floods in neighboring cells do not appear to have any impact on the focal cell in this specification. When using the same specification but the MA_3 transformed series of night lights in column (3), the contemporaneous positive effect of a flash flood disappears. When further including the additional controls as in Equation 3.6, there is a positive contemporaneous effect for flash floods that turns negative after some months. While not providing an estimate that should be taken literally due to the arbitrary cut-off at $m = 3$, this comparison is still informative and a few points can be noted. First, introducing both wind speed and neighboring cells flood does not change the coefficients of the flood indicators. Second, transforming the dependent variable first via moving average affects the result and should be considered further when including a longer time horizon. Lastly, controlling for province-specific seasonality, the coefficients of flood incidents become less negative, indicating a correlation between flood incidents with location-specific seasonality.[14]

3.5.1 Dynamics

Figure 3.3 shows dynamic effects for longer time horizons and added leads. The full model in use is shown in Equation 3.6. Results are once with moving average smoothing

[14]The change in coefficients moving from column 3) to column 4) is mainly driven by the month $\times$ province interaction, not by the country-specific (time) slopes. Coefficients becoming less negative thus indicates that there is a negative correlation between local seasonality in the probability of heavy rainfall episodes and economic activity in the following months that is not due to a flood event.

and once with the unaltered night lights. Leads show that there are no clear pre-trends before an event, be it a flash flood or a tropical storm. The effect upon impact starkly differs between the two hazards: for flash floods, we have a contemporaneous *increase* in the level of night light emissions, while for a tropical storm, there is a contemporaneous *decrease*. In the case of a tropical storm, this decrease in the level is then recovered in subsequent months. For flash floods, the dynamics are different. After the initial increase in emissions, the effect on the level becomes -1% to -2% three to six months after the event. Then, there is a quick recovery, and no effect is discernible eight months after the flash flood. The main difference in comparing MA_3 with direct night light measures is that the MA_3 dynamics are smoother and shrunk towards zero, as expected. No systematic bias is discernible such that using the direct night light measures is preferred in subsequent analysis for easier interpretation.

3.5.2 Spillovers

A flood in a neighboring location could have opposing effects on economic activity. For one, economic activity might be displaced from the flood-affected area over to unaffected areas in its vicinity. Then, coefficients ν_j in Equations 3.5 and 3.6 would be positive, especially for the first months after an event. On the other side, a flood could impede industry linkages in the affected area and close-by locations by, for instance, impassable roads, resulting in negative ν_j. A third option is that there are no spillovers where all effects are contained with the cells of size 11 km $\times$ 11 km. Figure 3.4 sheds some light on this question. There is a contemporaneous positive effect similar to a flood in the focal cell but of a smaller size. Then the effect becomes smaller until it becomes clearly negative up to -1% nine months after the event. Interestingly, this negative effect of a flood in a neighboring cell takes place later than in the case of a flood in the focal cell. This raises the question of the spillovers' nature. Arguably, the contemporaneous effect could be due to a similar mechanism for both neighboring and focal cells. On the other side, the following dynamics suggest some sort of hierarchy where negative impacts slowly spread out from the focal.

FIGURE 3.3: Dynamic Effects of Flash Floods an Tropical Storms

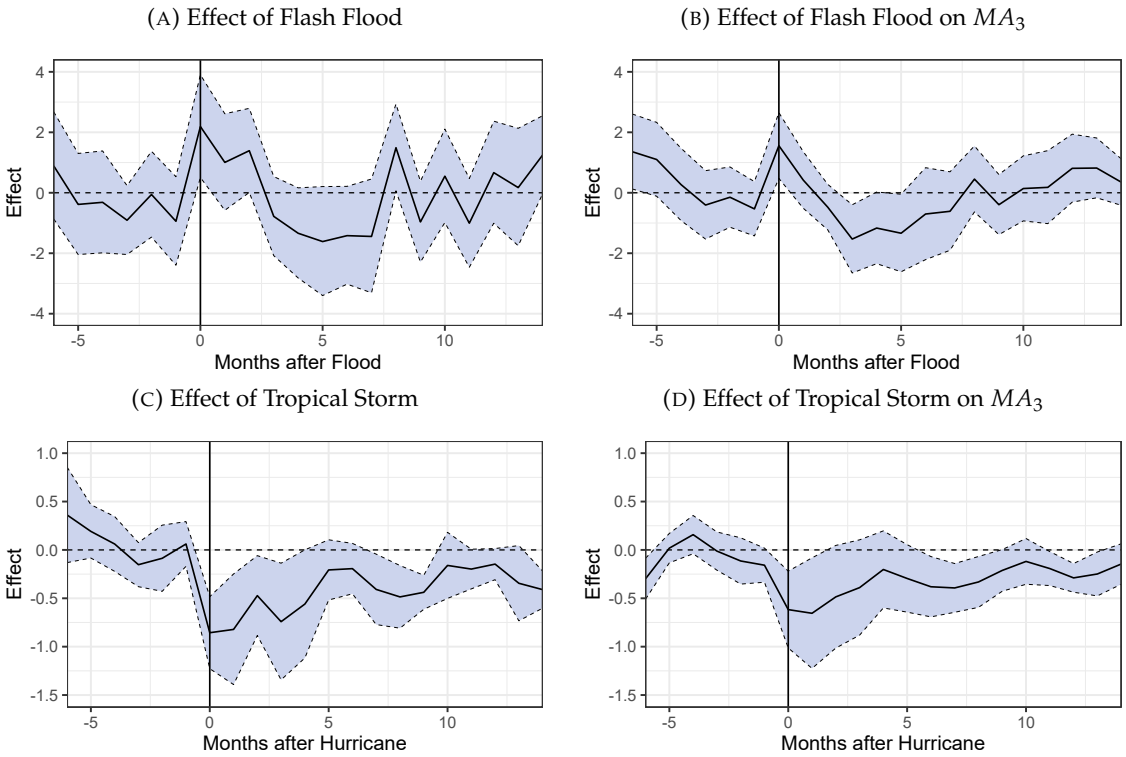

Notes: Dynamic effects of flash floods and tropical storms on night lights in percentage points. The black line plots the log-transformed coefficients with two-sided 90% confidence bands in blue. The regression model is as in Equation 3.6 with $log(ntl_{it})$ as the dependent variable in (a) and (c), and $log(MA_3(ntl_{it}))$ in (b) and (d).

3.5.3 Heterogeneity

The effect a flash flood has likely depends on local characteristics. These can include the history of previous floods, the share of built-up area, terrain ruggedness, elevation, or agricultural activity. A steeper, more rugged topography might be associated with more detrimental impacts in case of a flood. Previous exposure to floods could make households and firms more resilient or, conversely, scar their ability to recover from further shocks. Table 3.4 displays results of regressions that include interactions of the binary flood indicator with these local characteristics. Since we expect from the results so far that the effect is largest around four months post-flood, I only use the indicator fl_4 of a flood four months ago for the regression with interactions in order to keep the number

FIGURE 3.4: Dynamic Effects of Neighboring Flash Floods

(A) Effect of Neighboring Flash Flood

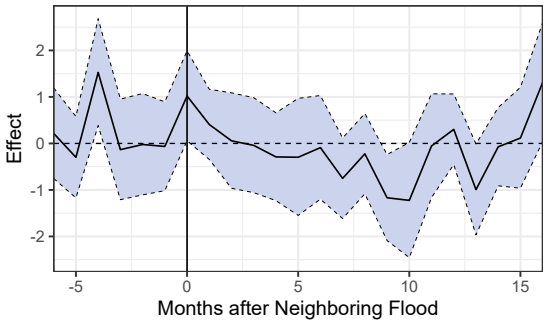

(B) Effect of Neighboring Flash Flood on MA_3

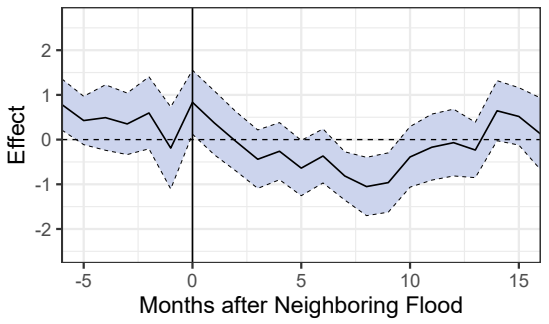

Notes: Dynamic effects of neighboring flash floods on night lights in percentage points. The black line plots the log-transformed coefficients with two-sided 90% confidence bands in blue. The regression model is as in Equation 3.6 with $log(ntl_{it})$ as the dependent variable in (a) and $log(MA_3(ntl_{it}))$ in (b).

of terms tractable for interpretation. The coefficient of fl_4 here thus gives the cumulative effect a flood has four months after the event while the interaction gives the change in cumulative effect per one unit change in the variable for heterogeneity. The local characteristics have been normalized to a mean of zero, which can be interpreted as a deviation from the mean. This will not change the direct effect of fl_4 mechanically. The coefficient of fl_4 is -2% in all but one specification. The number of floods between June 2000 and 2010 (# Hist. Floods) has no additional effect (model column 1). The same is true for the terrain ruggedness index (TRI) and elevation above sea level (models columns 2 and 3). The higher the share of built-up area, the weaker the effect of a flood (model column 4). The effect is not only statistically significant: the estimated coefficient of 0.5% lowers the flash flood effect per 1% of the built-up area, indicating that highly developed locations do not experience a reduction in night lights (the 75^{th} percentile of the area built is 0.74%).[15] Arguably, the built-up area is a measure of human settlement and economic activity. A higher development might be associated with higher quality infrastructure (paved roads vs. dirt roads, adequate drainage systems, more resilient electric grid). An alternative explanation is that emergency relief efforts for more built-up areas are better

[15]Data on land cover is from 2018. Thus, the cell fixed effects purge it from any direct impact, as it does so for elevation and TRI, and we have only the interaction for interpretation.

endowed by local decision-makers such that flash floods have less of a negative impact there. In contrast, the percentage of area covered by agricultural crops does not influence the impact of a flash flood (model column 5). The same holds for land coverage in forests, grassland, or shrubs (results not reported).

Floods in neighboring cells do not directly affect the night light level four months afterward, but its interaction with a flash flood in the focal cell is positive and statistically significant (model column 6).[16] This implies that a flood does not harm economic activity if there are floods in neighboring areas. Conversely, floods in neighboring areas are only having a negative impact if the focal area is not hit by a flood itself. There could be two interpretations of this effect. First, if a larger geographical area is subject to a hazard, there might be a more pronounced relief effort by a central state, explaining the positive interaction effect. A second interpretation is motivated by the basic reasoning of economic geography, namely that pull and push factors are involved in allocating economic activity across space. If there is only a negative shock in the focal cell but none in surrounding areas, an incentive exists for some activity to move to the unaffected area. Conversely, if all areas are hit by the negative shock in a similar fashion, no adjustment takes place.

Heterogeneity by Development

Besides heterogeneity concerning the focal cell, we can also consider heterogeneity with respect to their country's development. There is evidence that flood events mainly affect low- and medium-developed countries (Loayza et al., 2012). The human development index (HDI) is a summary measure of average achievement in key dimensions of human development and classifies countries into low, medium, high, and very high development.[17] The HDI is calculated on the country level and available for virtually all states worldwide. Some Caribbean islands are overseas territories of larger countries,

[16] Figure 3.4 suggests that a neighboring cell's flood impacts the focal cell with some longer lag. However, in this specification with interaction, I do not find any such evidence for lags of six or nine months either (not reported).

[17] The HDI itself is often the subject of critique. For instance, it does not consider inequality directly. Still, it is a measure that, compared to GDP, is more resourceful in comparing development.

such as the USA (Virgin Islands, Puerto Rico), France (Guadeloupe, Martinique), or the Netherlands (ABC Islands), for which the HDI predominantly represents mainland development. Nevertheless, these Islands boast comparatively high development and are expected to be similarly impacted to other very high-development states in the region, such as the Bahamas or Panama. Regressing an interaction between the HDI category as of 2021 and flash flood incidence onto log night light models potential heterogeneity in effect by country development. Again, I use the indicator of a flood four months ago fl_4 for interaction.

TABLE 3.3: Regressions: $m = 3$

	$log(ntl_{it})$		$log(MA_3(ntl_{it}))$	
	(1)	(2)	(3)	(4)
fl_0	0.04*** (0.02)	0.04*** (0.01)	0.005 (0.01)	0.02*** (0.005)
fl_1	-0.002 (0.01)	-0.002 (0.01)	-0.02** (0.01)	0.004 (0.005)
fl_2	-0.01 (0.01)	-0.02 (0.01)	-0.03*** (0.01)	-0.005 (0.004)
fl_3	-0.03** (0.01)	-0.04*** (0.01)	-0.04*** (0.01)	-0.01** (0.006)
wn_0		-0.008*** (0.002)	-0.005*** (0.002)	-0.006*** (0.002)
wn_1		-0.006** (0.003)	-0.004* (0.002)	-0.006** (0.003)
wn_2		-0.001 (0.002)	-0.002*** (0.0007)	-0.004 (0.003)
wn_3		-0.004*** (0.0006)	-0.003*** (0.0006)	-0.004 (0.002)
nfl_0		0.001 (0.009)	0.007 (0.005)	0.01*** (0.004)
nfl_1		0.0004 (0.007)	0.006 (0.005)	0.006 (0.004)
nfl_2		0.002 (0.006)	0.005 (0.005)	0.0006 (0.003)
nfl_3		0.007 (0.007)	0.004 (0.005)	-0.003 (0.003)
Observations	1,466,766	1,466,766	1,394,986	1,394,986
R^2	0.82	0.82	0.87	0.89
Fixed Effects				
Date	✓	✓	✓	✓
Location	✓	✓	✓	✓
Country				✓
Month × province				✓
Varying Slopes				
Country				✓

Notes: Table of regression results for a maximum lag length of $m = 3$ showing coefficients for flash floods, tropical storm wind speed and neighboring floods. The regression in column (1) follows Equation 3.4, column (2) follows Equation 3.5, column (3) also follows Equation 3.5 but with a moving average dependent variable and column (4) follows Equation 3.6. *p<0.1; **p<0.05; ***p<0.01

TABLE 3.4: Regressions: Heterogeneity

	$log(ntl_{it})$					
	(1)	(2)	(3)	(4)	(5)	(6)
fl_4	-0.01 (0.009)	-0.02* (0.009)	-0.02* (0.010)	-0.02* (0.009)	-0.02* (0.009)	-0.02** (0.009)
$fl_4 \times$ # Hist. Floods	-0.0006 (0.0005)					
$fl_4 \times$ TRI		-0.0007 (0.0004)				
$fl_4 \times$ Elevation			-1.6×10^{-5} (1.6×10^{-5})			
$fl_4 \times$ Built %				0.005*** (0.002)		
$fl_4 \times$ Agriculture %					-3×10^{-5} (0.0005)	
nfl_4						-0.008 (0.005)
$fl_4 \times nfl_4$						0.01** (0.005)
Observations	1,466,766	1,466,766	1,466,766	1,466,766	1,466,766	1,466,766
R^2	0.84	0.84	0.84	0.84	0.84	0.84
Fixed Effects						
Date	✓	✓	✓	✓	✓	✓
Location	✓	✓	✓	✓	✓	✓
Country	✓	✓	✓	✓	✓	✓
Month $\times$ province	✓	✓	✓	✓	✓	✓
Varying Slopes						
Country	✓	✓	✓	✓	✓	✓

Notes: Table of regression results with only fl_4 as the indicator for the interaction with various sources of potential effect heterogeneity. Variables for interaction are normalized such that the coefficient for fl_4 gives the estimate when the interacted variable is at its mean. Standard errors are in parentheses. *p<0.1; **p<0.05; ***p<0.01

TABLE 3.5: Regressions: HDI

	$log(ntl_{it})$	
	(1)	(2)
fl_4		-0.02* (0.009)
$fl_4 \times$ HDI = low	-0.07* (0.04)	
$fl_4 \times$ HDI = medium	-0.04** (0.02)	
$fl_4 \times$ HDI = high	0.01 (0.01)	
$fl_4 \times$ HDI = very high	-0.01 (0.02)	
$fl_4 \times$ HDI = Territory	-0.005 (0.04)	
Observations	1,466,766	1,466,766
R^2	0.84	0.84
Fixed Effects		
Date	✓	✓
Location	✓	✓
Country	✓	✓
Month × province	✓	✓
Varying Slopes		
Country	✓	✓

Notes: Table of regression results with only fl_4 as the indicator for the interaction with the five levels of HDI. Column (1) shows heterogenous effects from a regression with the interaction terms and column (2) the unconditional average effect from a regression without interaction. Standard errors are in parentheses. *p<0.1; **p<0.05; ***p<0.01

Table 3.5 shows results that point towards the importance of economic development in absorbing natural hazards. Results in column (1) suggest that cells that lie in low (medium) developed countries emit 7% (4%) less light at night four months after a flood, whereas cells in higher developed countries appear to not react locally to a flood. On average, for the study region, the level of night light decreases by 2% six months after a flash flood (column 2). This decrease of 2% of the level of night light emissions after four months is where the effect is most pronounced. Albeit small, this effect can still be economically significant given the high frequency of such heavy rainfall episodes. Assessing the dynamic response heterogeneity with respect to the countries' development while controlling for the dynamics due to tropical storms and spillovers would ask for a fixed effects model with many interactions where the serial correlation of the indicators

might become problematic. Instead, I use local projections introduced by Jordà (2005) and recently employed by Naguib et al. (2022) to study dynamic changes in night light due to tropical storms in India. Local projections are performed as a set of sequential regressions, where the dependent variable is shifted m steps ahead instead of introducing m lags of the flood indicator. An additional benefit of the local projection method is that they directly yield impulse-response-functions with correctly specified confidence bands. The specification I use is

$$\begin{aligned}\Delta ntl_{it+m} =& \beta_1 f_{it} + \alpha_1 wn_{it} + \nu_1 nfl_{it} + \\ & \gamma_i + \delta_t + \pi_c time_t + \omega_{pt}(month_t \times province_i) + \varepsilon_{it+m}\end{aligned} \tag{3.7}$$

where I run a series of m regressions with the coefficient β_1 associated with regression m gives the effect of a flash flood on Δntl_{it+m}, the cumulative growth between $t-1$ and $t+m$. I also estimate a variation of 3.7 with an interaction $fl_{it} \times HDI_{low,med.}$ which separates the effect a flood has on countries with low and medium HDI from those with at least high HDI:[18]

$$\begin{aligned}\Delta ntl_{it+m} =& \boldsymbol{\beta} fl_{it} \times HDI_{low,med.} + \alpha_1 wn_{it} + \nu_1 nfl_{it} + \\ & \gamma_i + \delta_t + \pi_c time_t + \omega_{pt}(month_t \times province_i) + \varepsilon_{it+m}.\end{aligned} \tag{3.8}$$

Figure 3.5 shows the dynamic effect of a flash flood on night light from local projections. As hinted by the results four months after a flood in Table 3.5, the aggregate effect is driven by those cells in low- to medium-developed countries. In both cases, there is an initial increase in night lights of 1% that quickly reverses and reaches a low of -2.6% on

[18]The only country with a low HDI is Haiti. Thus, I group it together with countries with a medium HDI: Guatemala, El Salvador, Honduras, Nicaragua and Venezuela.

FIGURE 3.5: Dynamic Effects of Flash Floods from Local Projections

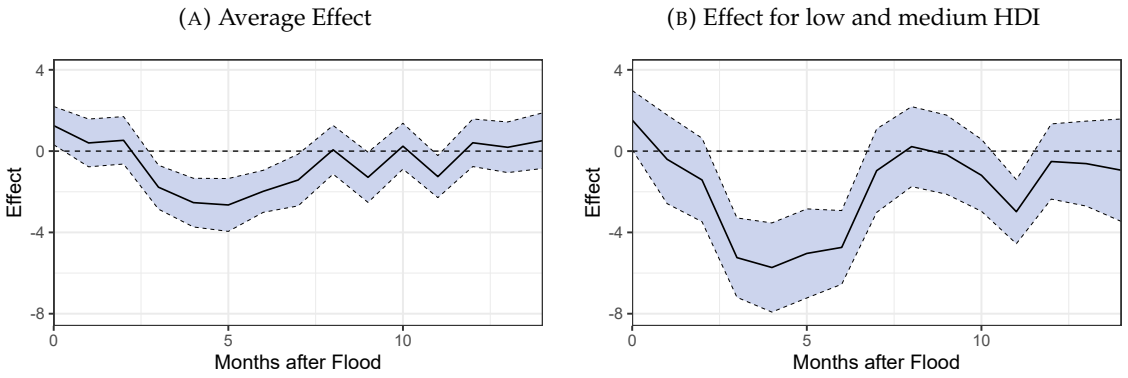

Notes: Dynamic effects of flash floods on night lights in percentage points. The black line plots the growth rate m months after a flood with two-sided 90% confidence bands in blue. (a) plots the average effects as in Equation 3.7 and (b) the effects for low and medium HDI countries as in Equation 3.8.

average and -5.7% in low- and medium-development countries. Note that in comparison to the dynamics in Figure 3.3 or 3.4, where the effect size can not be interpreted as direct impulse-response-function,[19] they can be interpreted that way with local projections. The IRFs from local projections confirm that there is indeed a 1) positive contemporaneous impact, 2) negative growth in the following months reaching its low four to five months after the event, and 3) recovery in the months following. Not only that, but the results from local projections suggest stronger and more pronounced reductions in night light emissions due to a flash flood than the results from the model in 3.6 suggest.

Alternative Event Definition

The main analysis already provides considerable robustness to the results. In this section, I provide further evidence that the event definition, when rainfall events are causing floods, is robust. In the main analysis, I require that a rainfall event needs to have an excess intensity of 2 mm/h above the threshold as determined in Collalti, Spencer, and Strobl (2023). Out of the total 63 Million rainfall events, where most are minor showers,

[19]The issue with the FE model with many lags in a dynamic setting is that the flood indicators fl_0, fl_1, etc. are serially correlated. To avoid issues with respect to growth, I chose to model night light in levels as in Brei, Mohan, and Strobl (2019).

FIGURE 3.6: Dynamic Effects of Flash Floods with Alternative Event Definition

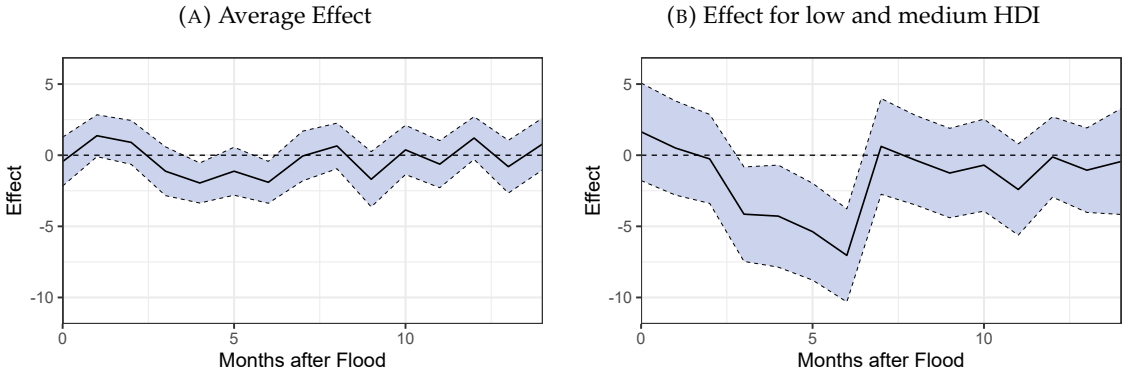

Notes: Dynamic effects of flash floods on night lights in percentage points with the definition of 5 mm/h above the classification threshold. The black line plots the growth rate m months after a flood with two-sided 90% confidence bands in blue. (a) plots the average effects as in Equation 3.7 and (b) the effects for low and medium HDI countries as in Equation 3.8.

1.06 Million or 1.7% are above this threshold. When focusing on the time period where night light data is available and aggregating these to the monthly level, around 15% of cell-by-month observations are treated by a potential flood. One might be concerned with the frequency of treatment, especially with regard to back-of-the-envelope calculations that rely on the estimated effect and the frequency of the natural hazard. Thus, I use a much more restrictive definition of 5 mm/h above the threshold calibrated with the universe of flash flood events for Jamaica since 2000. Then, only 2.9% of cell-by-month observations experience a rainfall event that likely triggers flash floods. The average return period is almost three years. Results of the local projections as in Equation 3.7 and 3.8 are shown in Figure 3.6. Confidence bands are wider, and the dynamics are the same as with the 2 mm/h classification. The effect size is, as expected, larger for low- and medium-development countries; for instance, after six months, the estimate suggests a reduction in night light activity of -7% instead of -5.7% in the main analysis. This suggests that the excess threshold of 2 mm/h is appropriate and by choosing a threshold of 5 mm/h, some hazardous events are ignored. Results are, therefore, driven by local characteristics that differ by country and not the event definition.

3.6 Discussion

The analysis has four key implications. First, episodes of extreme rainfall that likely trigger flash flooding have a sizeable negative effect on economic activity as measured by night light emissions. Second, the dynamics after the flood differs from a tropical storm. In the case of a flood, there is a brief contemporaneous positive effect that becomes negative in months four and five after before recovering in month ten. A tropical storm, in contrast, has a negative effect upon impact from where recovery is comparatively slower. This result is indicative of the different mechanisms through which either of the hazards influences economic activity. The third key implication is with regard to spatial spillovers. There is a spatial spillover from floods in neighboring areas onto the local economy but to a smaller degree. Also, there is a longer lag between event and effect than if the area had been hit directly. If several neighboring areas are hit simultaneously, then there is a *positive* spillover, reducing the negative effect of being hit. The fourth key implication is that the estimated negative effect of a flash flood is driven by locations in low- and medium-developed countries.

A natural next point is to assess how detrimental floods are in economic terms. Taking the estimates from the local projections, the total effect[20] in the year after an event is a -0.9% reduction in night lights for the study region and -2.2% for low and medium developed countries. In recent years, more attention has been given to the question of translating changes in night light emissions into economic variables such as GDP.[21] In their seminal paper, Henderson, Storeygard, and Weil (2012) lay foundations on the use of night light data to augment income growth measures. They find that the elasticity between the growth of lights and GDP growth is around 0.3. For low- and middle-income countries, there is an average of 1.27 flash floods in a cell per year, and assuming that

[20] Here, total effect relates conceptually to the integral of the IRF, which is, in the case of month-wise growth effects in the LP framework, equal to the mean effect for the first 12 months after an event.

[21] Chen and Nordhaus (2019) compare DMSP/OLS and VIIRS for predicting cross-sectional and time-series GDP data for the US. They find that VIIRS performs well at predicting metropolitan area night light growth. Gibson et al. (2021) compare the ability of the DMSP/OLS and VIIRS to predict local GDP for Indonesia and finds that the DMSP/OLS is twice as noisy as the VIIRS. They find elasticities around $0.17 - 0.19$ when using VIIRS night light to predict Indonesia's second-level sub-national GDP and elasticity of 0.5 for provincial-level GDP.

they are evenly distributed with respect to economic activity,[22] A back-of-the-envelope calculation implies that there is a decrease in the GDP growth rate by $-2.2\% \times 0.3 \times 1.27 = -0.84\%$. Note here that while each shock is transitory and can thus be thought of as a level change, the series of shocks are on such a high frequency that their cumulative impact is best represented by a change in the growth rate. To put this into perspective, the average GDP growth rate[23] for the countries in the low to medium category in the 10-year period 2012 to 2021 were: Haiti (0.82%), Guatemala (3.46%), El Salvador (2.09%), Honduras (3.26%), Nicaragua (3.16%), and Venezuela (1.02%). Clearly, pluvial floods do not explain the differences between these countries' growth rates and likely do not account for the current development. However, these countries would especially suffer if either the severity or frequency of extreme rainfall events increases.

To put the impacts of flash floods into perspective, it is informative to compare them to other natural hazards such as hurricanes and urban floods. Ishizawa, Miranda, and Strobl (2019) investigate the impacts of hurricanes on monthly economic activity in a similar setup as this study via night lights for the Dominican Republic. Their estimated effect is highly dependent on storm intensity but is said to peak 9 months after impact and go to zero after 15 months. For the average storm, the effect peaks at about -7.5%, more than $3\times$ the effect of the average flash flood as estimated in this study. Kocornik-Mina et al. (2020) studies floods in the context of cities and displacement due to flood risk. Conceptually, their focus on large-scale urban floods should lead to stronger impacts compared to the more general notion of flash floods used here.[24] They find that large floods *"... reduce a city's economic activity, as measured by nighttime lights, by between 2 and 8 percent in the year of the flood"*. The estimated average effect in the year of the flood in this study is smaller with -0.9%.

[22] Flood incidents are negatively correlated with the percentage of built area with a correlation coefficient of -0.02. There is thus more built-up area and economic activity in locations that experience fewer floods. However, the strength of the correlation is low enough that it can be ignored for this back-of-the-envelope calculation.

[23] World Bank annual national accounts data.

[24] Flash floods constructed via the IDF-curve approach likely generate more small-scale events than the subset of floods with at least 100'000 people displaced and detailed inundation maps in the DFO data as in Kocornik-Mina et al. (2020).

One can not only distinguish the differences in the effect size but also in the dynamic response after a natural hazard. There is a contemporaneous increase in night light emissions for floods which does not appear for hurricanes. Several factors can lead to this phenomenon. It is well-known that buildings and structures that have been flooded are prone to catch fire due to corrosion and damage to electrical circuits. Even a single fire in a relatively large region would lead to a significant increase in night lights. Gas flares, for instance, are a major source of night light emission in remote areas, and data on night lights have been used successfully to estimate their emissions (Elvidge et al., 2009). The second factor that leads to the phenomenon of a positive contemporaneous effect is disaster aid. While it is hard to quantify, it is easy to see that aid flowing into an area will increase light emissions for the duration of the endeavor. Still, this cannot explain why it would be different for different natural hazards. For this, we need to consider the type of destruction each hazard brings. Strong winds from hurricanes directly destroy buildings and damage overland power lines.[25] This destruction is immediately reflected in a lower night light emission. This contrasts with flash floods. While also causing destruction to buildings, flash floods directly destroy roads and other transportation structures that are only indirectly affected by hurricanes (Diakakis et al., 2020). Since most roads are unlit in Central America and the Caribbean, their destruction or deterioration does not directly cause night light emissions to fall. However, they do hamper economic activity by increasing the cost of transporting goods and commuting to work (Hallegatte et al., 2016). While in the short term of one to two months, this cost might be absorbed by firms and households, they cannot do so for a longer time. Repair and reconstruction occur but are only done six to eight months after an event. This story nicely fits the result that 1) more developed countries with a higher quality infrastructure are less affected, 2) areas with a higher percentage of built area, including paved roads, are less affected, 3) negative spillover effects from floods in neighboring areas exist but are smaller than local effects from floods. While 1) and 2) follow straightforward, points 3) concerning spatial spillovers requires explanation. In order to substantiate this line of argument, further

[25]See the Saffir-Simpson Hurricane Wind Scale, which directly describes the damage to houses and the electricity infrastructure in its classification.

research is necessary. For one, work has to be done to understand how firms are affected when there is a flood in their vicinity. A fruitful route might be to separately consider specific industries, such as the construction sector or manufacturing. Also, a better understanding of the way how gaps in the transportation network in developing countries affect economic activity is necessary.

The main strength of the paper, the construction of a flash flood indicator based on physical characteristics, is also its main weakness. On one side, it allows me to flexibly and consistently define a hazard across multiple countries. This is the first study in economics to rigorously define localized flood events from rainfall data directly. Others, such as Cavallo et al. (2013) and Kocornik-Mina et al. (2020), rely on event databases that are not necessarily consistent across time or countries. At the same time, by not directly observing the hazardous event but rather inferring it from a decision rule related to rainfall characteristics, I can not be certain to cover all events adequately. Strictly speaking, the results must be understood in terms of a rainfall event that likely causes some flooding in the cell's area. Since the classification method has been calibrated on high-quality, exhaustive data for all flood events in Jamaica since 2000, it should perform well for the study region. Extending the methodology here to other regions or doing a global analysis, however, requires appropriate calibration in each subject region (Hirpa et al., 2018).

Through empirical studies that focus on a specific type of natural disaster, we obtain a clearer picture of how various types can be discerned. The flash floods investigated here are characterized by their frequency, local occurrence, and the lagged dynamic reaction with a quick recovery. Other hazards do have different signatures. With hurricanes, it has been suggested that their imprint on the economy is important even several years afterward (Hsiang and Jina, 2014), while droughts trigger specific migratory reactions (Kaczan and Orgill-Meyer, 2020). These findings could be assessed more formally and more thoroughly in a general equilibrium growth model that takes into account different natural disasters and their potential trajectories concerning climate change. There is a great need for such an undertaking: most integrated assessment models assume climate change impacts to be a single, non-linear scalar of all outputs in all sectors in all locations.

This omits practically all insights gained in the economic natural disaster literature. In conjunction with this neglect, it has to be noted that the uncertainty for climate change projections from economic growth is magnitudes larger than the uncertainty from the natural sciences. Thus, it is necessary for economists to find precise, causal estimates for various channels through which climate change will impact the economy, natural disasters being one of them.

3.7 Conclusion

I study the dynamic effect of extreme rainfall events that lead to flash floods on local economic activity as measured by night light emission in Central America and the Caribbean. I find that such an event decreases local emissions by up to -5.7% in low and medium-development countries, while there is little effect in higher-development countries. My results further suggest that floods do cause a different dynamic reaction to hurricanes and other natural hazards. The impulse-response-function shows that, after a contemporaneous increase in night lights by 1.3%, the effect of a flood becomes -5% after three months and stays in that range until reversing back to zero in month seven. The average effect in the 12 months following a flash flood is -2.2% in low and medium-development countries. Back-of-the-envelope calculations indicate that for those countries, the total impact is equal to a reduction in the GDP growth rate of 0.84% due to the high frequency of flash floods.

I further find that flash floods cause spatial spillovers. The effect on night light emission when there is an event in a neighboring area is similar to a flood in that area itself but smaller in size and with a longer delay. This indicates that a flood disrupts production processes, for instance by destroying part of the transportation infrastructure, which affects not only those that are directly impacted. If several neighboring areas are hit simultaneously, then there is positive spillover, reducing the negative direct effect. Such negation of the negative effect of floods is consistent with reasoning from economic geography that relative differences balance out across space.

My findings have two main implications for policy. First, there is a distinctly negative effect of extreme rainfall episodes on economic activity in low and medium-developed countries. Before, the effect of extreme rainfall has often been masked by spatial or temporal aggregation. Since there appears to be little effect for higher-development countries, development in key areas could be a way out. Future research has to be conducted to investigate what those key areas are and how one can induce resilience in lower-development countries. Second, because flash floods are such a high-frequency natural hazard with return periods of less than one year in many parts of the study region, they can have direct effects on a country's growth rate. In a warming and humid climate, extreme rainfall events are projected to increase in frequency and severity. I show that such an increase will likely impact the growth of developing countries in Central America and the Caribbean. Consequentially, the cost of future emissions should take this into account.

Chapter 4

Flash Flood Hazard: an Economic Analysis for Central America and the Caribbean

---

"The first thing I learned about having money was that it gives you choices. People don't want to be rich. They want to be able to choose. The richer you are, the more choices you have. That is the freedom of money."

Trevor Noah, Born a Crime

Acknowledgments: I would like to thank Eric Strobl, the participants of the EAERE 2022 (Rimini), the VI Econometric Models of Climate Change Conference 2022 (Toulouse), the Swiss Climate Summer School 2022 (Grindelwald), WECON 2023 (Kingston), as well as seminar participants at the University of Bern, for their valuable comments. This research did not receive any specific grant from funding agencies in the public, commercial, or not-for-profit sectors.

4.1 Introduction

Natural hazards such as floods are becoming more prevalent with global warming. The direct flood damages are projected to increase non-linearly with rising global temperatures.[1] With a limited capacity to adapt to climate change, it is important to study the mechanisms through which climate change affects the economy in order to provide guidance for policymakers (Mendelsohn, 2012). The early literature on the economic consequences of natural disasters has studied them via cross-country models, where the results are somewhat mixed (Albala-Bertrand, 1993; Noy, 2009; Loayza et al., 2012; Cavallo et al., 2013). A frequent hypothesis is that the direct destruction of a hazard can stimulate economic activity through efficient re-organization or even creative destruction. A priori, it is therefore not clear whether an increase in direct flood damages will decrease economic activity or not. To the best of my knowledge, there is no study that focuses on the local economic impact of flash floods, even though they are one of the most common natural hazards.[2]

Flash floods are a type of flood that is caused by heavy rainfall in a short period of time, generally less than 6 hours, and are characterized by heavy torrents that sweep everything before them (NOAA Flood and Flash Flood Definition). Due to climate change, they are predicted to increase in frequency and severity in many parts of the world (Seneviratne et al., 2021). Since flash floods are triggered by episodes of extreme rainfall, they are particularly localized and can occur almost anywhere, even if the local climate is comparatively dry (Yin et al., 2023). It has been recognized that a large regional unit of analysis can aggregate out the economic effects of natural hazards (Elliott et al., 2019). It follows that an understanding of the mechanisms through which flash floods impact economic activity should be derived from micro-level evidence.

[1] IPCC 6^{th} Report, Summary for Policymakers.

[2] For instance, according to the Centre for Research on the Epidemiology of Disasters (CRED) Emergency Events Database (EM-DAT), the number of affected people in 2022 by flash floods (0.9 M) is closest to convective storms (1.6 M), more than river floods (0.1 M) or forest fires (0.03 M). Note, however, that the EM-DAT only catalogs disasters if there is a certain number of people affected or a minimum of monetary damages. Further, it has been suggested that the EM-DAT suffers from bias since it relies on the reporting of events by agencies or newspapers.

Impacts can be divided into direct impacts or damages and indirect economic impacts Cavallo and Noy (2011). Direct damages refer to the directly caused destruction to assets, for instance, property, at the time the natural hazard strikes. They commonly include the destruction of residential housing, establishments, infrastructure, and crops, but can also include health impacts.[3] Indirect impacts are the second-order effects of a natural hazard. In other words, they are due to changes in the behavior of economic agents, namely firms and households. Direct impacts are well understood, while there is large uncertainty in how natural hazards impact economic activity and growth (Botzen, Deschenes, and Sanders, 2019). Further empirical evidence is necessary to reduce this uncertainty with regard to indirect effects.

There are two main challenges in credibly analyzing the impacts of flash floods. First, since there exists no data that adequately captures flash floods, one needs to model their local occurrence.[4] The economic literature on tropical storms' economic effects has, for instance, produced physical measures to approximate local impacts in order to ensure comparability across regions without concerns of endogeneity (Strobl, 2012; Hsiang and Jina, 2014). The second challenge is with regard to the data on economic agents and identification. Sufficiently detailed micro-data of either firms or households do usually not provide exact locations or are unavailable for confidentiality reasons. Consequentially, identification of the effect is difficult. Ideally, one could observe establishments over a longer period of time before and after a flash flood event in a panel to estimate dynamic effects. Even then, the high frequency of flash floods makes the definition of an adequate control group difficult.

In this paper, I attempt to overcome these challenges by employing remote-sensing rainfall data to detect potential flash flood events on a high spatial resolution and linking

[3] For instances, Kousky (2016) summarizes the health impacts natural hazards have on children. These include malnutrition, diarrheal illness due to contaminated water, and various mental health problems.

[4] Recent studies that investigate the indirect effects of flood events use the Dartmouth Flood Observatory (DFO) data (Kocornik-Mina et al., 2020; Zhou and Botzen, 2021). However, flash floods are likely not captured by this data. The DFO relies on satellite imagery on cloud-free days to quantify the extent of flooded areas. Since floods often occur in combination with heavy rainfalls and thus cloud coverage, and because flash floods do usually not remain for a long time as shallow, standing floods, the DFO will not capture them adequately.

these to the Worldbank Enterprise Surveys for Central America and the Caribbean. I estimate the effect of flash floods on several measures of establishment performance while controlling for the history of previous events. The region of Central America and the Caribbean is arguably ideal to study flash flood impacts. Since the mid 20^{th} century, the magnitude and frequency of extreme precipitation events have increased significantly in the region (Seneviratne et al., 2021). Soil degradation is common, and urbanization is unregulated, acerbating the risk for flash floods (Charvériat, 2000; Pinos and Quesada-Román, 2021). Many countries in the study region are lower- to middle-income, such that the efficiency of adaptation and investment into resilience against natural hazards is crucial for further development.

The contribution to the literature in this paper is two-fold. First, in terms of the methodology, I detect potential flash floods via intensity-duration classification from Collalti, Spencer, and Strobl (2023) as a physical measure of incidence from satellite rainfall data. This classification is based on a conditional copula model and information on all confirmed flash flood events in Jamaica from 2001 to 2018. Jamaica shares a similar topography, soil composition, and climate with the whole region such that the method is well-calibrated. In addition, the confirmed events from the Jamaican Office of Disaster and Preparedness Management (ODPEM) constitute an exhaustive list for that time period in Jamaica, which is a rarity for the study region. Second, with the use of Worldbank Enterprise Survey data, I analyze the establishment impacts of natural hazards consistently across a large group of countries. After data cleaning, surveys from ten different countries[5] are used to estimate how establishments are affected in terms of sales, employment, investment choices and productivity of labor and capital.

There are two strands of the literature to which this study directly relates. One body of work investigates the firm and establishment-level impact of specific natural hazards. Leiter, Oberhofer, and Raschky (2009) have been pivotal by estimating the effects of floods on European firms' capital, labor, and productivity. They examine the impact on firms

[5]These countries are: Columbia, Venezuela, Panama, Nicaragua, El Salvador, Guatemala, Costa Rica, Mexico, Dominican Republic, and Haiti.

that are located in a region[6] hit by a major flood. They document higher growth rates of assets and employment but a decline in productivity. Similarly, Zhou and Botzen (2021) study the impacts of storms and floods on firm growth in Vietnam and find that flooding increases labor and capital growth but reduces sales. In contrast to this paper, both studies use data from large-scale flood events and aggregate these onto the province level, which likely aggregates out some of the impacts. Elliott et al. (2019) estimates the direct and indirect impact of typhoons on manufacturing plant performance in China. Plant sales decrease significantly, but the effects are relatively short-lived. Some studies analyze the firm-level effect of a single event: Okubo and Strobl (2021) investigate the 1959 Ise Bay Typhoon and find that firms in retail and wholesale are less likely to exit the market, whereas those in manufacturing and construction are more likely to upgrade their capital. Several studies analyze a specific earthquake to investigate the role of creative destruction: Tanaka (2015) and Cole et al. (2019) study the 1995 Great Kobe Earthquake and Okazaki, Okubo, and Strobl (2019) the 1923 Great Kanto Earthquake. Evidence is mixed with Tanaka (2015) finding negative effects while Cole et al. (2019) and Okazaki, Okubo, and Strobl (2019) are more positive.

This study also relates to the literature that studies the economic impacts of weather anomalies (Dell, Jones, and Olken, 2012; Felbermayr et al., 2022; Kotz, Levermann, and Wenz, 2022). Positive temperature anomalies have generally been associated with negative economic impacts, whereas results have been mixed for rainfall (Dell, Jones, and Olken, 2012). An exception to this is Barrios, Bertinelli, and Strobl (2010) who find that the declining rainfall rates in sub-Saharan Africa are a significant determinant of the regions' lower economic growth rates. These earlier studies focus on the long-run climatic variation on the country level with panels of country-by-year rainfall data. Arguably, this cannot be informative with respect to floods, in general. Spatial and temporal aggregation masks out extreme events, such that excess rainfall has an ambiguous interpretation.[7] With the advent of satellite data in recent years, the spatial resolution improved.

[6] NUTS-II region, of which there are 268 for Europe at that time.

[7] Excess rainfall in a country in a given year could be evenly distributed rainfall throughout the year or short, extreme rainfall in a specific region - with likely different effects on the economy.

Kotz, Levermann, and Wenz (2022) estimate the effects on sub-national region's economic growth. They find that growth is reduced by the number of wet days and in extreme daily rainfall, while the annual total rainfall is positively associated with growth. Felbermayr et al. (2022) connect monthly weather anomalies with night light data on a 0.5×0.5 grid (approx. 55 km $\times$ 55 km at the equator). They find that rainfall anomalies reduce night light growth contemporaneously with a rebound in the next periods and contemporaneous positive spatial spillover into neighboring areas. This study has been influenced by the development of increasing resolution to capture the economic impacts of weather anomalies. In some sense, it ties together the weather anomaly with the natural hazard literature in the case of extreme rainfall and flash flood events.

To briefly summarize the results, I show that flash floods impact establishment performance, resulting in less output, fewer workers employed, a change in investment dynamics, and an increase in capital productivity. Financial market access plays a central role. Establishments for whom financial market access is an obstacle drive the documented reduction in output. They further have a decreased labor productivity, whereas firms that are not constrained experience the increase in capital productivity found in the overall analysis. I further explore heterogeneity by industry. There is comparatively little variation in the effects of flash floods across sectors, with the notable exception of the construction sector. The construction sector is not negatively impacted as it does not see a reduction in output or workers employed but still reacts strongly in investment dynamics. This might indicate that flash floods affect establishments through more than one mechanism.[8]

The remainder of the paper is organized as follows: Section 4.2 provides background and discusses theoretical considerations. Section 4.3 presents the flash flood classification and describes the data. In Section 4.4, the empirical strategy is detailed, and results are shown in Section 4.5. Section 4.6 then discusses the main implications and concludes.

[8]There is a literature that documents how natural disasters impact across supply chain (Rose and Liao, 2005; Altay and Ramirez, 2010; Henriet, Hallegatte, and Tabourier, 2012). For instance, Altay and Ramirez (2010) show that the impact of a flood depends on the flood's position in the supply chain: upstream firms are positively, and downstream firms are negatively affected.

4.2 Background

Episodes of heavy rainfall and flash floods are projected to become more prevalent in a warming climate (Seneviratne et al., 2021). Flash floods are a subtype of pluvial floods, which are caused by extreme rainfall. These can be categorized into flash and surface water floods. Surface water floods are shallow, standing floods that occur when rain falls over a prolonged period of time, and the water cannot run off. Flash floods are characterized by their quick onset and ravageous, debris-sweeping flow. Meteorological conditions that cause flash floods are mostly convective and orographic, which are naturally localized. Since most precipitation in the tropics is convective, the potential for frequent flash floods is given almost anywhere in the study region.

While flash floods are local events, some have disastrous impacts. On July 20^{th} and August 12^{th} 2021, two flash floods hit Zhengzhou and Suizhou in Central China, claiming human lives and destroying infrastructure. The two events were due to heavy rainfall, peaking at 201.9 mm/h and 117.9 mm/h in intensity, respectively (China Meteorological Administration). There are many other instances where heavy rainfall led to disastrous flash floods: 2013 in La Plata, Argentina, 2009 in Messina, Italy, and 2016 in Maryland, USA, to name a few. However, not every flash flood causes such destruction. The risk of natural hazards can be decomposed into vulnerability, exposure, and hazard (Field and Barros, 2014). A higher exposure is given by a larger population and more assets in the hazard's location. Depending on the vulnerability, the natural hazard becomes a disaster. In the case of flash flood hazard, changes in the socio-economic dimension can strongly affect the risk (Terti et al., 2015). It follows that evaluating the impact of flash floods has significant economic and social implications, which requires knowledge across disciplines of social and physical sciences (Ruin et al., 2014).

The vulnerability to flash floods has, so far, only been investigated in non-economic terms. These include Špitalar et al. (2014) who evaluate fatalities from flash floods in the United States 2006 - 2012. While most fatalities accrued in rural areas, impacts on humans are said to be higher in urban areas. Vulnerability to flash floods can also be

in terms of the built environment where structural parameters are assessed relative to the hazard intensity (Milanesi et al., 2018). From a socio-economic perspective, there have been some efforts to evaluate flash flood vulnerability by creating an index for the United States (Khajehei et al., 2020) and Spain (Aroca-Jiménez et al., 2018). This study is, however, the first to consider economic consequences on firms on the establishment level.

4.2.1 Hypotheses

Theoretical considerations can establish a set of hypotheses to be evaluated empirically. With the data in mind, these are concerned with single establishments. The theoretical literature on the economic impact of natural disasters mainly focuses on the macroeconomic perspective. However, some recent papers specifically model firm behavior in response to natural hazards even if the objective is the macroeconomic impact (Hallegatte, Hourcade, and Dumas, 2007; Hallegatte and Dumas, 2009; Henriet, Hallegatte, and Tabourier, 2012; Barrot and Sauvagnat, 2016; Hallegatte and Vogt-Schilb, 2019; Strulik and Trimborn, 2019). I subsequently summarize the main insights into hypotheses for the empirical analysis in this paper.

Hallegatte and Vogt-Schilb (2019) model impacts of natural hazards with different layers of capital and assume that part of a firm's capital is destroyed and thus output and labor decrease. Because a natural hazard does not discriminate between capital types in its destruction, total losses relate to the average and not the marginal productivity of capital. In most instances, capital productivity increases, whereas labor productivity decreases. Further echoing the insight from Hallegatte, Hourcade, and Dumas (2007), the reconstruction phase is crucial for economic dynamics. For instance, if investments in reconstruction are limited due to financial and technical constraints, the economy recovers more slowly. Strulik and Trimborn (2019) model impacts of natural disasters and distinguish between a firm's productive capital and durable goods. They find that if a natural disaster destroys either predominantly productive capital or durable goods (which is the assumed mechanism), the initial decline in output can become an increase

over time. In turn, the investment choices of firms are impacted by natural disasters. Barrot and Sauvagnat (2016) analyze whether natural disasters propagate in production networks. They derive hypotheses based on the static network model analysis of Acemoglu et al. (2012), assuming that when a firm is hit by a natural hazard, some share of output is destroyed. The model predicts positive horizontal and downstream pass-through rates that are confirmed empirically. This implies that heterogeneity in impact across sectors and layers of the value chain is limited.

In summary, five hypotheses emerge on the establishment impact of a natural hazard, which will guide the empirical analysis and frame the discussion. After a flash flood,

1. Output Y and labor L decrease.
2. The productivity of capital increases, and the productivity of labor decreases.
3. Investments of establishments hit differ from those that have been spared.
4. Establishments with constrained financial access are more impacted.
5. Heterogeneity in impacts across industries is limited.

Note that not all implications are voiced in unison in the literature. While output and capital decrease by assumption, the impact on labor depends on model specification. The choice of dynamic versus static and general versus partial equilibrium models can alter some of the predictions stated. The hypotheses are chosen so as to describe the case that likely corresponds to frequent and localized natural hazards such as flash floods.

4.3 Data

To study the stated hypotheses empirically, information regarding flash flood occurrence and establishment-level data is necessary. I derive information on flash flood occurrence with a physical hazard indicator. Specifically, I use satellite rainfall data and employ a classification scheme that is based on hydrological modeling of extreme rainfall events.

Establishment-level data is taken from the Worldbank Enterprise Survey, which provides a wide array of data on establishment performance. Subsequent sections detail the procedure and data preparation.

4.3.1 Study Region

The study region of Central America and the Caribbean is characterized by a high propensity to natural disasters. The region knows various geographical definitions. Central America is often defined as all countries from Mexico to Panama[9], though some exclude Mexico, and others include Colombia and Venezuela. Similarly, the Caribbean knows various definitions. There is a well-defined core of islands that are part of the Caribbean that includes all the islands in the Caribbean Sea. For the remainder of this paper, Central America and the Caribbean refers to an encompassing definition of the region that includes all countries mentioned. Specific details and restrictions apply due to data availability.

4.3.2 Flash Flood

The flash flood classification is based on Collalti, Spencer, and Strobl (2023) who model extreme rainfall events via copula functions, and use data on confirmed flash flood events in Jamaica to classify above which threshold in the intensity-duration space an extreme rainfall event likely triggers a flash flood. Information about confirmed Jamaican' flash floods comes from the Office of Disaster and Preparedness Management (ODPEM), whose responsibility includes monitoring extreme weather events in Jamaica and implementing measures to mitigate their impact. The procedure is tailored to the Global Precipitation Measurement (GPM) Integrated Multi-satellitE Retrievals (IMERG) data, which is globally available since June 2000 (Huffman et al., 2015b).[10] The data contains

[9] as defined by the United Nations in their geoscheme for the Americas. This includes Mexico, Guatemala, Belize, Honduras, El Salvador, Nicaragua, Costa Rica, and Panama.

[10] The satellite precipitation algorithm combines various microwave and infrared precipitation measurements to produce precipitation estimates, adjusted with surface gauge data.

half-hourly rainfall measurements on a $0.1^\circ \times 0.1^\circ$ (approx. 11 km $\times$11 km at the equator) grid. From the half-hourly data, meteorological distinct events are defined with a 12 h inter-event time. The most extreme rainfall events are then used to model the dependence between the intensity and duration of an event with copula functions to generate intensity-duration-frequency (IDF) curves. Such a curve relates points in the intensity-duration space to a given frequency or return period. In that sense, one can interpret it as a measure of severity or extremness. With comprehensive data on all flash flood events since 2000, Collalti, Spencer, and Strobl (2023) define the IDF curve as the threshold for classification above which the ratio of hazardous events is maximized.

As a decision rule, I require that a rainfall event must have an intensity of at least 2 mm/h above the IDF curve from Collalti, Spencer, and Strobl (2023) in order to reduce the number of false positives.[11] Every time the GPM/IMERG cell within which an establishment is located experiences a rainfall event above that threshold, I treat it as being affected by a flash flood. Note that this does not imply that there has been direct damage to the establishment, as it could be that the extreme rainfall event did not cause flooding where the establishment is located exactly. In that case, it is still very likely that it has been affected by the extreme rain, as the inundation of roads and sweeping torrents of water are expected in close vicinity.

4.3.3 Enterprise Surveys

Data on firms are from the World Bank Enterprise Surveys. They are firm-level surveys of a representative sample of the economy's private sector and cover a broad range of topics, from corruption and crime to competition, infrastructure, and various other measures. Since 2005, the methodology has been globally standardized, and a total of 177'000 surveys in 153 countries have been carried out in various rounds. Table 4.1 displays the countries of the study region for which surveys were conducted. It further shows for how many rounds and in which year those surveys were conducted for a total of 37 surveys

[11] In robustness Section 4.5.3 I employ a more restrictive threshold of 3 mm/h. This approximately halves the number of events, but results do not change significantly.

FIGURE 4.1: Map of Establishments

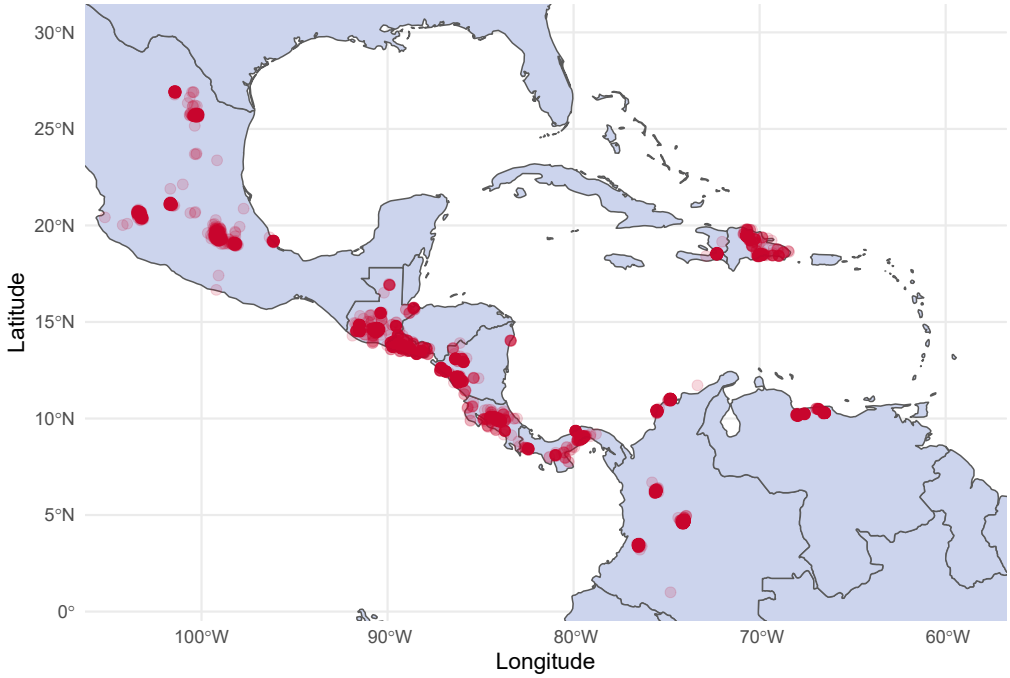

Map of all 7'755 geographically located establishments.

with 16'414 establishments. The Worldbank Development Economics Enterprise Analysis Unit (DECEA) provided me with information about each establishment's location. Due to confidentiality reasons, the locations come in the form of masked coordinates that have been randomly displaced by 500 m to 2'000 m in each axis. This results in a random displacement of approximately 700 meters to 2400 meters. Unfortunately, establishment locations were not captured as part of all surveys. In earlier rounds in 2005 and 2006, the surveyors were not equipped with tablets to record GPS coordinates as they were in later rounds. A total of 7'755 establishments remain for which detailed surveys and their approximate location are combined. Figure 4.1 depicts their geographical distribution in the study region.

TABLE 4.1: Summary of Surveys

Country/Year	2005	2006	2010	2016	2017	2019	Geo-Coded
Antigua & Barbuda			✓				
Bahamas			✓				
Barbados			✓				
Belize			✓				
Colombia		✓	✓		✓		2010, 2017
Costa Rica	✓		✓				2010
Dominica			✓				
Dominican Republic	✓		✓	✓			2016
El Salvador		✓	✓	✓			2010, 2016
Grenada			✓				
Guatemala		✓	✓		✓		2010, 2017
Guyana						✓	
Haiti			✓			✓	2019
Jamaica	✓		✓				
Mexico		✓	✓				2010
Nicaragua		✓	✓	✓			2010, 2016
Panama		✓	✓				2010
St. Kitts & Nevis			✓				
St. Lucia			✓				
St. Vincent & Grenadines			✓				
Trinidad & Tobago			✓				
Venezuela		✓	✓				2010

Notes: List of all countries in the region for which there were any Worldbank Enterprise Surveys. Columns of the years indicate whether a survey was conducted in a specific year. A majority of surveys were conducted in 2010. Geo-Coded indicates the countries and surveys for which the establishment's location was surveyed.

4.3.4 Sample Restriction

Not all of these 7'755 surveys can be used for the analysis. For one, many respondents do report questions with regard to the firm and not the single establishment. When a firm has several establishments, connecting a single establishment to a flash flood incident would not be informative. The sample is therefore reduced to those 6'423 surveys where either the firm is a single establishment or where the financial statements are separately prepared for each establishment. Further, not all surveys contain all relevant information for the analysis. Only 1'925 establishments did report sales, the number of full-time

employees, investments, labor, and electricity cost.[12] Even then, some surveys are implausible. There is, for instance, the establishment from Colombia that produces corn syrup and allegedly reports revenue of 327 B USD in 2010. I remove all observations that report sales, investments, or the number of employees 5 times larger than the 0.99 quantile, which reduces the sample by 25 observations. While I cannot verify that these 25 surveys were indeed faulty in the reporting or transcription, the manual inspection of these surveys reveals that at least some are implausible.[13]

4.3.5 Two Indices for Floods

Flash floods can occur continuously in time, whereas the establishment surveys constitute a cross-section. In order to relate one with the other, we need to consider that questions in the surveys are always in relation to the last fiscal year. Therefore, for every establishment, I construct an index of the number of potential flash floods in the 12 months of the last fiscal year,

$$Flood_j^t = \sum_{t=0}^{12} Flash\ Flood_{jt} \tag{4.1}$$

where j is the establishment identifier, and t denotes the time-shift relative to the establishment j's end of the last fiscal year. The variable $Flash\ Flood_{jt}$ gives the number of flash floods in the rainfall cell where j is located for the month t. If the end of the fiscal year was not collected in the survey, I assume that the fiscal ends on 31^{st} of December.

Similarly, I create an index of previous (*"historic"*) flash flood events to control for location-specific flash flood risk in the analysis,

$$Flood_h^t = \sum_{t=13}^{96} Flash\ Flood_{jt}. \tag{4.2}$$

[12] Electricity cost will be used as a proxy of capital cost.

[13] As another example, there is an establishment that deals with raw material products with 8 full-time employees that invested 150 B USD in machines and equipment and 15 B USD in land and buildings while only selling goods for 0.26 M USD in that year. In the robustness Section 4.5.3, I estimate the main model without removing the 25 surveys, and the results do not change.

The variable $Flood_h^t$ thus gives the number of flash floods in the rainfall cell where j is located for 7 years before the start of the last fiscal year. The choice of 7 years is due to rainfall data availability - ideally, one would provide a longer history of events.

TABLE 4.2: Summary Statistics

Statistic	Mean	St. Dev.	Min	Max
Floods Fiscal Year	2.65	2.46	0	10
Prior Floods	18.03	11.02	0	50
Access to Finance	0.54	0.50	0	1
Sales Last Year (M USD)	23.79	105.90	0.003	1'872.31
Full-Time Employees	145.95	325.53	3	6'513
Inv. Land & Buildings (M USD)	0.13	0.75	0.0000	16.03
Inv. Machines & Equipment (M USD)	0.95	10.08	0.0000	374.70
Firm Age	25.31	17.69	1	127
Power Outages	0.60	0.49	0	1
Generator Owned	0.23	0.42	0	1
% of Direct Exports	8.83	21.01	0	100
Female Ownership	0.39	0.49	0	1

Notes: Summary statistics after data cleaning for the remaining 1'900 observations.

4.3.6 Summary Statistics

Table 4.1 displays summary statistics. There are 1'900 establishments that experienced an average of 2.65 potential flash flood rainfall events in their last fiscal year and 18.03 in the 7 years before that. For 54% of establishments, access to finance is no major obstacle. In the last fiscal year, average sales were 23.8 M USD with 146 full-time employees, though there can be as little as 3 and as many as 6'513 people employed at the single establishment. All monetary values have first been transformed to USD with exchange rates at the end of the fiscal year and then inflated to December 2021. Investments also exhibit large variation, with an average of 1.08 M USD in total investments. Of that, the majority (88%) is in the category of machines, equipment, and vehicles. The oldest establishment in the sample is 127 years old, five times more than the average of 25.31 years. Many report issues with regard to electricity, where 60% report at least one power outage in the last fiscal year and 23% own a generator. Some establishments engage in direct exports

with an average value of 8.8% of directly exported goods. Lastly, in about 40% of firms, at least one of the owners is female.

4.4 Empirical Strategy

The data are cross-sectional, which can be a source of endogeneity bias. To estimate a causal effect, treatment assignment should be independent of potential outcomes after conditioning on observed covariates. In the case of flash floods, treatment can arguably be viewed as quasi-random in the case of extreme weather events. The specific timing of an extreme rainfall event in a location in one year versus another cannot be forecasted in any way. Therefore, the only way the occurrence of a flash flood in the fiscal year prior to the survey is correlated with establishment outcomes is through the underlying probability of treatment in that area. In other words, if one conditions for the location-specific differences in the likelihood of flood occurrence, then an estimate of the effect of flash floods on establishment outcomes should not suffer from endogeneity bias. In this cross-sectional setting, all relevant unit-specific time invariants can be captured with the unit-specific treatment history. I do that with the number of flood events 7 years before the last fiscal year. A regression that further controls for the country, industry, and year-fixed effects can be written as

$$log\left(Y_j\right) = \beta_1 Flood_j^t + \beta_2 Flood_j^h + \beta_3 Access_j^f + \delta X_j + C_j + V_j + T_j + \varepsilon_j \tag{4.3}$$

where Y_j is a variable of performance for establishment j, $Flood_j^t$ the flood index from Equation 4.1 and β the corresponding constant coefficient. $Flood_j^h$ is the number of floods in the years 1 to 8 after the end of the last fiscal year in the cell of establishment j from Equation 4.2, and $Access_j^f$ is an indicator of financial market access. X_j is a vector of establishment-specific control variables, C_j are country fixed effects, V_j industry fixed effects and T_j year fixed effects. The error term ε_j is assumed to be two-way clustered at the country and industry level.

4.4.1 Hypotheses

With a regression in 4.3 and the appropriate dependent variable Y_j, I can study Hypotheses 1, 2 and 3. That is, whether a flash flood causes an establishment's output and labor to decrease, whether the productivity of capital increases and that of labor decreases, and whether investment choices are affected. For output, I use sales in the last fiscal year in M USD. Labor is proxied by the number of full-time workers, whereas investments are reported separately for *Land & Buildings* and *Machines, Equipment & Vehicles* in M USD. Productivity can be estimated as the ratio between output and factor input in monetary terms. For the average productivity of labor, I use sales per labor cost.[14] I approximate capital cost with electricity cost to calculate the average productivity of capital as sales per electricity cost.[15]

To explore Hypothesis 4, I modify the model in Equation 4.3 with an interaction between $Flood_j^h$ and financial market access,

$$\begin{aligned} log\left(Y_j\right) =& \beta_1 Flood_j^t + \gamma\left(Flood_j^t \times Access_j^f\right) + \beta_2 Flood_j^h + \beta_3 Access_j^f + \\ & \delta X_j + C_j + V_j + T_j + \varepsilon_j \end{aligned} \tag{4.4}$$

where $Access_j^f$ denotes a binary indicator of whether access to financial services is considered no or a minor obstacle to operations (0) or a medium, severe, or very severe obstacle to operations (1). Conveniently, 54% fall into the first category such that the indicator can be approximately interpreted relative to the average outcome.

To review Hypothesis 5, the model should allow for heterogeneity with respect to an establishment's industry sector. There are 29 industry codes in the data, with sometimes only one entry. I group industries into larger sectors: Chemical & Plastic (n=309), Construction (n=41)[16], Food (n=329), Metals & Minerals (n=225), Textile & Garments (n=241),

[14] Labor cost is surveyed as *"total annual cost of labor including wages, salaries, bonuses, and social payments"*.

[15] This strategy has been used before in the literature, see e.g. Cole et al. (2018).

[16] The choice of a separate construction sector as an indicator is driven by theoretical considerations albeit the small number of establishments in that industry. Specifically, the reconstruction after a natural hazard is often associated with a boom in the construction sector. It is thus of interest to see whether there is a distinct heterogeneity.

Other Manufacturing (n=272) and Other (n=483).[17]. I modify the model in Equation 4.3 with an interaction between $Flood_j^h$ and industry,

$$log\left(Y_j\right) = \theta\left(Flood_j^t \times Industry_j\right) + \beta_2 Flood_j^h + \beta_3 Access_j^f + \delta X_j + C_j + V_j + T_j + \varepsilon_j \tag{4.5}$$

where $Industry_j$ is an indicator of the different industry sector groups. With this specification, I estimate the effect a flash flood has on each industry and compare for heterogeneity.

4.5 Results

Regression results of the model in Equation 4.3, estimated with ordinary least squares (OLS), are displayed in Table 4.3. Each flash flood in an establishment's fiscal year reduces sales by 3.3% and the number of full-time employees by 2.9%, consistent with Hypothesis 1. The productivity of capital as measured by sales per electricity cost E_{cost} increases by 6% while labor productivity measured with sales per labor cost L_{cost} is not affected. This is consistent with Hypothesis 2. Investments in land and buildings $Inv_{L\&}$ decrease by 8.3%[18] while investments in machines, equipment, and vehicles $Inv_{M\&E}$ increase by 12.5% (statistically not significant). This is some indication for Hypothesis 3. Floods before the last fiscal year are associated with 0.7% higher sales but no effect otherwise. Obstacles to financial access are more important, with negative effects across the board that are significant in the three variables measuring productivity: -13.9% in sales per worker, -12.4% in labor productivity and -8.3% in capital productivity. Together, this suggests a story where firms that have difficulties accessing the financial market are less productive, probably due to outdated capital.

To put the impacts of flash floods into perspective, it is informative to compare them to other natural hazards. Zhou and Botzen (2021) analyze large floods in Vietnam and

[17] Other includes diverse sub-sectors such as IT or transportation that could not be grouped otherwise.
[18] All effects are calculated from the coefficients with $(exp(\beta) - 1) \times 100$.

TABLE 4.3: Regressions: Establishment Impacts

ln log(·)	Sales/Worker (1)	Worker (2)	Sales (3)	$Inv_{L\&B}$ (4)	$Inv_{M\&E}$ (5)	Sales/L_{cost} (6)	Sales/E_{cost} (7)
$Floods_j^t$	-0.006	-0.029**	-0.034**	-0.087**	0.118	-0.015	0.058***
	(0.012)	(0.011)	(0.011)	(0.037)	(0.076)	(0.011)	(0.014)
$Floods_j^h$	0.004*	0.003	0.007**	0.010	-0.021	0.001	-0.006
	(0.002)	(0.002)	(0.002)	(0.007)	(0.025)	(0.002)	(0.003)
$Access_j^f$	-0.150*	-0.021	-0.170	-0.143	0.032	-0.132**	-0.087***
	(0.070)	(0.045)	(0.095)	(0.133)	(0.304)	(0.053)	(0.004)
Observations	1,883	1,883	1,883	1,883	1,883	1,880	1,877
R^2	0.41	0.82	0.71	0.29	0.08	0.92	0.83
Fixed Effects:							
Industry	✓	✓	✓	✓	✓	✓	✓
Country	✓	✓	✓	✓	✓	✓	✓
Year	✓	✓	✓	✓	✓	✓	✓

Notes: Table of regression results of the model in Equation 4.3 without coefficients of the control variables X_j for brevity. The full table with all the coefficient estimates is D.1 in the Appendix. Standard errors are in parentheses. *p<0.1; **p<0.05; ***p<0.01

find immediate effects of -1.5% and -2.9% on sales growth if there is a flood in an establishments province with a measure based on casualties and damages, respectively.[19] While methodologically different from this paper, it is striking how comparable these estimates are. They, however, do find evidence of delayed positive impacts on capital and labor growth for up to three years, while I cannot directly study the dynamics in the following years. However, from the coefficient of flood history, we can infer that the negative impacts in the first year are also reverted after some time. Elliott et al. (2019) study the effect of typhoons on Chinese manufacturing plants. Their estimates suggest that the average damaging storm reduces a plant's turnover by 1% in the year of the strike for an average reduction of 3.7% due to typhoon activity, comparable to the estimate of flash floods. They do not find any evidence of an effect beyond the year of impact. Tanaka (2015) investigates the effect of the Great Kobe Earthquake and finds 11.1% lower value added of manufacturing plants in the most devastated area of Kobe. Naturally, the effect

[19]The measure determines which provinces are affected, given a certain threshold. If they use their physical-based measure with DFO inundation maps, they find an effect of -2.3% on growth in the next year.

of a severe earthquake is expected to be magnitudes larger than that of one flash flood.

Because the Worldbank Enterprise Surveys is a representative sample of an economy's private sector, we can perform some back-of-the-envelope calculations with regard to the economic cost caused by flash floods. Taking the average of 2.65 potential flash floods per fiscal year multiplied by the estimated -3.3% in the baseline specification in Equation 4.3 for $Floods_j^t$ on sales, the yearly average reduction in sales is $2.65 \times -3.3\% = -8.745\%$. That is under the assumption that the establishment surveys are also representative with respect to flash flood risk and vulnerability such that external validity is given. If we further assume that the establishment's reduction in output is proportional to direct flood damages, which, according to the 6^{th} IPCC Report, are approximately doubling with a 2°C compared to a 1.5°C warming, it is likely that flash floods in Central America and the Caribbean will cause substantial overall economic loss in the future.

4.5.1 Financial Access

OLS regression results of the model with the financial access interaction in Equation 4.4 are displayed in Table 4.4. Coefficients of $Flood_j^t$ are similar to those in Table 4.3 of the model without interaction, but smaller in size and no longer statistically significant. Only capital productivity is significantly increasing by 7.4%. Coefficients of the interaction term $Floods_j^t \times Access_j^f$ then can be interpreted as the effect of a flash flood for those establishments for whom financial access poses an obstacle. Sales significantly decrease by 4.8% while the number of workers is unaffected, resulting in a 3.4% lower Sales/Worker ratio. The productivity of labor decreases by 3.9% as well. In summary, establishments that are facing obstacles with regard to their financing are more negatively impacted by flash floods, consistent with Hypothesis 4.

Financial market access has been suggested to facilitate and accelerate recovery after a natural disaster (Benson and Clay, 2004). For instance, De Janvry, Del Valle, and Sadoulet (2016) find for Mexico that access to disaster funding boosts local economic activity between 2% and 4% in the year following a disaster, as measured by night light. Here, I

can confirm this mechanism for flash floods and establishment-level impacts. Namely, adequate financing opportunities makes establishments resilient to flash floods and can be part of the efforts to decrease natural hazard vulnerability for economic development in Central America and the Caribbean.

TABLE 4.4: Regressions: Financial Access

In log(·)	Sales/Worker (1)	Worker (2)	Sales (3)	$Inv_{L\&B}$ (4)	$Inv_{M\&E}$ (5)	Sales/L_{cost} (6)	Sales/E_{cost} (7)
$Floods_j^t$	0.013	-0.020	-0.007	-0.077	0.143	0.008	0.071***
	(0.015)	(0.012)	(0.014)	(0.046)	(0.082)	(0.015)	(0.010)
$Floods_j^t \times$	-0.034*	-0.015	-0.049***	-0.017	-0.044	-0.040***	-0.022
$Access_j^f$	(0.018)	(0.016)	(0.013)	(0.029)	(0.072)	(0.008)	(0.014)
$Floods_j^h$	0.004**	0.003	0.007*	0.010	-0.021	0.0009	-0.006*
	(0.002)	(0.002)	(0.003)	(0.007)	(0.025)	(0.004)	(0.003)
$Access_j^f$	-0.060	0.019	-0.041	-0.097	0.148	-0.024	-0.028
	(0.085)	(0.063)	(0.088)	(0.144)	(0.361)	(0.047)	(0.046)
Observations	1,883	1,883	1,883	1,883	1,883	1,880	1,877
R^2	0.41	0.82	0.71	0.29	0.08	0.92	0.83
Fixed Effects:							
Industry	✓	✓	✓	✓	✓	✓	✓
Country	✓	✓	✓	✓	✓	✓	✓
Year	✓	✓	✓	✓	✓	✓	✓

Notes: Table of regression results of the model in Equation 4.4 with the interaction for financial access, without coefficients of the control variables X_j for brevity. The full table with all the coefficient estimates is D.2 in the Appendix. Standard errors are in parentheses. *p<0.1; **p<0.05; ***p<0.01

4.5.2 Sector Heterogeneity

I study heterogeneity across different industries with the model in Equation 4.5. Figure 4.2 displays the results of regressions with OLS.[20] The first row shows the results from regressions without any interaction, as in Equation 4.3, for comparison. Studying the heterogeneity with respect to the industry by comparing coefficients of a single column, it is apparent that there is little variation. That is, most industries are affected similarly by a flash flood. For instance, all industries but construction see a reduction in workers

[20]The full results are in Table D.3 in the Appendix.

FIGURE 4.2: Industry-Specific Effects

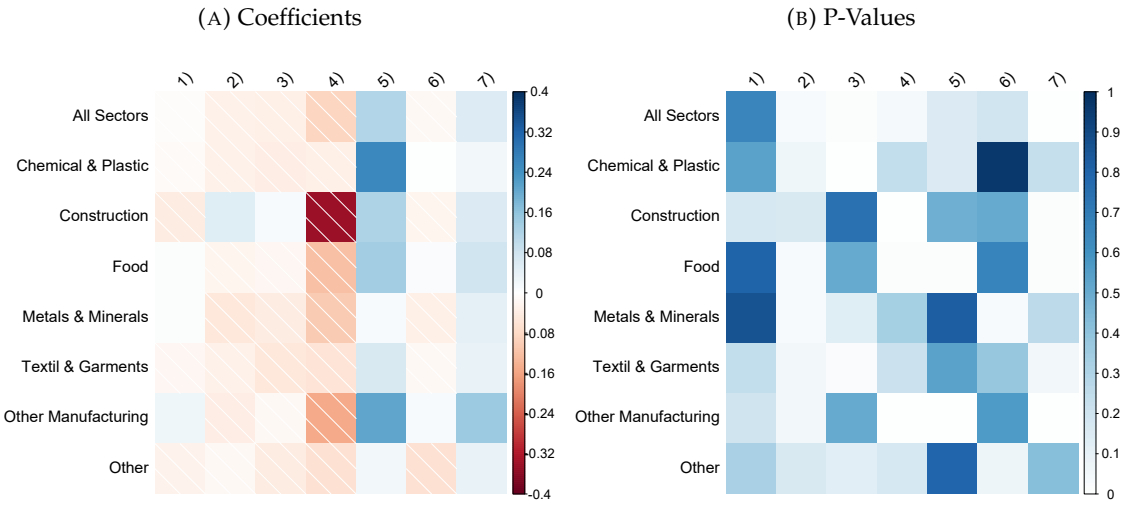

Notes: Matrix-plot of coefficients from regressions with industry indicator and matrix-plot of corresponding p-values. The columns relate to the various dependent variables Y_j: column 1) is the regression with $Sales/Worker$, column 2) with $Worker$, column 3) with $Sales$, column 4) with $Inv_{L\&B}$, column 5) with $Inv_{M\&E}$, column 6) with $Sales/L_{cost}$ and column 7) with $Sales/E_{cost}$. The first row shows the result from the regressions without interaction as in Equation 4.3 whereas the other rows are results from Equation 4.5.

by 2% to 5% and a reduction in sales by 1% to 5%. The construction sector is indeed out of line: instead of a decrease in workers and sales as for all other industries, coefficients are positive, albeit not statistically significant. Investment dynamics also show more variation across industries: investment into land & buildings decreases by 4% to 29% while investment into machines, equipment, and vehicles increases by 2% to 30%. Variation in coefficients for investment is comparatively large, which might be due to the worse model fit compared to the other regressions. The productivity of capital and labor is similarly affected by flash floods across industries. For labor productivity, the effect is slightly negative between 0% and -6% and is not statistically significant in most cases. The effect on capital productivity is positive throughout between 2% to 16%.

From a qualitative point of view, the differences across industries are not substantial for any measure of firm performance, with the exception of the construction sector. The construction sector is less negatively affected in terms of workers and sales but stands

out for reducing land & building investments significantly. Note that the lower statistical confidence in industry-specific effects in a model with interactions is mechanically driven by a smaller group size. Also, there might be heterogeneity within the relatively large industry categories. In summary, there is evidence for Hypothesis 5 that there is little effect-heterogeneity across industries.

4.5.3 Robustness

While the lack of heterogeneity in the estimates with respect to an establishment's industry is already an indicator of the effects' robustness, I perform a number of further checks. I start by relaxing the sample restriction and estimate the model in Equation 4.4 without removing either missing values for any of the other Y_j or implausible observations. Table D.4 in Appendix D.2 reports the estimates of the variables of interest. The main implications remain the same if we compare it to Table 4.4. Establishments that have no obstacles with regard to financial access are not affected in terms of workers or sales but see an increase in capital productivity by around 7%, whereas establishments with obstacles to financial market access are negatively affected in terms of workers and sales and also see a decrease of labor productivity by 4%.

I next check whether the results are driven by the flood definition of being 2 mm/h in intensity above the respective IDF curve. More precisely, one might be cautious that the average of 2.65 events over all establishments in the last fiscal year is producing some false positives. Thus, I use a much more restrictive 3 mm/h above the threshold, such that there is only an average of 1.38 events in the last fiscal year. I estimate the model in Equation 4.4 and report the coefficient estimates for $Flood_j^t$ and $Flood_j^t \times Access_j^f$ in Table 4.5. Results remain similar though the coefficients of $Flood_j^t \times Access_j^f$ are more strongly negative. This can be expected since the 3 mm/h minimum excess selects more extreme and potentially hazardous events, compared to the 2 mm/h definition.

I next run a series of permutation tests for each dependent variable Y_j. That is, I randomly permute the order of the Y_j relative to the rest of the data. Then, I estimate Equation 4.3

TABLE 4.5: Regressions: Alternative Event Definition

In log(·)	Sales/Worker (1)	Worker (2)	Sales (3)	$Inv_{L\&B}$ (4)	$Inv_{M\&E}$ (5)	Sales/L_{cost} (6)	Sales/E_{cost} (7)
2 mm/h Definition							
$Floods_j^t$	0.013	-0.020	-0.007	-0.077	0.143	0.008	0.071***
	(0.015)	(0.012)	(0.014)	(0.046)	(0.082)	(0.015)	(0.010)
$Floods_j^t \times$	-0.034*	-0.015	-0.049***	-0.017	-0.044	-0.040***	-0.022
$Access_j^f$	(0.018)	(0.016)	(0.013)	(0.029)	(0.072)	(0.008)	(0.014)
3 mm/h Definition							
$Floods_j^t$	0.030	-0.011	0.018	-0.101	0.155	0.018	0.043*
	(0.021)	(0.018)	(0.024)	(0.056)	(0.094)	(0.019)	(0.021)
$Floods_j^t \times$	-0.057**	-0.029	-0.087***	-0.055	-0.076	-0.058***	-0.013
$Access_j^f$	(0.025)	(0.025)	(0.009)	(0.033)	(0.130)	(0.009)	(0.016)

Notes: Table of regression results of the model in Equation 4.4 for event definition with 2 mm/h and 3 mm/h minimum excess intensity. Standard errors are in parentheses. *p<0.1; **p<0.05; ***p<0.01

TABLE 4.6: Regressions: P-Values from Permutation

In log(·)	Sales/Worker (1)	Worker (2)	Sales (3)	$Inv_{L\&B}$ (4)	$Inv_{M\&E}$ (5)	Sales/L_{cost} (6)	Sales/E_{cost} (7)
$Floods_j^t$	-0.006	-0.029	-0.034	-0.087	0.118	-0.015	0.058
p-value Reg.	0.657	0.037	0.015	0.042	0.156	0.195	0.003
p-value Perm.	0.390	0.127	0.171	0.033	0.073	0.378	0.140

Notes: Table of regression results of the model in Equation 4.3 with p-values from regression estimation and permutation.

and obtain the coefficient β_1 of $Flood_j^h$.[21] I repeat this process 10'000 times and calculate the quantile of the coefficient estimate with un-permuted data relative to the 10'000 permutations' estimates as p-value. I repeat that process for all dependent variables Y_j. Table 4.6 shows coefficients and p-values from the regression as in Table 4.3 together with the p-values from permutation. The p-values from the permutation are, in most cases, larger than their counterpart. This is due to the more conservative nature of permutation tests, which make no assumptions about the distributional properties of the data. This is especially the case for the variables Worker, Sales, and Sales/E_{cost}, which have a p-value

[21] I choose the model in Equation 4.3 over the one in Equation 4.4 because the evaluation of the interaction in a permutation setting to calculate p-values is not straightforward and requires treatment of joint-significance.

that is around 0.1 larger when calculated by permutation compared to the OLS regression. Thus, these estimates that do not differentiate between an establishment's financial access should be understood with some caution. In the case of investments, however, the p-values by permutation are smaller. Histograms of the 10'000 permutation coefficient estimates are shown in Figure D.1 in Appendix D.2.

4.6 Conclusion

I study the effect of extreme rainfall events that lead to flash floods on local economic activity as measured by establishment performance in Central America and the Caribbean. A major contribution is the physical definition of flash flood occurrence in a large region across many countries in a consistent manner with satellite rainfall data. I find that one such flash flood in a fiscal year decreases sales and the number of employees by around 3%, the investments into land and buildings by 8.3%, and increases capital productivity by 6%. This indicates that a flash flood is a negative shock to an establishment, while the increase in capital productivity could be due to mechanisms such as build-back-better or creative destruction.

My results further suggest that obstacles to financial access are a major determinant of impact. Establishments that report no obstacles to financial access do not see a reduction in sales or workers but experience an increase in capital productivity, whereas establishments that report obstacles to financial access see a decrease in sales of 4.8% and even a decrease in labor productivity. Back-of-the-envelope calculations indicate that the yearly flash flood impact on establishments is equal to a reduction in output of 8.745% due to their high frequency. I find no evidence of heterogeneous effects across industries, with the exception of the construction sector. Estimates on sales and employees are consistently negative for all other sectors, with the exception of the construction sector that sees a zero effect on these two measures.

The paper is the first that studies the establishment-level economic impacts of flash floods. It does so with a physically derived index of the hazard for a region that is

especially at risk (Pinos and Quesada-Román, 2021). There is both the contribution to the literature in terms of the hazard methodology and the implication with regard to climate change adaptation. In that sense, the focus on countries in Central America and the Caribbean is a double-edged sword. Since countries in that region would be affected gravely by an increase in flash floods (Seneviratne et al., 2021), knowledge of adaptation is crucial. Consistent data across several countries that provide geo-located information on establishment performance is, however, scarce. The attempt to identify the effects of flash floods with cross-sectional data from the Establishment Surveys is a difficult endeavor. Since the effects are likely dynamic in nature, these dynamics cannot be adequately modeled with the data, which is the main weakness of this analysis. However, by exploiting the timing of flash floods in the period prior to the last fiscal year, concerns for endogeneity can be relaxed. In other words, since the occurrence of a flood in a given year against the underlying risk of floods in that area is quasi-random, the identified effects serve as a credible baseline for policy recommendations. Nonetheless, future studies should aim at obtaining panel data on establishment performance to identify the dynamic effects.

My findings have two main implications for policy. First, flash floods negatively impact establishment performance within the fiscal year of the flood. Evidence in the literature for other hazards is somewhat mixed (Leiter, Oberhofer, and Raschky, 2009; Tanaka, 2015; Elliott et al., 2019; Cole et al., 2019; Okazaki, Okubo, and Strobl, 2019; Zhou and Botzen, 2021). Spatial as well as temporal aggregation of the research design as well as the severity of the hazard and institutional context, play an important role in the outcome. A warming and more humid climate will likely further increase the frequency and severity of flash floods in countries with an already high risk. Second, financial access is an effective modulator of impact in the case of flash floods. Adequate financing opportunities appear to make establishments resilient to flash floods and can be part of the efforts to decrease natural hazard vulnerability for economic development in Central America and the Caribbean. This finding echoes Hallegatte et al. (2016) who advocate for better financial inclusion to increase resilience and reduce the impacts of natural hazards in the

light of climate change. Hence, the possibility of quickly refunding destroyed productive capacity is a way to manage what cannot be avoided.

Appendix A

Economic Damages due to Extreme Precipitation during Tropical Storms: Evidence from Jamaica

A.1 Panel Summary Statistics

TABLE A.1: Hurricane Michelle Parish Statistics

	Damage M USD	Max. Rain mm/h	Total Rain mm	Max. Wind km/h	Population 1'000
Clarendon	2.38	3.39	9.49	61.02	245.10
Hanover	1.51	4.98	17.93	69.56	69.53
Manchester	1.36	3.47	10.73	61.59	189.80
Portland	9.41	26.24	70.16	52.10	81.74
St. Andrew & Kingston	20.49	7.90	22.79	58.99	662.43
St. Ann	3.20	8.82	26.04	63.35	172.36
St. Catherine	3.91	3.39	8.95	59.95	516.22
St. Elizabeth	4.86	5.38	13.95	64.62	150.21
St. James	2.48	2.80	12.55	68.24	93.90
St. Mary	11.79	17.06	51.19	60.61	113.61
St. Thomas	2.47	6.85	27.72	50.05	93.90
Trelawny	1.62	5.28	14.56	66.79	75.16
Westmoreland	1.77	5.24	17.14	68.67	144.10

Notes: Parish level data for Hurricane Michelle.

TABLE A.2: Hurricane Dean Parish Statistics

	Damage M USD	Max. Rain mm/h	Total Rain mm	Max. Wind km/h	Population 1'000
Clarendon	63.31	20.65	63.11	212.31	245.10
Hanover	10.61	12.15	37.07	184.64	69.53
Manchester	59.98	22.29	64.19	213.99	189.80
Portland	6.69	18.88	46.15	173.90	81.74
St. Andrew & Kingston	49.05	18.45	52.94	196.53	662.43
St. Ann	18.91	16.24	43.06	187.85	172.36
St. Catherine	33.34	20.93	58.62	200.10	516.22
St. Elizabeth	36.22	12.16	35.64	218.23	150.21
St. James	18.89	10.84	29.67	196.60	93.90
St. Mary	22.87	21.94	47.19	179.63	113.61
St. Thomas	51.80	26.71	59.31	184.71	93.90
Trelawny	13.05	20.49	49.72	192.85	75.16
Westmoreland	31.19	16.61	43.22	196.08	144.10

Notes: Parish level data for Hurricane Dean.

TABLE A.3: Storm Gustav Parish Statistics

	Damage M USD	Max. Rain mm/h	Total Rain mm	Max. Wind km/h	Population 1'000
Clarendon	19.22	13.16	66.25	71.24	245.10
Hanover	6.43	9.13	50.90	71.23	69.53
Manchester	3.43	11.88	57.70	74.06	189.80
Portland	3.55	24.13	79.69	71.88	81.74
St. Andrew & Kingston	57.04	13.67	80.60	70.99	662.43
St. Ann	2.41	14.32	58.53	71.10	172.36
St. Catherine	34.39	17.18	67.66	71.08	516.22
St. Elizabeth	5.06	7.29	45.06	75.84	150.21
St. James	8.39	9.56	41.65	72.37	93.90
St. Mary	47.06	14.33	88.08	71.63	113.61
St. Thomas	24.80	31.49	82.28	70.88	93.90
Trelawny	1.66	7.88	45.39	74.45	75.16
Westmoreland	40.07	7.77	45.54	71.05	144.10

Notes: Parish level data for Tropical Storm Gustav.

TABLE A.4: Storm Nicole Parish Statistics

	Damage M USD	Max. Rain mm/h	Total Rain mm	Max. Wind km/h	Population 1'000
Clarendon	23.60	44.62	120.05	18.71	245.10
Hanover	9.03	22.11	82.52	21.26	69.53
Manchester	14.39	33.98	110.84	19.11	189.80
Portland	35.85	23.24	71.27	13.16	81.74
St. Andrew & Kingston	38.91	48.35	100.30	17.24	662.43
St. Ann	16.41	51.84	117.43	18.97	172.36
St. Catherine	24.57	56.75	123.19	17.83	516.22
St. Elizabeth	28.48	51.61	156.35	19.60	150.21
St. James	16.48	34.86	120.90	20.17	93.90
St. Mary	26.81	24.06	64.41	18.71	113.61
St. Thomas	16.27	21.86	72.53	11.30	93.90
Trelawny	8.21	77.84	197.15	20.15	75.16
Westmoreland	25.33	35.25	130.96	21.08	144.10

Notes: Parish level data for Tropical Storm Nicole.

TABLE A.5: Hurricane Sandy Parish Statistics

	Damage M USD	Max. Rain mm/h	Total Rain mm	Max. Wind km/h	Population 1'000
Clarendon	3.25	12.95	85.69	87.72	245.10
Hanover	0.57	4.50	12.23	63.74	69.53
Manchester	0.68	18.21	96.09	78.98	189.80
Portland	0.20	52.07	169.02	96.25	81.74
St. Andrew & Kingston	10.74	38.78	133.27	95.92	662.43
St. Ann	4.47	30.89	102.31	90.88	172.36
St. Catherine	26.85	27.99	107.04	92.45	516.22
St. Elizabeth	0.23	13.51	59.39	72.04	150.21
St. James	1.82	8.38	26.90	71.28	93.90
St. Mary	30.84	51.34	130.15	101.62	113.61
St. Thomas	26.85	17.54	120.78	93.75	93.90
Trelawny	1.41	17.21	59.93	75.13	75.16
Westmoreland	32.90	5.06	12.92	63.57	144.10

Notes: Parish level data for Hurricane Sandy.

A.2 Wind Field Model

In terms of implementing Equation (1.1), one should note that the maximum sustained wind velocity anywhere in the storm V_{mst} is given by the storm track data, the forward velocity of the storm V_{hst} can be directly calculated by following the storm's movements between successive locations along its track, and the radial distance R_{cst} and the clockwise angle T_{cst} are calculated relative to the point of interest c. All other parameters have to be estimated or values assumed. For instance, we have no information on the gust wind factor G, but several studies (see e.g. Paulsen and Schroeder, 2005) have measured G to be around 1.5, and we also use this value. For S we follow Boose, Serrano, and Foster (2004) and assume it to be 1. While we also do not know the surface friction to determine D directly, Vickery, Masters, Powell, and Wadhera (2009) note that in open water, the reduction factor is about 0.7 and reduces by 14% on the coast and 28% further 50 km inland. We thus adopt a reduction factor that decreases linearly within this range as we consider points c further inland from the coast. Finally, to determine the shape of the wind profile curve B, we employ the approximation method of Holland (1980) where B is assumed to be in the range of $1.5 - 2.5$ and negatively correlated with central pressure. We use the parametric model estimated by Xiao, Xiao, and Duan (2009) to estimate the radius of maximum winds R_{mst}.

A.3 PPP Parameter Estimates

FIGURE A.1: Location Parameters

(A) μ_{1c}

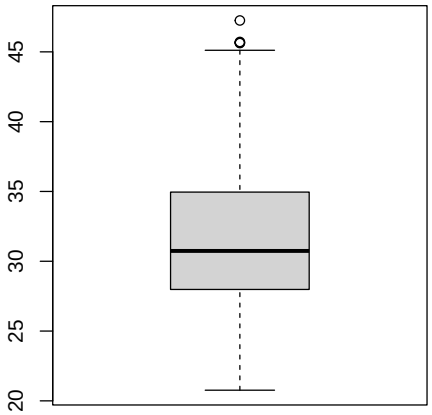

(B) μ_{2c}

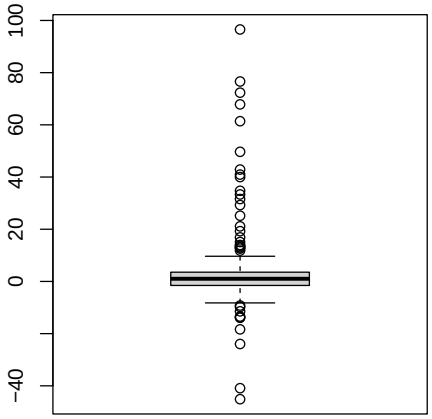

(C) μ_{3c}

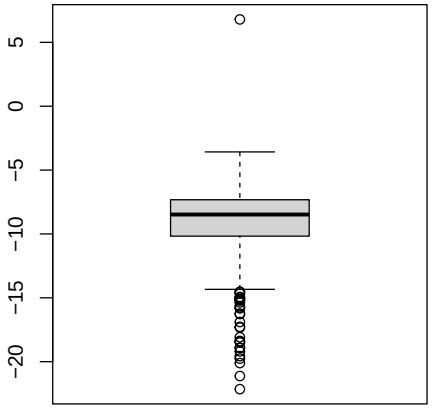

(D) μ_{4c}

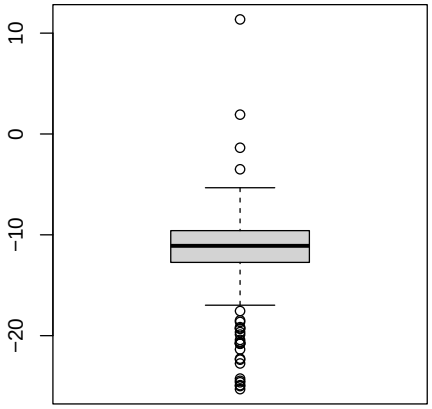

Notes: Boxplot of the location parameters as outlined in Equations 1.10 and 1.11.

FIGURE A.2: Location Parameters

(A) σ_{1c}

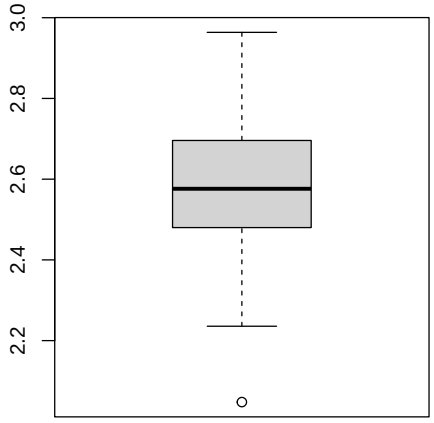

(B) σ_{2c}

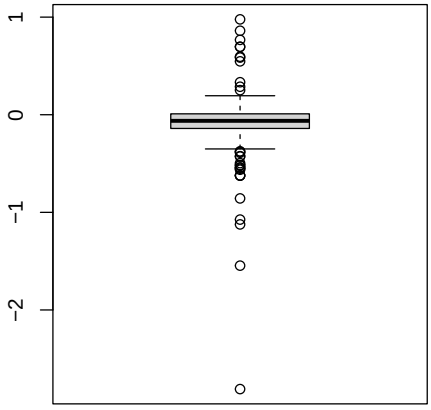

(C) σ_{3c}

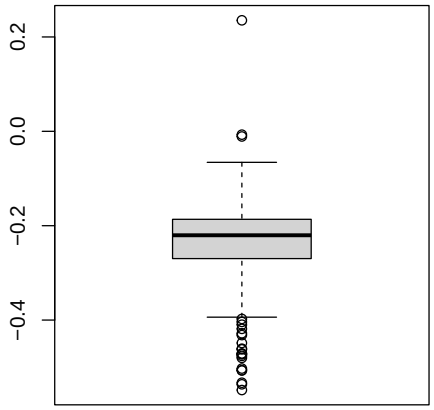

(D) σ_{4c}

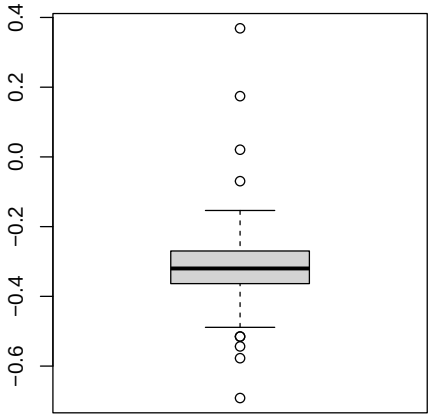

Notes: Boxplot of the scale parameters as outlined in Equations 1.10 and 1.11.

Appendix B

Flash Flood Detection via Copula-based IDF Curves: Evidence from Jamaica

B.1 Event Definition

Depending on the IETD, the statistical properties of the events change. Values of IETD between 4h and 24h are considered. Figure B.1 shows how the average intensity and duration changes for the flash flood event data with different values of the IETD. There is a relatively sudden drop in mean intensity for IETDs above 21 hours. Also, the mean duration increases one to one up until an IETD of 12 hours after which the slope becomes flatter. Both indicate that the IETD above 12 and 21 hours results in imprecisely delimited events with regard to duration and intensity, respectively. Figure B.2 shows the probability density function of duration and intensity for the confirmed flash flood event data (green) and maximum rainfall events (blue). In order to apply the two-sample approach, they should follow the same marginal distribution. The maximum rainfall events are more intense but shorter compared to the confirmed flash flood events. The resemblance between duration increases with higher IETD while there is no clear pattern for intensity. In conclusion, an IETD of 12 hours is best suitable for the data at hand. Note

that in section 2.4.3, where marginals are estimated for the conditional copula modeling, Kolmogorov-Smirnov tests indicate that the marginal distributions of the maximum rainfall event data are suitable for the smaller confirmed events data as well.

FIGURE B.1: Intensity and Duration for Different IETD

(A) Mean Event Intensity

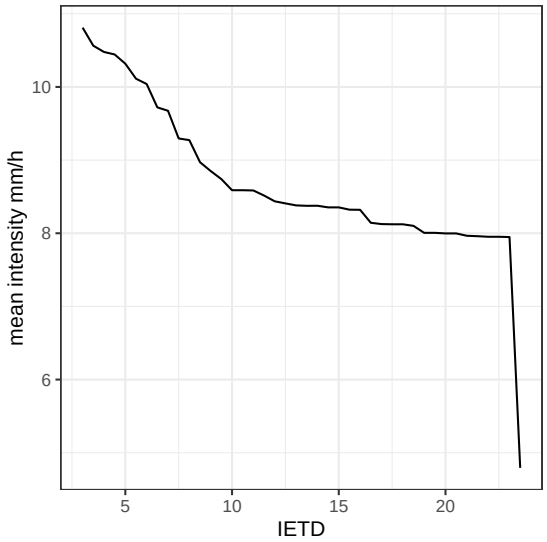

(B) Mean Event Duration

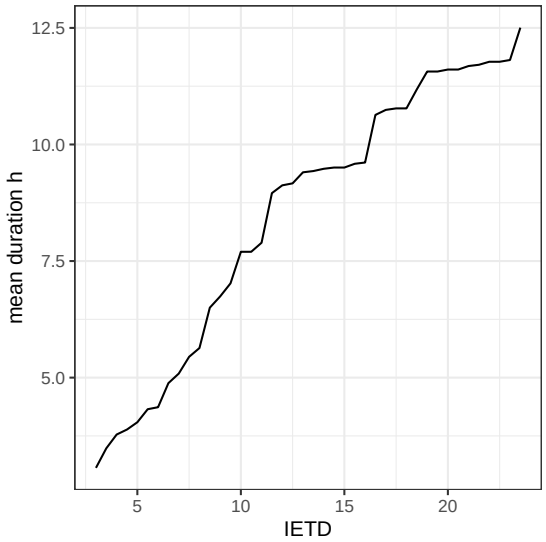

Notes: Mean event intensity and duration for different values of IETD.

FIGURE B.2: Marginal Distribution for Different IETD

(A) Duration IETD = 6 h

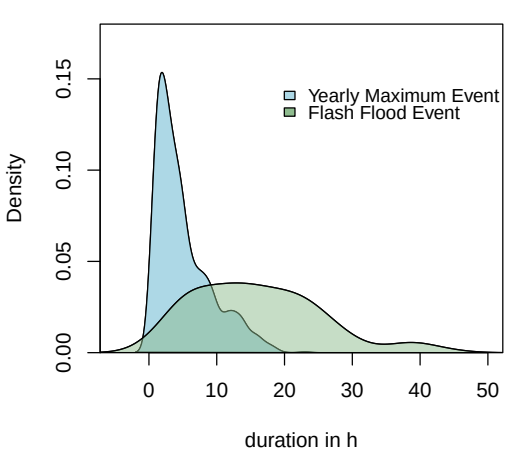

(B) Intensity IETD = 6 h

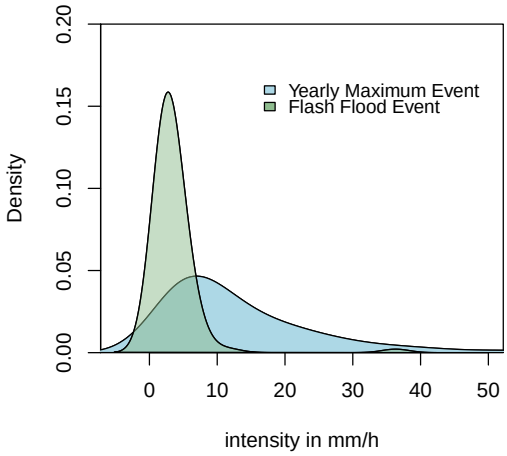

(C) Duration IETD = 12 h

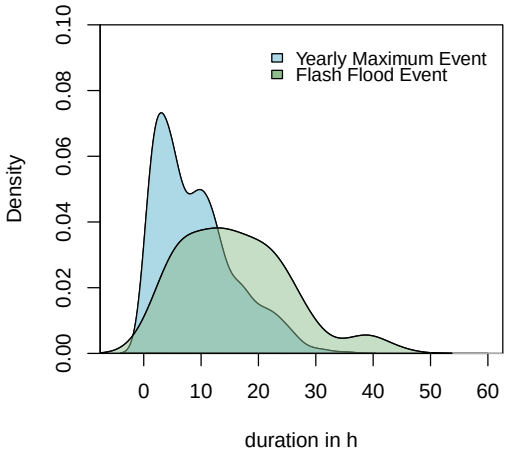

(D) Intensity IETD = 12 h

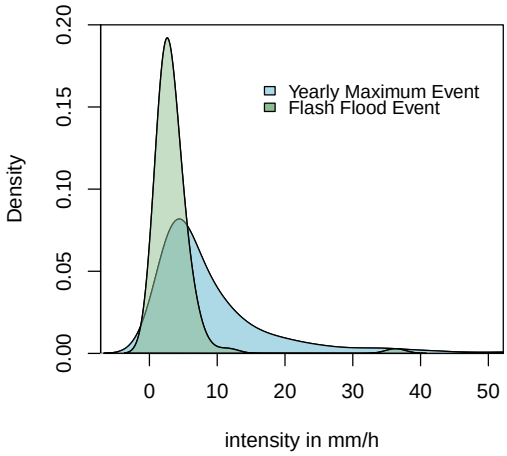

(E) Duration IETD = 24 h

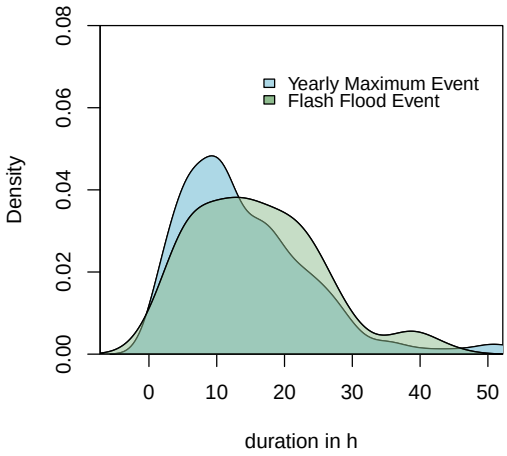

(F) Intensity IETD = 24 h

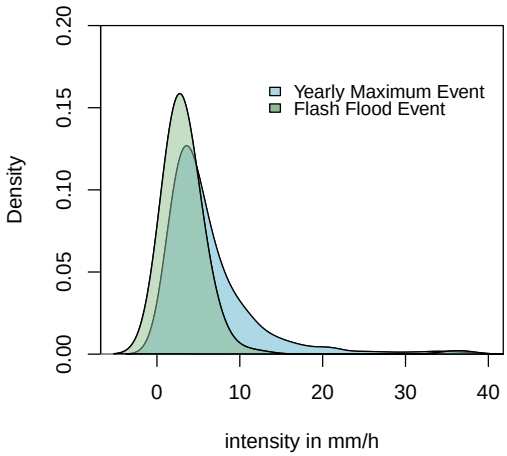

Notes: Probability density plots for duration and intensity for an IETD of 6 h, 12h, and 24 h.

B.2 Summary Statistics

The event data's summary statistics are given in Table B.1.

TABLE B.1: Summary Statistics

	Maximum Yearly Events				
	N	Mean	St. Dev.	Min	Max
Total Rainfall	1,120	47.542	24.522	6.705	148.485
Event Duration	1,120	9.031	6.811	0.500	36.000
Rainfall Intensity	1,120	9.927	12.089	0.905	120.000
	Confirmed flash flood Events				
	N	Mean	St. Dev.	Min	Max
Total Rainfall	93	73.677	53.283	12.120	240.100
Event Duration	93	11.419	8.325	17.000	32.000
Rainfall Intensity	93	5.169	7.271	0.962	54.760

Notes: Summary table of events with IETD of 12 hours for all locations with a confirmed flash flood event.

Appendix C

The Economic Dynamics after a Flood: Evidence from Satellite Data

C.1 Wind Field Model

In terms of implementing Equation 3.1 one should note that the maximum sustained wind velocity anywhere in the storm V_{mst} is given by the storm track data, the forward velocity of the storm V_{hst} can be directly calculated by following the storm's movements between successive locations along its track, the radial distance R_{cst} and the clockwise angle T_{cst} which are calculated relative to the point of interest c. All other parameters have to be estimated or values assumed. For instance, we have no information on the gust wind factor G, but a number of studies (see e.g. Paulsen and Schroeder, 2005) have measured G to be around 1.5, and I also use this value. For S, I follow Boose, Serrano, and Foster (2004) and assume it to be 1. While we also do not know the surface friction to determine D directly, Vickery, Masters, Powell, and Wadhera (2009) note that in open water, the reduction factor is about 0.7 and reduces by 14% on the coast and 28% further 50 km inland. I thus adopt a reduction factor that decreases linearly within this range as we consider points c further inland from the coast. Finally, to determine the shape of the wind profile curve B, I employ the approximation method of Holland (1980) where B is negatively correlated with central pressure and falls in the range of $1.5 - 2.5$ (Xiao et al.,

2011). I use the parametric non-basin-specific model estimated by Vickery and Wadhera (2008) to calculate the radius of maximum winds R_{mst}.

Appendix D

Flash Flood Hazard: an Economic Analysis for Central America and the Caribbean

D.1 Regression Tables

TABLE D.1: Regressions: Establishment Impacts

In log(·)	Sales/Worker (1)	Worker (2)	Sales (3)	$Inv_{L\&B}$ (4)	$Inv_{M\&E}$ (5)	Sales/L_{cost} (6)	Sales/E_{cost} (7)
$Floods_j^t$	-0.006	-0.029**	-0.034**	-0.087**	0.118	-0.015	0.058***
	(0.012)	(0.011)	(0.011)	(0.037)	(0.076)	(0.011)	(0.014)
$Floods_j^h$	0.004*	0.003	0.007**	0.010	-0.021	0.001	-0.006
	(0.002)	(0.002)	(0.002)	(0.007)	(0.025)	(0.002)	(0.003)
$Access_j^f$	-0.150*	-0.021	-0.170	-0.143	0.032	-0.132**	-0.087***
	(0.070)	(0.045)	(0.095)	(0.133)	(0.304)	(0.053)	(0.004)
Firm: Small	0.429	0.641***	1.07*	-0.093	1.16***	-0.043	0.709
	(0.436)	(0.131)	(0.532)	(0.148)	(0.175)	(0.294)	(0.425)
Firm: Medium	0.651	1.90***	2.55***	0.987***	1.39***	0.121	0.769
	(0.430)	(0.208)	(0.567)	(0.281)	(0.189)	(0.286)	(0.432)
Firm: Large	1.08**	3.45***	4.53***	2.32***	2.91***	0.272	0.834*
	(0.442)	(0.324)	(0.656)	(0.427)	(0.638)	(0.275)	(0.419)
Firm: V. Large	1.29**	4.49***	5.78***	3.35***	3.04***	0.396	0.845
	(0.442)	(0.259)	(0.622)	(0.443)	(0.375)	(0.287)	(0.475)
% Public	0.003	0.007	0.010	0.023	0.034	-0.0002	-0.019***
	(0.004)	(0.004)	(0.007)	(0.019)	(0.043)	(0.007)	(0.004)
Firm Age	0.005**	0.008***	0.013***	0.009	-0.006	0.0008	-0.0009
	(0.002)	(0.001)	(0.003)	(0.007)	(0.010)	(0.0006)	(0.003)
% Direct Exports	0.005**	0.005***	0.010***	0.008	0.006	0.003**	0.0008
	(0.002)	(0.001)	(0.002)	(0.006)	(0.008)	(0.001)	(0.002)
Size of City	0.057*	0.013	0.070**	0.063	-0.078	-0.003	-0.0005
	(0.026)	(0.012)	(0.025)	(0.073)	(0.104)	(0.025)	(0.016)
Observations	1,725	1,725	1,725	1,725	1,725	1,722	1,719
R^2	0.40	0.83	0.71	0.28	0.08	0.93	0.83
Fixed Effects:							
Industry	✓	✓	✓	✓	✓	✓	✓
Country	✓	✓	✓	✓	✓	✓	✓
Year	✓	✓	✓	✓	✓	✓	✓

Notes: Table of regression results of the model in Equation 4.3. Standard errors are in parentheses. *p<0.1; **p<0.05; ***p<0.01

TABLE D.2: Regressions: Financial Access

ln log(·)	Sales/Worker (1)	Worker (2)	Sales (3)	$Inv_{L\&B}$ (4)	$Inv_{M\&E}$ (5)	Sales/L_{cost} (6)	Sales/E_{cost} (7)
$Floods_j^t$	0.013	-0.020	-0.007	-0.077	0.143	0.008	0.071***
	(0.015)	(0.012)	(0.014)	(0.046)	(0.082)	(0.015)	(0.010)
$Floods_j^t \times$	-0.034*	-0.015	-0.049***	-0.017	-0.044	-0.040***	-0.022
$Access_j^f$	(0.018)	(0.016)	(0.013)	(0.029)	(0.072)	(0.008)	(0.014)
$Access_j^f$	-0.060	0.019	-0.041	-0.097	0.148	-0.024	-0.028
	(0.085)	(0.063)	(0.088)	(0.144)	(0.361)	(0.047)	(0.046)
$Floods_j^h$	0.004**	0.003	0.007*	0.010	-0.021	0.0009	-0.006*
	(0.002)	(0.002)	(0.003)	(0.007)	(0.025)	(0.004)	(0.003)
Firm: Small	0.428	0.641***	1.07*	-0.094	1.16***	-0.045	0.707
	(0.450)	(0.133)	(0.551)	(0.152)	(0.177)	(0.308)	(0.435)
Firm: Medium	0.647	1.89***	2.54***	0.985***	1.39***	0.116	0.766
	(0.446)	(0.210)	(0.589)	(0.286)	(0.174)	(0.303)	(0.444)
Firm: Large	1.07**	3.45***	4.52***	2.32***	2.90***	0.263	0.830*
	(0.456)	(0.325)	(0.674)	(0.428)	(0.631)	(0.292)	(0.430)
Firm: V. Large	1.28**	4.49***	5.77***	3.34***	3.03***	0.390	0.842
	(0.458)	(0.260)	(0.641)	(0.447)	(0.356)	(0.305)	(0.485)
% Public	0.002	0.007	0.009	0.023	0.033	-0.0008	-0.019***
	(0.004)	(0.004)	(0.007)	(0.023)	(0.043)	(0.009)	(0.005)
Firm Age	0.005**	0.008***	0.013***	0.009	-0.006	0.0008	-0.0009
	(0.002)	(0.002)	(0.003)	(0.006)	(0.010)	(0.003)	(0.003)
% Direct Exports	0.005**	0.005**	0.010***	0.008	0.006	0.003	0.0008
	(0.002)	(0.001)	(0.002)	(0.007)	(0.011)	(0.003)	(0.002)
Size of City	0.058*	0.013	0.072**	0.063	-0.077	-0.002	0.0002
	(0.026)	(0.012)	(0.025)	(0.077)	(0.106)	(0.028)	(0.018)
Observations	1,883	1,883	1,883	1,883	1,883	1,880	1,877
R^2	0.41	0.82	0.71	0.29	0.08	0.92	0.83
Within R^2	0.13	0.80	0.66	0.20	0.03	0.04	0.009
Fixed Effects:							
Industry	✓	✓	✓	✓	✓	✓	✓
Country	✓	✓	✓	✓	✓	✓	✓
Year	✓	✓	✓	✓	✓	✓	✓

Notes: Table of regression results of the model in Equation 4.4 with the interaction for financial access. Standard errors are in parentheses. *p<0.1; **p<0.05; ***p<0.01

TABLE D.3: Regressions: Industry Heterogeneity

In log(·)	Sales/Worker (1)	Worker (2)	Sales (3)	$Inv_{L\&B}$ (4)	$Inv_{M\&E}$ (5)	Sales/L_{cost} (6)	Sales/E_{cost} (7)
$Floods_j^t$ ×	-0.010	-0.029*	-0.040***	-0.035	0.259	0.0007	0.021
Chemicals/Plastic	(0.016)	(0.014)	(0.009)	(0.028)	(0.165)	(0.017)	(0.017)
$Floods_j^t$ ×	-0.042	0.056	0.014	-0.341***	0.121	-0.022	0.062**
Construction	(0.028)	(0.037)	(0.041)	(0.062)	(0.168)	(0.032)	(0.019)
$Floods_j^t$ ×Food	0.005	-0.024**	-0.018	-0.119**	0.139**	0.011	0.077**
	(0.022)	(0.010)	(0.026)	(0.039)	(0.043)	(0.024)	(0.026)
$Floods_j^t$ × Metals	0.004	-0.048**	-0.044	-0.102	0.014	-0.033**	0.046
& Minerals	(0.026)	(0.020)	(0.027)	(0.099)	(0.063)	(0.013)	(0.039)
$Floods_j^t$ × Textile	-0.018	-0.032*	-0.050**	-0.058	0.067	-0.015	0.039*
&Garments	(0.014)	(0.014)	(0.019)	(0.044)	(0.104)	(0.016)	(0.018)
$Floods_j^t$ × Other	0.024	-0.036*	-0.012	-0.149***	0.209***	0.015	0.146***
Manufacturing	(0.018)	(0.016)	(0.017)	(0.044)	(0.058)	(0.026)	(0.022)
$Floods_j^t$ × Other	-0.027	-0.016	-0.043	-0.061	0.024	-0.063*	0.038
	(0.026)	(0.010)	(0.025)	(0.042)	(0.090)	(0.031)	(0.045)
$Floods_j^h$	0.005**	0.003	0.007***	0.010	-0.019	0.002	-0.006
	(0.002)	(0.002)	(0.002)	(0.010)	(0.021)	(0.003)	(0.005)
$Access_j^f$	-0.150*	-0.019	-0.170	-0.148	0.031	-0.132**	-0.087**
	(0.072)	(0.042)	(0.098)	(0.137)	(0.300)	(0.055)	(0.035)
Firm: Small	0.428	0.643***	1.07*	-0.082	1.18***	-0.030	0.694
	(0.427)	(0.131)	(0.525)	(0.156)	(0.170)	(0.271)	(0.417)
Firm: Medium	0.645	1.90***	2.55***	0.994***	1.42***	0.132	0.744
	(0.420)	(0.207)	(0.561)	(0.276)	(0.200)	(0.256)	(0.420)
Firm: Large	1.08**	3.45***	4.53***	2.34***	2.93***	0.283	0.813*
	(0.434)	(0.324)	(0.652)	(0.420)	(0.590)	(0.247)	(0.411)
Firm: V. Large	1.29**	4.49***	5.78***	3.34***	3.09***	0.416	0.841
	(0.435)	(0.258)	(0.620)	(0.431)	(0.360)	(0.259)	(0.467)
% Public	0.003	0.007	0.010	0.022	0.030	-0.0005	-0.018
	(0.004)	(0.005)	(0.006)	(0.022)	(0.040)	(0.010)	(0.010)
Firm Age	0.005**	0.008***	0.013***	0.009	-0.006	0.0007	-0.0010
	(0.002)	(0.002)	(0.003)	(0.008)	(0.012)	(0.003)	(0.005)
% Direct Exports	0.005*	0.005***	0.010***	0.009	0.006	0.003	0.0007
	(0.002)	(0.001)	(0.002)	(0.006)	(0.010)	(0.003)	(0.004)
Size of City	0.058**	0.014	0.071**	0.059	-0.079	-0.004	0.003
	(0.025)	(0.012)	(0.026)	(0.078)	(0.116)	(0.028)	(0.024)
Observations	1,883	1,883	1,883	1,883	1,883	1,880	1,877
R^2	0.41	0.82	0.71	0.30	0.08	0.92	0.83
Fixed Effects:							
Industry	✓	✓	✓	✓	✓	✓	✓
Country	✓	✓	✓	✓	✓	✓	✓
Year	✓	✓	✓	✓	✓	✓	✓

Notes: Table of regression results of the model in Equation 4.5 with the interactions for industry. Standard errors are in parentheses. *p<0.1; **p<0.05; ***p<0.01

D.2 Robustness

TABLE D.4: Regressions: All Observations

In log(·)	Sales/Worker (1)	Worker (2)	Sales (3)	$Inv_{L\&B}$ (4)	$Inv_{M\&E}$ (5)	Sales/L_{cost} (6)	Sales/E_{cost} (7)
$Floods_j^t$	0.030	-0.004	0.028	-0.098**	0.205	0.011	0.073***
	(0.022)	(0.010)	(0.029)	(0.034)	(0.133)	(0.012)	(0.016)
$Floods_j^t \times Access_j^f$	-0.018	-0.017*	-0.034*	0.027	-0.060	-0.040***	-0.021
	(0.019)	(0.007)	(0.017)	(0.027)	(0.060)	(0.008)	(0.014)
$Floods_j^h$	5.21×10^{-5}	-0.0001	-0.0001	0.004	-0.023	0.003*	-0.005
	(0.002)	(0.001)	(0.002)	(0.007)	(0.023)	(0.002)	(0.008)
$Access_j^f$	-0.034	0.014	-0.012	-0.281*	-0.025	-0.009	-0.013
	(0.055)	(0.033)	(0.036)	(0.146)	(0.310)	(0.049)	(0.027)
Observations	5,313	6,230	5,323	2,654	2,725	4,904	4,291
R^2	0.40	0.82	0.66	0.28	0.15	0.90	0.79
Fixed Effects:							
Industry	✓	✓	✓	✓	✓	✓	✓
Country	✓	✓	✓	✓	✓	✓	✓
Year	✓	✓	✓	✓	✓	✓	✓

Notes: Table of regression results of the model in Equation 4.4 with all observations. The table is without coefficients of the control variables X_j for brevity. Standard errors are in parentheses. *p<0.1; **p<0.05; ***p<0.01

FIGURE D.1: Histograms of Coefficients from Permutation

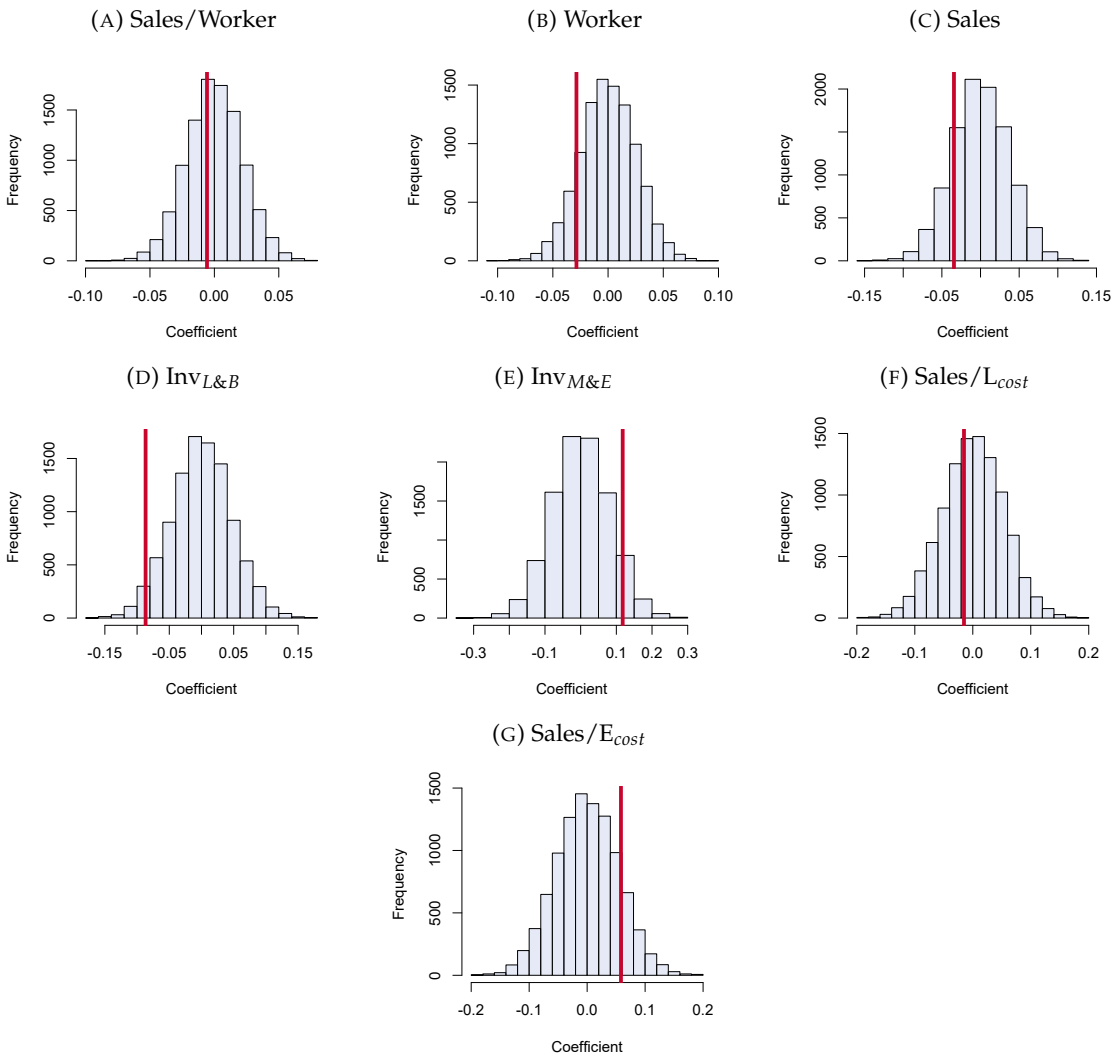

Notes: Histograms of the coefficient estimates with random permutation in Y_j. The red line indicates the estimate with unpermuted data. The regression model estimated is in Equation 4.3.

Bibliography

Acemoglu, Daron, Philippe Aghion, Leonardo Bursztyn, and David Hemous. 2012. "The environment and directed technical change." *American economic review* 102 (1):131–166.

Albala-Bertrand, Jose-Miguel. 1993. "Natural disaster situations and growth: A macroeconomic model for sudden disaster impacts." *World Development* 21 (9):1417–1434.

Aleotti, Pietro. 2004. "A warning system for rainfall-induced shallow failures." *Engineering geology* 73 (3-4):247–265.

Altay, Nezih and Andres Ramirez. 2010. "Impact of disasters on firms in different sectors: implications for supply chains." *Journal of Supply Chain Management* 46 (4):59–80.

Amatulli, Giuseppe, Sami Domisch, Mao-Ning Tuanmu, Benoit Parmentier, Ajay Ranipeta, Jeremy Malczyk, and Walter Jetz. 2018. "A suite of global, cross-scale topographic variables for environmental and biodiversity modeling." *Scientific data* 5 (1):1–15.

Anderson, Malcolm G., Elizabeth Holcombe, James R. Blake, Francis Ghesquire, Niels Holm-Nielsen, and Tiguist Fisseha. 2011. "Reducing landslide risk in communities: Evidence from the Eastern Caribbean." *Applied Geography* 31 (2):590–599.

Arenas, Andres Diaz. 1983. "Tropical storms in Central America and the Caribbean: characteristic rainfall and forecasting of flash floods." *Hydrology of humid tropical regions. International Association of Hydrological Sciences (IAHS) Publication* (140):39–51.

Ariff, Noratiqah Mohd, Abdul Aziz Jemain, Kamarulzaman Ibrahim, and Wan Zawiah Wan Zin. 2012. "IDF relationships using bivariate copula for storm events in Peninsular Malaysia." *Journal of Hydrology* 470:158–171.

Aroca-Jiménez, Estefanía, José M. Bodoque, Juan A. García, and Andrés Díez-Herrero. 2018. "A quantitative methodology for the assessment of the regional economic vulnerability to flash floods." *Journal of hydrology* 565:386–399.

Bakkensen, Laura A., Doo-Sun R. Park, and Raja Shanti Ranjan Sarkar. 2018. "Climate costs of tropical cyclone losses also depend on rain." *Environmental Research Letters* 13 (7):074034.

Bakkensen, Laura A., Xiangying Shi, and Brianna D. Zurita. 2018. "The impact of disaster data on estimating damage determinants and climate costs." *Economics of Disasters and Climate Change* 2 (1):49–71.

Baradaranshoraka, Mohammad, Jean-Paul Pinelli, Kurt Gurley, Xinlai Peng, and Mingwei Zhao. 2017. "Hurricane wind versus storm surge damage in the context of a risk prediction model." *Journal of Structural Engineering* 143 (9):04017103.

Barone, Guglielmo and Sauro Mocetti. 2014. "Natural disasters, growth and institutions: a tale of two earthquakes." *Journal of Urban Economics* 84:52–66.

Barrios, Salvador, Luisito Bertinelli, and Eric Strobl. 2010. "Trends in rainfall and economic growth in Africa: A neglected cause of the African growth tragedy." *The Review of Economics and Statistics* 92 (2):350–366.

Barrot, Jean-Noël and Julien Sauvagnat. 2016. "Input specificity and the propagation of idiosyncratic shocks in production networks." *The Quarterly Journal of Economics* 131 (3):1543–1592.

Beguería, Santiago, Marta Angulo-Martínez, Sergio M. Vicente-Serrano, J. Ignacio López-Moreno, and Ahmed El-Kenawy. 2011. "Assessing trends in extreme precipitation events intensity and magnitude using non-stationary peaks-over-threshold analysis:

a case study in northeast Spain from 1930 to 2006." *International Journal of Climatology* 31 (14):2102–2114.

Benson, Charlotte and Edward J. Clay. 2004. *Understanding the economic and financial impacts of natural disasters*. 4. World Bank Publications.

Bertinelli, Luisito and Eric Strobl. 2013. "Quantifying the local economic growth impact of hurricane strikes: an analysis from outer space for the Caribbean." *Journal of Applied Meteorology and Climatology* 52 (8):1688–1697.

Bezak, Nejc, Mojca Šraj, and Matjaž Mikoš. 2016. "Copula-based IDF curves and empirical rainfall thresholds for flash floods and rainfall-induced landslides." *Journal of Hydrology* 541:272–284.

Boose, Emery R., Mayra I. Serrano, and David R. Foster. 2004. "Landscape and regional impacts of hurricanes in Puerto Rico." *Ecological Monographs* 74 (2):335–352.

Borga, Marco, Paolo Boscolo, Francesco Zanon, and Marco Sangati. 2007. "Hydrometeorological analysis of the 29 August 2003 flash flood in the Eastern Italian Alps." *Journal of hydrometeorology* 8 (5):1049–1067.

Botzen, Wouter, Olivier Deschenes, and Mark Sanders. 2019. "The economic impacts of natural disasters: A review of models and empirical studies." *Review of Environmental Economics and Policy* .

Bourque, Linda B., Judith M. Siegel, Megumi Kano, and Michele M. Wood. 2006. "Weathering the storm: The impact of hurricanes on physical and mental health." *The Annals of the American Academy of Political and Social Science* 604 (1):129–151.

Bradshaw, Sarah. 2003. "Handbook for estimating the socio-economic and environmental effects of disasters." *ECLAC & International Bank for Reconstruction & Development* .

Brei, Michael, Preeya Mohan, and Eric Strobl. 2019. "The impact of natural disasters on the banking sector: Evidence from hurricane strikes in the Caribbean." *The Quarterly Review of Economics and Finance* 72:232–239.

Buchhorn, Marcel, Myroslava Lesiv, Nandin-Erdene Tsendbazar, Martin Herold, Luc Bertels, and Bruno Smets. 2020. "Copernicus global land cover layers—collection 2." *Remote Sensing* 12 (6):1044.

Burgess, Christopher P., Michael A. Taylor, Tannecia Stephenson, and Arpita Mandal. 2015. "Frequency analysis, infilling and trends for extreme precipitation for Jamaica (1895–2100)." *Journal of Hydrology: Regional Studies* 3:424–443.

Caine, Nel. 1980. "The rainfall intensity-duration control of shallow landslides and debris flows." *Geografiska annaler: series A, physical geography* 62 (1-2):23–27.

Carby, Barbara. 2018. "Integrating disaster risk reduction in national development planning: experience and challenges of Jamaica." *Environmental Hazards* 17 (3):219–233.

Cavallo, Eduardo, Sebastian Galiani, Ilan Noy, and Juan Pantano. 2013. "Catastrophic natural disasters and economic growth." *Review of Economics and Statistics* 95 (5):1549–1561.

Cavallo, Eduardo and Ilan Noy. 2011. "Natural disasters and the economy—a survey." *International Review of Environmental and Resource Economics* 5 (1):63–102.

Charvériat, Céline. 2000. "Natural disasters in Latin America and the Caribbean: An overview of risk." .

Chen, Shuyi S., John A. Knaff, and Frank D. Marks Jr. 2006. "Effects of vertical wind shear and storm motion on tropical cyclone rainfall asymmetries deduced from TRMM." *Monthly Weather Review* 134 (11):3190–3208.

Chen, Xi and William D. Nordhaus. 2011. "Using luminosity data as a proxy for economic statistics." *Proceedings of the National Academy of Sciences* 108 (21):8589–8594.

Chen, Xi and William D Nordhaus. 2019. "VIIRS nighttime lights in the estimation of cross-sectional and time-series GDP." *Remote Sensing* 11 (9):1057.

Cole, Matthew A., Robert J. R. Elliott, Giovanni Occhiali, and Eric Strobl. 2018. "Power outages and firm performance in Sub-Saharan Africa." *Journal of Development Economics* 134:150–159.

Cole, Matthew A., Robert J. R. Elliott, Toshihiro Okubo, and Eric Strobl. 2019. "Natural disasters and spatial heterogeneity in damages: the birth, life and death of manufacturing plants." *Journal of Economic Geography* 19 (2):373–408.

Coles, Stuart, Joanna Bawa, Lesley Trenner, and Pat Dorazio. 2001. *An introduction to statistical modeling of extreme values*, vol. 208. Springer.

Collalti, Dino, Nekeisha Spencer, and Eric Strobl. 2023. "Flash Flood detection via copula-based IDF curves." Unpublished.

Collalti, Dino and Eric Strobl. 2022. "Economic damages due to extreme precipitation during tropical storms: evidence from Jamaica." *Natural Hazards* 110 (3):2059–2086.

Collischonn, Bruno, Walter Collischonn, and Carlos Eduardo Morelli Tucci. 2008. "Daily hydrological modeling in the Amazon basin using TRMM rainfall estimates." *Journal of Hydrology* 360 (1-4):207–216.

Conceição, Pedro. 2019. *Human Development Report 2019: Beyond Income, Beyond Averages, Beyond Today: Inequalities in Human Development in the 21st Century*. United Nations Development Programme.

Cook, R. Dennis. 1977. "Detection of Influential Observation in Linear Regression." *Technometrics* 19 (1):15–18. URL `http://www.jstor.org/stable/1268249`.

Crespo Cuaresma, Jesús, Jaroslava Hlouskova, and Michael Obersteiner. 2008. "Natural disasters as creative destruction? Evidence from developing countries." *Economic Inquiry* 46 (2):214–226.

Czajkowski, Jeffrey, Kevin Simmons, and Daniel Sutter. 2011. "An analysis of coastal and inland fatalities in landfalling US hurricanes." *Natural hazards* 59 (3):1513–1531.

Davison, Anthony C. and Richard L. Smith. 1990. "Models for exceedances over high thresholds." *Journal of the Royal Statistical Society: Series B (Methodological)* 52 (3):393–425.

De Janvry, Alain, Alejandro Del Valle, and Elisabeth Sadoulet. 2016. "Insuring growth: the impact of disaster funds on economic reconstruction in Mexico." *World Bank Policy Research Working Paper* (7714).

De Michele, Carlo, Gianfausto Salvadori, Renata Vezzoli, and Silvano Pecora. 2013. "Multivariate assessment of droughts: Frequency analysis and dynamic return period." *Water Resources Research* 49 (10):6985–6994.

Dell, Melissa, Benjamin F. Jones, and Benjamin A. Olken. 2012. "Temperature shocks and economic growth: Evidence from the last half century." *American Economic Journal: Macroeconomics* 4 (3):66–95.

Dell, Melissa, Benjamin F Jones, and Benjamin A Olken. 2014. "What do we learn from the weather? The new climate-economy literature." *Journal of Economic literature* 52 (3):740–798.

Demirdjian, Levon, Yaping Zhou, and George J. Huffman. 2018. "Statistical modeling of extreme precipitation with TRMM data." *Journal of applied meteorology and climatology* 57 (1):15–30.

Demuth, Julie L., Mark DeMaria, and John A. Knaff. 2006. "Improvement of Advanced Microwave Sounding Unit tropical cyclone intensity and size estimation algorithms." *Journal of applied meteorology and climatology* 45 (11):1573–1581.

Deryugina, Tatyana. 2017. "The fiscal cost of hurricanes: Disaster aid versus social insurance." *American Economic Journal: Economic Policy* 9 (3):168–198.

Diakakis, M., G. Deligiannakis, Z. Antoniadis, M Melaki, N. K. Katsetsiadou, E. Andreadakis, N. I. Spyrou, and M. Gogou. 2020. "Proposal of a flash flood impact severity scale for the classification and mapping of flash flood impacts." *Journal of Hydrology* 590:125452.

Do, Trung Q., John W. van de Lindt, and Daniel T. Cox. 2020. "Hurricane Surge-Wave Building Fragility Methodology for Use in Damage, Loss, and Resilience Analysis." *Journal of Structural Engineering* 146 (1):04019177.

Dou, Jie, Ali P. Yunus, Yueren Xu, Zhongfan Zhu, Chi-Wen Chen, Mehebub Sahana, Khabat Khosravi, Yong Yang, and Binh Thai Pham. 2019. "Torrential rainfall-triggered shallow landslide characteristics and susceptibility assessment using ensemble data-driven models in the Dongjiang Reservoir Watershed, China." *Natural Hazards* 97 (2):579–609.

Driscoll, John C. and Aart C. Kraay. 1998. "Consistent covariance matrix estimation with spatially dependent panel data." *Review of economics and statistics* 80 (4):549–560.

Eberenz, Samuel, Samuel Lüthi, and David N. Bresch. 2021. "Regional tropical cyclone impact functions for globally consistent risk assessments." *Natural Hazards and Earth System Sciences* 21 (1):393–415.

Eichenauer, Vera Z., Andreas Fuchs, Sven Kunze, and Eric Strobl. 2020. "Distortions in aid allocation of United Nations flash appeals: Evidence from the 2015 Nepal earthquake." *World development* 136:105023.

Elliott, Robert J. R., Yi Liu, Eric Strobl, and Meng Tong. 2019. "Estimating the direct and indirect impact of typhoons on plant performance: Evidence from Chinese manufacturers." *Journal of Environmental Economics and Management* 98:102252.

Elliott, Robert J. R., Eric Strobl, and Puyang Sun. 2015. "The local impact of typhoons on economic activity in China: A view from outer space." *Journal of Urban Economics* 88:50–66.

Elvidge, Christopher D., Daniel Ziskin, Kimberly E. Baugh, Benjamin T. Tuttle, Tilottama Ghosh, Dee W. Pack, Edward H. Erwin, and Mikhail Zhizhin. 2009. "A fifteen year record of global natural gas flaring derived from satellite data." *Energies* 2 (3):595–622.

Emanuel, Kerry. 2005. "Increasing destructiveness of tropical cyclones over the past 30 years." *Nature* 436 (7051):686.

———. 2011. "Global warming effects on US hurricane damage." *Weather, Climate, and Society* 3 (4):261–268.

———. 2013. "Downscaling CMIP5 climate models shows increased tropical cyclone activity over the 21st century." *Proceedings of the National Academy of Sciences* 110 (30):12219–12224.

Encyclopedia Britannica. 2022. "Central America." Website. Https://www.britannica.com/place/Central-America.

Fabian, Marius, Christian Lessmann, and Tim Sofke. 2019. "Natural disasters and regional development–the case of earthquakes." *Environment and Development Economics* 24 (5):479–505.

Felbermayr, Gabriel and Jasmin Gröschl. 2014. "Naturally negative: The growth effects of natural disasters." *Journal of development economics* 111:92–106.

Felbermayr, Gabriel, Jasmin Gröschl, Mark Sanders, Vincent Schippers, and Thomas Steinwachs. 2022. "The economic impact of weather anomalies." *World Development* 151:105745.

Field, Christopher B. and Vicente R. Barros. 2014. *Climate change 2014–Impacts, adaptation and vulnerability: Regional aspects*. Cambridge University Press.

Fomby, Thomas, Yuki Ikeda, and Norman V Loayza. 2013. "The growth aftermath of natural disasters." *Journal of applied econometrics* 28 (3):412–434.

Frost, Chris and Simon G. Thompson. 2000. "Correcting for regression dilution bias: comparison of methods for a single predictor variable." *Journal of the Royal Statistical Society: Series A (Statistics in Society)* 163 (2):173–189.

Furrer, Eva M. and Richard W. Katz. 2008. "Improving the simulation of extreme precipitation events by stochastic weather generators." *Water Resources Research* 44 (12).

Gencer, Ebru. 2013. "An overview of urban vulnerability to natural disasters and climate change in Central America & the Caribbean Region." .

Gibson, John, Susan Olivia, Geua Boe-Gibson, and Chao Li. 2021. "Which night lights data should we use in economics, and where?" *Journal of Development Economics* 149:102602.

Gilewski, Paweł and Marek Nawalany. 2018. "Inter-comparison of rain-gauge, radar, and satellite (IMERG GPM) precipitation estimates performance for rainfall-runoff modeling in a mountainous catchment in Poland." *Water* 10 (11):1665.

Gilleland, Eric and Richard W Katz. 2006. "Analyzing seasonal to interannual extreme weather and climate variability with the extremes toolkit." In *18th Conference on Climate Variability and Change, 86th American Meteorological Society (AMS) Annual Meeting*, vol. 29. Citeseer.

Gilleland, Eric and Richard W. Katz. 2016. "extRemes 2.0: An extreme value analysis package in R." *Journal of Statistical Software* 72 (8):1–39.

Grønneberg, Steffen and Nils Lid Hjort. 2014. "The copula information criteria." *Scandinavian Journal of Statistics* 41 (2):436–459.

Grossmann, Iris and M. Granger Morgan. 2011. "Tropical cyclones, climate change, and scientific uncertainty: what do we know, what does it mean, and what should be done?" *Climatic Change* 108 (3):543–579.

Hallegatte, Stéphane and Patrice Dumas. 2009. "Can natural disasters have positive consequences? Investigating the role of embodied technical change." *Ecological Economics* 68 (3):777–786.

Hallegatte, Stéphane, Jean-Charles Hourcade, and Patrice Dumas. 2007. "Why economic dynamics matter in assessing climate change damages: illustration on extreme events." *Ecological economics* 62 (2):330–340.

Hallegatte, Stephane and Valentin Przyluski. 2010. *The economics of natural disasters: concepts and methods*. The World Bank.

Hallegatte, Stephane and Adrien Vogt-Schilb. 2019. *Are losses from natural disasters more than just asset losses? the role of capital aggregation, sector interactions, and investment behaviors*. Springer.

Hallegatte, Stephane, Adrien Vogt-Schilb, Mook Bangalore, and Julie Rozenberg. 2016. *Unbreakable: building the resilience of the poor in the face of natural disasters*. World Bank Publications.

Hatzikyriakou, Adam and Ning Lin. 2018. "Assessing the vulnerability of structures and residential communities to storm surge: An analysis of flood impact during Hurricane Sandy." *Frontiers in Built Environment* 4:4.

Hence, Deanna A. and Robert A. Houze Jr. 2011. "Vertical structure of hurricane eyewalls as seen by the TRMM Precipitation Radar." *Journal of the Atmospheric Sciences* 68 (8):1637–1652.

Henderson, J. Vernon, Adam Storeygard, and David N. Weil. 2012. "Measuring economic growth from outer space." *American economic review* 102 (2):994–1028.

Hendricks, Eric A., Melinda S. Peng, Bing Fu, and Tim Li. 2010. "Quantifying environmental control on tropical cyclone intensity change." *Monthly Weather Review* 138 (8):3243–3271.

Henriet, Fanny, Stéphane Hallegatte, and Lionel Tabourier. 2012. "Firm-network characteristics and economic robustness to natural disasters." *Journal of Economic Dynamics and Control* 36 (1):150–167.

Hirpa, Feyera A., Peter Salamon, Hylke E. Beck, Valerio Lorini, Lorenzo Alfieri, Ervin Zsoter, and Simon J. Dadson. 2018. "Calibration of the Global Flood Awareness System (GloFAS) using daily streamflow data." *Journal of Hydrology* 566:595–606.

Hofert, Marius, Ivan Kojadinovic, Martin Mächler, and Jun Yan. 2018. *Elements of copula modeling with R*. Springer.

Hofert, Marius, Martin Mächler, and Alexander J. McNeil. 2012. "Likelihood inference for Archimedean copulas in high dimensions under known margins." *Journal of Multivariate Analysis* 110:133–150.

Holcombe, Elizabeth and Malcolm Anderson. 2010. "Tackling landslide risk: Helping land use policy to reflect unplanned housing realities in the Eastern Caribbean." *Land Use Policy* 27 (3):798–800.

Holland, G. 1980. "An Analytic Model of the Wind and Pressure Profiles in Hurricanes." *Monthly Weather Review* 106:1212–1218.

Hornbeck, Richard. 2012. "The enduring impact of the American Dust Bowl: Short- and long-run adjustments to environmental catastrophe." *American Economic Review* 102 (4):1477–1507.

Hornbeck, Richard and Suresh Naidu. 2014. "When the levee breaks: black migration and economic development in the American South." *American Economic Review* 104 (3):963–90.

Hou, Arthur Y., Ramesh K. Kakar, Steven Neeck, Ardeshir A. Azarbarzin, Christian D. Kummerow, Masahiro Kojima, Riko Oki, Kenji Nakamura, and Toshio Iguchi. 2014. "The global precipitation measurement mission." *Bulletin of the American Meteorological Society* 95 (5):701–722.

Hsiang, Solomon M. and Amir S. Jina. 2014. "The causal effect of environmental catastrophe on long-run economic growth: Evidence from 6,700 cyclones." Tech. rep., National Bureau of Economic Research.

Hu, Xuan, Bingsheng Liu, Zheng Yi Wu, and Jie Gong. 2016. "Analysis of dominant factors associated with hurricane damages to residential structures using the rough set theory." *Natural Hazards Review* 17 (3):04016005.

Huff, Floyd A. 1967. "Time distribution of rainfall in heavy storms." *Water resources research* 3 (4):1007–1019.

Huffman, George J., David T. Bolvin, Dan Braithwaite, Kuolin Hsu, Robert Joyce, Pingping Xie, and Soo-Hyun Yoo. 2015a. "NASA global precipitation measurement (GPM) integrated multi-satellite retrievals for GPM (IMERG)." *Algorithm theoretical basis document, version* 4:30.

Huffman, George J., David T. Bolvin, Eric J. Nelkin, and Tan Jackson. 2020. "Integrated Multi-satellitE Retrievals for GPM (IMERG) Technical Documentation." Tech. rep., Mesoscale Atmospheric Processes Laboratory, NASA Goddard Space Flight Center, Science Systems and Applications, Inc.

Huffman, George J., David T. Bolvin, Eric J. Nelkin, David B. Wolff, Robert F. Adler, Guojun Gu, Yang Hong, Kenneth P. Bowman, and Erich F. Stocker. 2007. "The TRMM multisatellite precipitation analysis (TMPA): Quasi-global, multiyear, combined-sensor precipitation estimates at fine scales." *Journal of hydrometeorology* 8 (1):38–55.

Huffman, George J, David T Bolvin, Eric J Nelkin et al. 2015b. "Integrated Multi-satellitE Retrievals for GPM (IMERG) technical documentation." *NASA/GSFC Code* 612 (47):2019.

IPCC. 2012. "Managing the Risks of Extreme Events and Disasters to Advance Climate Change Adaptation." In *Summary for Policymakers*. Cambridge University Press, 3–21.

Ishizawa, Oscar A., Juan José Miranda, and Eric Strobl. 2019. "The impact of Hurricane strikes on short-term local economic activity: evidence from nightlight images in the Dominican Republic." *International Journal of Disaster Risk Science* 10 (3):362–370.

Jiang, Haiyan, Jeffrey B. Halverson, Joanne Simpson, and Edward J. Zipser. 2008. "Hurricane "rainfall potential" derived from satellite observations aids overland rainfall prediction." *Journal of applied meteorology and climatology* 47 (4):944–959.

Jiang, Haiyan, Chuntao Liu, and Edward J. Zipser. 2011. "A TRMM-based tropical cyclone cloud and precipitation feature database." *Journal of applied meteorology and climatology* 50 (6):1255–1274.

Joe, Harry. 2014. *Dependence modeling with copulas*. Chapman Hall/CRC Monographs on Statistics Applied Probability.

Johnston, Jake and Juan A Montecino. 2012. *Update on the Jamaican economy*. Center for Economic and Policy Research Washington DC.

Jonkman, Sebastiaan N. 2005. "Global perspectives on loss of human life caused by floods." *Natural hazards* 34 (2):151–175.

Jordà, Òscar. 2005. "Estimation and inference of impulse responses by local projections." *American economic review* 95 (1):161–182.

Kaczan, David J. and Jennifer Orgill-Meyer. 2020. "The impact of climate change on migration: a synthesis of recent empirical insights." *Climatic Change* 158 (3-4):281–300.

Keefer, David K., Raymond C. Wilson, Robert K. Mark, Earl E. Brabb, William M. Brown, Stephen D. Ellen, Edwin L. Harp, Gerald F. Wieczorek, Christopher S. Alger, and Robert S. Zatkin. 1987. "Real-time landslide warning during heavy rainfall." *Science* 238 (4829):921–925.

Khajehei, Sepideh, Ali Ahmadalipour, Wanyun Shao, and Hamid Moradkhani. 2020. "A place-based assessment of flash flood hazard and vulnerability in the contiguous United States." *Scientific Reports* 10 (1):448.

Klomp, Jeroen. 2016. "Economic development and natural disasters: A satellite data analysis." *Global Environmental Change* 36:67–88.

Klomp, Jeroen and Kay Valckx. 2014. "Natural disasters and economic growth: A meta-analysis." *Global Environmental Change* 26:183–195.

Knutson, Thomas, Suzana J. Camargo, Johnny C. L. Chan, Kerry Emanuel, Chang-Hoi Ho, James Kossin, Mrutyunjay Mohapatra, Masaki Satoh, Masato Sugi, and Kevin Walsh. 2019. "Tropical Cyclones and Climate Change Assessment: Part I: Detection and Attribution." *Bulletin of the American Meteorological Society* 100 (10):1987–2007.

Kocornik-Mina, Adriana, Thomas K. J. McDermott, Guy Michaels, and Ferdinand Rauch. 2020. "Flooded cities." *American Economic Journal: Applied Economics* 12 (2):35–66.

Kojadinovic, Ivan and Jun Yan. 2010. "Modeling multivariate distributions with continuous margins using the copula R package." *Journal of Statistical Software* 34 (1):1–20.

Koks, Elco E., Julie Rozenberg, Conrad Zorn, Mersedeh Tariverdi, Michalis Vousdoukas, S. A. Fraser, J. W. Hall, and Stephane Hallegatte. 2019. "A global multi-hazard risk analysis of road and railway infrastructure assets." *Nature communications* 10 (1):1–11.

Kotz, Maximilian, Anders Levermann, and Leonie Wenz. 2022. "The effect of rainfall changes on economic production." *Nature* 601 (7892):223–227.

Kousky, Carolyn. 2016. "Impacts of natural disasters on children." *The Future of children* :73–92.

Koutsoyiannis, Demetris, Demosthenes Kozonis, and Alexandros Manetas. 1998. "A mathematical framework for studying rainfall intensity-duration-frequency relationships." *Journal of hydrology* 206 (1-2):118–135.

Laing, Arlene G. 2004. "Cases of heavy precipitation and flash floods in the Caribbean during El Nino winters." *Journal of Hydrometeorology* 5 (4):577–594.

Landsea, C. W. and J. L. Franklin. 2013. "Atlantic Hurricane Database Uncertainty and Presentation of a New Database Format." *Monthly Wearther Review* 141:3576–3592.

Larsen, Matthew C. and Andrew Simon. 1993. "A rainfall intensity-duration threshold for landslides in a humid-tropical environment, Puerto Rico." *Geografiska Annaler: Series A, Physical Geography* 75 (1-2):13–23.

Lau, K.-M., Y. P. Zhou, and H.-T. Wu. 2008. "Have tropical cyclones been feeding more extreme rainfall?" *Journal of Geophysical Research: Atmospheres* 113 (D23).

Leiter, Andrea M., Harald Oberhofer, and Paul A. Raschky. 2009. "Creative disasters? Flooding effects on capital, labour and productivity within European firms." *Environmental and Resource Economics* 43 (3):333–350.

Lenzen, Manfred, Arunima Malik, Steven Kenway, Peter Daniels, Ka Leung Lam, and Arne Geschke. 2019. "Economic damage and spillovers from a tropical cyclone." *Natural Hazards and Earth System Sciences* 19 (1):137–151.

Li, Heshu, Dong Wang, Vijay P. Singh, Yuankun Wang, Jianfeng Wu, Jichun Wu, Jiufu Liu, Ying Zou, Ruimin He, and Jianyun Zhang. 2019. "Non-stationary frequency analysis of annual extreme rainfall volume and intensity using Archimedean copulas: A case study in eastern China." *Journal of hydrology* 571:114–131.

Li, Xiang-Hu, Qi Zhang, and Chong-Yu Xu. 2012. "Suitability of the TRMM satellite rainfalls in driving a distributed hydrological model for water balance computations in Xinjiang catchment, Poyang lake basin." *Journal of Hydrology* 426:28–38.

Li, Yi, Weihua Fang, and Xiaogang Duan. 2019. "On the driving forces of historical changes in the fatalities of tropical cyclone disasters in China from 1951 to 2014." *Natural Hazards* 98 (2):507–533.

Lin, Ning, James A. Smith, Gabriele Villarini, Timothy P. Marchok, and Mary Lynn Baeck. 2010. "Modeling extreme rainfall, winds, and surge from Hurricane Isabel (2003)." *Weather and forecasting* 25 (5):1342–1361.

Lindell, Michael K. and Carla S. Prater. 2003. "Assessing community impacts of natural disasters." *Natural hazards review* 4 (4):176–185.

Linkin, Megan E. 2014. "Excess Rainfall Product for the Caribbean Region-Developed by The CCRIF and Swiss Re." In *AGU Fall Meeting Abstracts*, vol. 2014. NH51C–04.

Loayza, Norman V., Eduardo Olaberria, Jamele Rigolini, and Luc Christiaensen. 2012. "Natural disasters and growth: Going beyond the averages." *World Development* 40 (7):1317–1336.

Lonfat, Manuel, Frank D. Marks Jr, and Shuyi S. Chen. 2004. "Precipitation distribution in tropical cyclones using the Tropical Rainfall Measuring Mission (TRMM) microwave imager: A global perspective." *Monthly Weather Review* 132 (7):1645–1660.

López-Marrero, Tania and Abimael Castro-Rivera. 2019. "Let's not forget about non-landfalling cyclones: tendencies and impacts in Puerto Rico." *Natural Hazards* 98 (2):809–815.

Lumbroso, D. M., S. Boyce, H. Bast, and N. Walmsley. 2011. "The challenges of developing rainfall intensity–duration–frequency curves and national flood hazard maps for the Caribbean." *Journal of Flood Risk Management* 4 (1):42–52.

Lung, Tobias, Carlo Lavalle, Roland Hiederer, Alessandro Dosio, and Laurens M. Bouwer. 2013. "A multi-hazard regional level impact assessment for Europe combining indicators of climatic and non-climatic change." *Global Environmental Change* 23 (2):522–536.

Masoomi, Hassan, John W. van de Lindt, Mohammad R. Ameri, Trung Q. Do, and Bret M. Webb. 2019. "Combined wind-wave-surge hurricane-induced damage prediction for buildings." *Journal of Structural Engineering* 145 (1):04018227.

Matyas, Corene J. and Julie A. Silva. 2013. "Extreme weather and economic well-being in rural Mozambique." *Natural hazards* 66 (1):31–49.

Mendelsohn, Robert. 2012. "The economics of adaptation to climate change in developing countries." *Climate Change Economics* 3 (02):1250006.

Milanesi, Luca, Marco Pilotti, Andrea Belleri, Alessandra Marini, and Sven Fuchs. 2018. "Vulnerability to flash floods: a simplified structural model for masonry buildings." *Water Resources Research* 54 (10):7177–7197.

Miller, Servel, Tim Brewer, and Norman Harris. 2009. "Rainfall thresholding and susceptibility assessment of rainfall-induced landslides: application to landslide management in St Thomas, Jamaica." *Bulletin of Engineering Geology and the Environment* 68 (4):539.

Monioudi, Isavela N., Regina Asariotis, Austin Becker, Cassandra Bhat, Danielle Dowding-Gooden, Miguel Esteban, Luc Feyen, Lorenzo Mentaschi, Antigoni Nikolaou, Leonard Nurse et al. 2018. "Climate change impacts on critical international

transportation assets of Caribbean Small Island Developing States (SIDS): the case of Jamaica and Saint Lucia." *Regional Environmental Change* 18 (8):2211–2225.

Murnane, Richard J. and James B. Elsner. 2012. "Maximum wind speeds and US hurricane losses." *Geophysical Research Letters* 39 (16).

Naguib, Costanza, Martino Pelli, David Poirier, and Jeanne Tschopp. 2022. "The impact of cyclones on local economic growth: Evidence from local projections." *Economics letters* 220:110871.

Nandi, Arpita, Arpita Mandal, Matthew Wilson, and David Smith. 2016. "Flood hazard mapping in Jamaica using principal component analysis and logistic regression." *Environmental Earth Sciences* 75 (6):1–16.

Nelsen, Roger B. 2007. *An introduction to copulas*. Springer Science & Business Media.

Nkemdirim, Lawrence C. 1979. "Spatial and seasonal distribution of rainfall and runoff in Jamaica." *Geographical Review* :288–301.

NOAA. 2019. "NOAA increases chance for above-normal hurricane season." URL `https://www.noaa.gov/media-release/noaa-increases-chance-for-above-normal-hurricane-season`.

Nolasco-Javier, Dymphna and Lalit Kumar. 2018. "Deriving the rainfall threshold for shallow landslide early warning during tropical cyclones: a case study in northern Philippines." *Natural hazards* 90 (2):921–941.

Nolasco-Javier, Dymphna, Lalit Kumar, and Arlene Mae P. Tengonciang. 2015. "Rapid appraisal of rainfall threshold and selected landslides in Baguio, Philippines." *Natural hazards* 78 (3):1587–1607.

Norbiato, Daniele, Marco Borga, Silvia Degli Esposti, Eric Gaume, and Sandrine Anquetin. 2008. "Flash flood warning based on rainfall thresholds and soil moisture conditions: An assessment for gauged and ungauged basins." *Journal of Hydrology* 362 (3-4):274–290.

Nordhaus, William D. 2006. "The economics of hurricanes in the United States." Tech. rep., National Bureau of Economic Research.

———. 2010. "The economics of hurricanes and implications of global warming." *Climate Change Economics* 1 (01):1–20.

Northrop, Paul J., Nicolas Attalides, and Philip Jonathan. 2017. "Cross-validatory extreme value threshold selection and uncertainty with application to ocean storm severity." *Journal of the Royal Statistical Society: Series C (Applied Statistics)* 66 (1):93–120.

Noy, Ilan. 2009. "The macroeconomic consequences of disasters." *Journal of Development economics* 88 (2):221–231.

Okazaki, Tetsuji, Toshihiro Okubo, and Eric Strobl. 2019. "Creative destruction of industries: Yokohama city in the Great Kanto Earthquake, 1923." *The journal of economic history* 79 (1):1–31.

Okubo, Toshihiro and Eric Strobl. 2021. "Natural disasters, firm survival, and growth: Evidence from the Ise Bay Typhoon, Japan." *Journal of regional science* 61 (5):944–970.

Panwar, Vikrant and Subir Sen. 2020. "Disaster damage records of EM-DAT and DesInventar: a systematic comparison." *Economics of disasters and climate change* 4 (2):295–317.

Park, Doo-Sun R, Chang-Hoi Ho, Chaehyeon C Nam, and Hyeong-Seog Kim. 2015. "Evidence of reduced vulnerability to tropical cyclones in the Republic of Korea." *Environmental Research Letters* 10 (5):054003.

Park, Sangki, John W van de Lindt, and Yue Li. 2013. "Application of the hybrid ABV procedure for assessing community risk to hurricanes spatially." *Natural hazards* 68 (2):981–1000.

Paulsen, Becca M. and John L. Schroeder. 2005. "An examination of tropical and extratropical gust factors and the associated wind speed histograms." *Journal of Applied Meteorology and Climatology* 44 (2):270–280.

Peduzzi, Pascal, Bruno Chatenoux, H. Dao, Andréa De Bono, Christian Herold, James Kossin, Frédéric Mouton, and Ola Nordbeck. 2012. "Global trends in tropical cyclone risk." *Nature climate change* 2 (4):289–294.

Peterson, Thomas C., Michael A. Taylor, Rodger Demeritte, Donna L. Duncombe, Selvin Burton, Francisca Thompson, Avalon Porter, Mejia Mercedes, Elba Villegas, Rony Semexant Fils et al. 2002. "Recent changes in climate extremes in the Caribbean region." *Journal of Geophysical Research: Atmospheres* 107 (D21):ACL–16.

Pinos, Juan and Adolfo Quesada-Román. 2021. "Flood risk-related research trends in Latin America and the Caribbean." *Water* 14 (1):10.

Rappaport, Edward N. 2014. "Fatalities in the United States from Atlantic tropical cyclones: New data and interpretation." *Bulletin of the American Meteorological Society* 95 (3):341–346.

Rawlins, B. G., A. J. Ferguson, P. J. Chilton, R. S. Arthurton, J. G. Rees, and J. W. Baldock. 1998. "Review of agricultural pollution in the Caribbean with particular emphasis on small island developing states." *Marine Pollution Bulletin* 36 (9):658–668.

Rezapour, Mehdi and Tom E. Baldock. 2014. "Classification of hurricane hazards: The importance of rainfall." *Weather and Forecasting* 29 (6):1319–1331.

Román, Miguel O., Zhuosen Wang, Qingsong Sun, Virginia Kalb, Steven D. Miller, Andrew Molthan, Lori Schultz, Jordan Bell, Eleanor C. Stokes, Bhartendu Pandey et al. 2018. "NASA's Black Marble nighttime lights product suite." *Remote Sensing of Environment* 210:113–143.

Rose, Adam and Shu-Yi Liao. 2005. "Modeling regional economic resilience to disasters: A computable general equilibrium analysis of water service disruptions." *Journal of regional science* 45 (1):75–112.

Rosenzweig, Bernice R., Lauren McPhillips, Heejun Chang, Chingwen Cheng, Claire Welty, Marissa Matsler, David Iwaniec, and Cliff I. Davidson. 2018. "Pluvial flood risk and opportunities for resilience." *Wiley Interdisciplinary Reviews: Water* 5 (6):e1302.

Rözer, Viktor, Heidi Kreibich, Kai Schröter, Meike Müller, Nivedita Sairam, James Doss-Gollin, Upmanu Lall, and Bruno Merz. 2019. "Probabilistic models significantly reduce uncertainty in Hurricane Harvey pluvial flood loss estimates." *Earth's Future* 7 (4):384–394.

Ruin, Isabelle, Céline Lutoff, Brice Boudevillain, Jean-Dominique Creutin, Sandrine Anquetin, M Bertran Rojo, Laurent Boissier, Laurent Bonnifait, Marco Borga, L Colbeau-Justin et al. 2014. "Social and hydrological responses to extreme precipitations: An interdisciplinary strategy for postflood investigation." *Weather, climate, and society* 6 (1):135–153.

Salvadori, Gianfausto and Carlo De Michele. 2004. "Frequency analysis via copulas: Theoretical aspects and applications to hydrological events." *Water resources research* 40 (12).

Salvadori, Gianfausto, Fabrizio Durante, Carlo De Michele, Mauro Bernardi, and Lea Petrella. 2016. "A multivariate copula-based framework for dealing with hazard scenarios and failure probabilities." *Water Resources Research* 52 (5):3701–3721.

Scarrott, Carl and Anna MacDonald. 2012. "A review of extreme value threshold estimation and uncertainty quantification." *REVSTAT–Statistical Journal* 10 (1):33–60.

Seneviratne, Sonia I., Xuebin Zhang, Muhammad Adnan, Wafae Badi, Claudine Dereczynski, Alejandro Di Luca, Sergio M. Vicente-Serrano, Michael Wehner, and Botao Zhou. 2021. "11 Chapter 11: Weather and climate extreme events in a changing climate." .

Singh, Vijay P. and Lan Zhang. 2007. "IDF curves using the Frank Archimedean copula." *Journal of hydrologic engineering* 12 (6):651–662.

Skidmore, Mark and Hideki Toya. 2002. "Do natural disasters promote long-run growth?" *Economic inquiry* 40 (4):664–687.

Spekkers, M. H., M. Kok, F. H. L. R. Clemens, and J. A. E. Ten Veldhuis. 2013. "A statistical analysis of insurance damage claims related to rainfall extremes." *Hydrology & Earth*

System Sciences 17 (3).

Spencer, Nekeisha and Solomon Polachek. 2015. "Hurricane watch: Battening down the effects of the storm on local crop production." *Ecological Economics* 120:234–240.

Špitalar, Maruša, Jonathan J. Gourley, Celine Lutoff, Pierre-Emmanuel Kirstetter, Mitja Brilly, and Nicholas Carr. 2014. "Analysis of flash flood parameters and human impacts in the US from 2006 to 2012." *Journal of Hydrology* 519:863–870.

Statistical Institute of Jamaica. 2011. "Population Usually Resident in Jamaica, by Parish." *Population Census* .

Strobl, Eric. 2011. "The economic growth impact of hurricanes: evidence from US coastal counties." *Review of Economics and Statistics* 93 (2):575–589.

———. 2012. "The economic growth impact of natural disasters in developing countries: Evidence from hurricane strikes in the Central American and Caribbean regions." *Journal of Development economics* 97 (1):130–141.

Strulik, Holger and Timo Trimborn. 2019. "Natural disasters and macroeconomic performance." *Environmental and resource economics* 72:1069–1098.

Sugahara, Shigetoshi, Rosmeri Porfírio Da Rocha, and Reinaldo Silveira. 2009. "Non-stationary frequency analysis of extreme daily rainfall in Sao Paulo, Brazil." *International Journal of Climatology: A Journal of the Royal Meteorological Society* 29 (9):1339–1349.

Tanaka, Ayumu. 2015. "The impacts of natural disasters on plants' growth: Evidence from the Great Hanshin-Awaji (Kobe) earthquake." *Regional Science and Urban Economics* 50:31–41.

Tang, Guoqiang, Martyn P Clark, Simon Michael Papalexiou, Ziqiang Ma, and Yang Hong. 2020. "Have satellite precipitation products improved over last two decades? A comprehensive comparison of GPM IMERG with nine satellite and reanalysis datasets." *Remote sensing of environment* 240:111697.

Terti, Galateia, Isabelle Ruin, Sandrine Anquetin, and Jonathan J. Gourley. 2015. "Dynamic vulnerability factors for impact-based flash flood prediction." *Natural Hazards* 79:1481–1497.

The World Bank Group. 2018. "Advancing Disaster Risk Finance in Jamaica." *International Bank for Reconstruction and Development* .

Tramblay, Yves, Luc Neppel, Julie Carreau, and Kenza Najib. 2013. "Non-stationary frequency analysis of heavy rainfall events in southern France." *Hydrological Sciences Journal* 58 (2):280–294.

U.S. Bureau of Labor Statistics. 2019. "Consumer Price Index for All Urban Consumers: All Items [CPIAUCSL], retrieved from FRED." *Federal Reserve Bank of St. Louis* .

Van Oldenborgh, Geert Jan, Karin Van Der Wiel, Antonia Sebastian, Roop Singh, Julie Arrighi, Friederike Otto, Karsten Haustein, Sihan Li, Gabriel Vecchi, and Heidi Cullen. 2017. "Attribution of extreme rainfall from Hurricane Harvey, August 2017." *Environmental Research Letters* 12 (12):124009.

Van Ootegem, Luc, Kristine Van Herck, Tom Creten, Elsy Verhofstadt, Loris Foresti, Edouard Goudenhoofdt, Maarten Reyniers, Laurent Delobbe, D. Murla Tuyls, and Patrick Willems. 2018. "Exploring the potential of multivariate depth-damage and rainfall-damage models." *Journal of Flood Risk Management* 11:S916–S929.

Van Ootegem, Luc, Elsy Verhofstadt, Kristine Van Herck, and Tom Creten. 2015. "Multivariate pluvial flood damage models." *Environmental Impact Assessment Review* 54:91–100.

Vickery, Peter J., Forrest J. Masters, Mark D. Powell, and Dhiraj Wadhera. 2009. "Hurricane hazard modeling: The past, present, and future." *Journal of Wind Engineering and Industrial Aerodynamics* 97 (7-8):392–405.

Vickery, Peter J. and Dhiraj Wadhera. 2008. "Statistical models of Holland pressure profile parameter and radius to maximum winds of hurricanes from flight-level pressure and H* Wind data." *Journal of Applied Meteorology and climatology* 47 (10):2497–2517.

Villarini, Gabriele, Radoslaw Goska, James A. Smith, and Gabriel A. Vecchi. 2014a. "North Atlantic tropical cyclones and US flooding." *Bulletin of the American Meteorological Society* 95 (9):1381–1388.

Villarini, Gabriele, David A. Lavers, Enrico Scoccimarro, Ming Zhao, Michael F. Wehner, Gabriel A. Vecchi, Thomas R. Knutson, and Kevin A. Reed. 2014b. "Sensitivity of tropical cyclone rainfall to idealized global-scale forcings." *Journal of climate* 27 (12):4622–4641.

Villarini, Gabriele, James A. Smith, Mary Lynn Baeck, Timothy Marchok, and Gabriel A. Vecchi. 2011. "Characterization of rainfall distribution and flooding associated with US landfalling tropical cyclones: Analyses of Hurricanes Frances, Ivan, and Jeanne (2004)." *Journal of Geophysical Research: Atmospheres* 116 (D23).

Walsh, Kevin J. E., John L. McBride, Philip J. Klotzbach, Sethurathinam Balachandran, Suzana J. Camargo, Greg Holland, Thomas R. Knutson, James P. Kossin, Tsz-cheung Lee, Adam Sobel, and Masato Sugi. 2016. "Tropical cyclones and climate change." *Wiley Interdisciplinary Reviews: Climate Change* 7 (1):65–89.

Wilson, Matthew, Arpita Mandal, Michael Taylor, Christopher Burgess, Jayaka Campbell, and Tannecia Stepphenson. 2014. "Flood Risk and Climate Change in Negril, Jamaica: An Assessment of Combined Terrestrial and Coastal Flood Risk Driven by Projections of Future Climate." In *WCrP Conference for Latin America and the Caribbean: Developing, Linking and Applying Climate knowledge, Montevideo, Uruguay, March*. 17–21.

World Bank Group. 2020. "Population, total - Latin America & Caribbean." URL `https://data.worldbank.org/indicator/SP.POP.TOTL?locations=ZJ`.

Xiao, Y. F., Z. D. Duan, Y. Q. Xiao, J. P. Ou, L. Chang, and Q. S. Li. 2011. "Typhoon wind hazard analysis for southeast China coastal regions." *Structural Safety* 33 (4-5):286–295.

Xiao, Yu-Feng, Y-Quing Xiao, and Zhong-Dong Duan. 2009. "The Typhoon Wind Hazard Analysis in Hong Kong of China with the New Formula for Holland B Parameter and

the CE Wind Field Model." The Seventh Asia-Pacific Conference on Wind Engineering, 8-12 Nov., Taipei, Taiwan.

Yin, Jie, Yao Gao, Ruishan Chen, Dapeng Yu, Robert Wilby, Nigel Wright, Yong Ge, Jeremy Bricker, Huili Gong, and Mingfu Guan. 2023. "Flash floods: why are more of them devastating the world's driest regions?" *Nature* 615 (7951):212–215.

Yu, Zifeng, Yuqing Wang, Haiming Xu, Noel Davidson, Yandie Chen, Yimin Chen, and Hui Yu. 2017. "On the relationship between intensity and rainfall distribution in tropical cyclones making landfall over China." *Journal of Applied Meteorology and Climatology* 56 (10):2883–2901.

Yumul, Graciano P., Nathaniel T. Servando, Leilanie O. Suerte, Mae Y. Magarzo, Leo V. V. Juguan, and Carla B. Dimalanta. 2012. "Tropical cyclone–southwest monsoon interaction and the 2008 floods and landslides in Panay island, central Philippines: meteorological and geological factors." *Natural hazards* 62 (3):827–840.

Zhai, Alice R. and Jonathan H. Jiang. 2014. "Dependence of US hurricane economic loss on maximum wind speed and storm size." *Environmental Research Letters* 9 (6):064019.

Zhou, Fujin and Wouter Botzen. 2021. "Firm level evidence of disaster impacts on growth in Vietnam." *Environmental and Resource Economics* 79 (2):277–322.

Zscheischler, Jakob, Rene Orth, and Sonia I. Seneviratne. 2017. "Bivariate return periods of temperature and precipitation explain a large fraction of European crop yields." *Biogeosciences* 14 (13):3309–3320.